RESIDUAL AND GOAL-ORIENTED H- AND HP-ADAPTIVE FINITE ELEMENT; APPLICATION FOR ELLIPTIC AND SADDLE POINT PROBLEMS

A Dissertation

by

AREZOU GHESMATI

Submitted to the Office of Graduate and Professional Studies of
Texas A&M University
in partial fulfillment of the requirements for the degree of

DOCTOR OF PHILOSOPHY

Chair of Committee,	Wolfgang Bangerth
Committee Members,	Jean-Luc Guermond
	Andrea Bonito
	Jean C. Ragusa
Head of Department,	Emil J. Straube

May 2018

Major Subject: Mathematics

ABSTRACT

We propose and implement an automatic hp-adaptive refinement algorithm for the Stokes model problem. In this work, the strategy is based on the earlier work done by Dörfler at al. in 2007 for the Poisson problem. Similar to any other adaptivity approach, an a posteriori estimator is needed to control the error in areas with high residuals. We define a family of residual-based estimators $\eta_\alpha,\ \alpha \in [0,1]$ for the hp-adaptive finite element approximation of the exact solution. Moreover, we show the reliability and efficiency of the estimators η_α. Finally, numerical examples illustrate the exponential convergence rate of the hp-AFEM in comparison with the h-AFEM.

In many applications, such as analysis of fluid flows in our case, we are not interested in computing the solution itself, but instead the aim is finding a good approximation for some functional of interest. In these cases, the idea is to develop some a posteriori error estimates to generate a sequence of h- or hp-adaptive grids that minimize the error in our goal functional with respect to the problem size. In this work, we apply local averaging interpolation operators such as Scott-Zhang and Clément type operators to formulate the dual weight of our proposed goal-oriented error estimator. This idea was recently used in an application to the Poisson problem. We extend those results to saddle-point problems and provide a dual-weighted goal estimator for each cell. The reliability of the goal estimator is proved and numerical examples demonstrate the performance of the locally defined dual-weighted goal-estimator in terms of reliability, efficiency, and convergence.

Another important aspect of this research is providing a goal-oriented adaptive finite element method for symmetric second-order linear elliptic problems. We prove that the product of primal and dual estimators, which is a reliable upper bound for the error in the goal functional, decays at the optimal rate. The results reported in the numerical experiments confirm the quasi-optimality behavior of our goal-oriented algorithm.

DEDICATION

To Amir, love of my life, and our darling little boy, Borna.

To my kind and lovely parents Bahman and Tooran.

ACKNOWLEDGMENTS

I would like to express my gratitude to the department of Mathematics at Texas A&M University for giving me the opportunity to meet lots of world renowned mathematicians over the past five years. Great people who have helped me and influenced my research, especially my supervisor Dr. Wolfgang Bangerth.

Having Prof. Bangerth as my supervisor was a great privilege through my Ph.D. journey. His insights, advices, and his patient guidances shed light to my professional academic path. I am also thankful for his generous support during my Ph.D. years and giving me the chances to attend various conferences and workshops.

I would like to thank all my committee members, Dr. Bonito, Dr. Guermond, and Dr. Ragusa for all insightful advices and for their time and patience. I also want to thank Dr. Bruno Turksin for his friendly support and sharing his valuable experience in programing.

I want to give my deepest appreciation to my kind parents for their unconditional love and backup throughout my education from elementary school to my Ph.D. studies, abroad. I am blessed to have such an encouraging parents, always granting care and support.

Last but not the least, I would like to specially thank to my beloved husband, Amir, for his unlimited love, support and encouragement in the past seven years being my life companion. Without his support, this journey would not be joyful and easy to follow.

CONTRIBUTORS AND FUNDING SOURCES

Contributors

This work was supervised by a dissertation committee consisting of Professor Wolfgang Bangerth of the Department of Mathematics (chair), Professor Jean-Luc Guermond of the Department of Mathematics, Professor Andrea Bonito of the Department of Mathematics, and Professor Jean C. Ragusa of the Department of Nuclear Engineering.

All work for the dissertation was completed independently by the student, under the advisement of Professor Wolfgang Bangerth of the Department of Mathematics.

Funding Sources

This work was made possible in part by National Science Foundation (NSF) under grant number OCI-1148116 to develop computational algorithms and implement them in open source software deal.II.

TABLE OF CONTENTS

Page

LIST OF FIGURES

FIGURE Page

LIST OF TABLES

TABLE Page

1. INTRODUCTION

1.1 Motivation and background

We consider the Stokes equations as an example of saddle point problems. The Stokes flow models the motion of fluid when the inertia effects can be neglected. We assume the fluid is incompressible and give the formulation for the stationary flow. Given $f \in L^2(\Omega)^2$, $\nu > 0$, the momentum and the mass equations are formulated as follows: Find velocity, $u : \overline{\Omega} \to \mathbb{R}^2$, and pressure, $\varrho : \Omega \to \mathbb{R}$, such that

$$\begin{aligned} -2\nu\nabla \cdot \varepsilon(u) + \nabla\varrho &= f \qquad \text{in} \quad \Omega \\ -\nabla \cdot u &= 0 \qquad \text{in} \quad \Omega \\ u &= 0 \qquad \text{on} \quad \Gamma. \end{aligned} \tag{1.1}$$

Where we define the symmetric gradient as $\varepsilon(u) = \frac{1}{2}[(\nabla u)+(\nabla u)^T]$. The main technical difficulty in dealing with the Stokes problem is that unlike linear elliptic problems it does not satisfy the coercivity property and is not a definite problem. The pressure can be seen as the Lagrange multiplier associated with the constraint on the velocity. As a quick note on discretization, the velocity and pressure as two dependent variables with different roles leads us to formulate these equations into a category of finite element method, namely the mixed finite elements approximations. Therefore, in creating the weak formulation for the mixed finite element method, the corresponding spaces are the Cartesian products of the appropriate Sobolev spaces associated with the velocity and the pressure variables. In chapter 2, we will discuss on the necessary and sufficient condition, namely the inf-sup condition, to ensure the mixed finite element formulation is well-posed.

In the previous application of adaptive finite element methods for the Stokes equations in the deal.ii library, the error estimator has been defined by applying the so-called Kelly error estimator

to the velocity. In this method, one computes the error estimator η_K for cell K as:

$$\eta_K^2 := \sum_{e \in \mathcal{E}(K)} C_e \left\| \left[\frac{\partial u_{\text{FE}}}{\partial n_K} \right] \right\|_e^2 .$$

The problem with this method is that even though it gives good hints for the mesh refinement, the error estimator is not to be trusted. For example, in using higher order polynomial spaces, the estimator computed here tends to zero even faster than the actual error itself. Therefore, we consider the need to define a residual based estimator containing both cell and jumped residuals. While investigation through references related to a posteriori error estimator, and learning about exponential convergence rate using the hp-AFEM, the article by Melenk et al. [2] inspired us to define a residual based a posteriori error estimator in conforming hp-AFEM for the Stokes problem:

$$\eta_K^2 := \eta_{K;R}^2 + \eta_{K;B}^2,$$

where $\eta_{K;R}$ denotes the cell residual-based term and $\eta_{K;B}$ indicates the jump-based term. In Chapter 3, we introduce hp-residual-based error estimator for the Stokes equations in the context of conforming finite elements. We also prove the most important property of a posteriori estimators – the reliability and the efficiency – for a family of weighted error estimators $\eta_\alpha,\ \alpha \in [0, 1]$. The numerical results reported in that chapter verify the capability of our hp-estimator and also the exponential decay rate of the energy error and error estimator is observed in our test cases.

Meanwhile, working on the aforementioned residual estimator, we use the proposed hp residual-based a posteriori error estimator to define a new local dual-weighted h- and hp-goal-oriented estimator for the Stokes equations. It is important to mention that in many real world applications, such as working on fluid structure iterations, the primary goal is not finding the solution to a problem in every single point. Most of the time, the main aim is being able to recover stresses or forces with high accuracy in some specific sub-areas of the problem domain. When this is the goal of interest, then applying uniform refinement or traditional adaptive strategies using the energy error estimator may not be effective enough to achieve high accuracy in that quantity of interest. In

2015, Bürg and Nazarov in [1] defined a new reliable and efficient goal-oriented estimator for the Poisson equation, and in their numerical examples they showed the optimality in decay rate in the goal-oriented mesh refinement procedure. Based on this work, we define a new goal oriented dual-weighted error estimator for the Stokes model problem. For each cell K, we consider the corresponding patch cells ω_K, and then apply Clément and Scott-Zhang type interpolation operators on ω_k to get the dual-weight in our goal-oriented estimator definition. The details of the proof of the reliability and efficiency of the goal-oriented estimator are given in Chapter 4. In this study, we tried to obtain close to optimal meshes to calculate the specified quantity of interest. In the benchmark numerical examples, the exponential convergence rate for the goal-oriented hp-AFEM is presented. The optimal error decay rate, as is expected for $(u, z) \in \mathbb{A}^s \times \mathbb{A}^t$ is achieved in our numerical test cases which were close to $\mathcal{O}(\text{DOF}^{s+t})$. Where $\mathbb{A}^s$ and $\mathbb{A}^t$ are the standard approximation classes, and DOF presents the number of degrees of freedom. In our attempt to prove optimal decay rate in the error of goal-functional, we consider class of general second-order elliptic problems, and propose a goal-oriented marking strategy that will be described in Chapter 5. In the spirit of Feischl et al. [3], we prove our primal and dual estimators satisfy the well-known *axioms of adaptivity* that were first introduced in 2008 by Cascon et al. [4] and then enhanced in 2014 by Carstensen et al. [5]. As our main result in this chapter, we prove the product of primal and dual estimator, which is a reliable upper bound for error in the goal functional, decays in optimal rate as a function of number of degrees of freedom. Our numerical test cases validate our analytical discussion and the corresponding plots visualize the aforementioned results. Finally we conclude and summarize our findings of these three studies in Chapter 6.

1.2 Overview on related work on adaptivity and objectives

Adaptive approaches for the numerical solution of PDEs are now standard tools in both science and engineering of phenomena modeled by PDEs. The idea of adaptivity goes back to the history of enhancements of the solution for PDEs by the classical finite element method. In that approach, if the accuracy of the approximated finite element solution did not satisfy a pre-defined tolerance, then the whole triangulation was refined to smaller cells. In 1970, Babŭska [6] showed that the

existence of singularities such as singularity at corners of the boundary has great influence on the convergence rate of finite element methods. It was shown that proper local refinement of the finite element mesh near the singular part of the domain leads to the expected convergence rate. Based on this, the h-adaptive finite element method was born. By developing the idea of a posteriori error estimation, its application extended to a wide variety of model problems [7, 8]. Babuška in [9] showed that the p-version of the finite element method is another approach to increase the accuracy of the finite element solution. In 1981, Babůska et al. [10] showed the approximation order depends on the both mesh size h and its element degrees p, and they introduced the idea of combining h and p versions of the finite element method. It was shown that the hp-adaptive FEM can achieve exponential rates of convergence with respect to the number of degrees of freedom [11, 12, 13, 14].

Continuing the idea of adaptivity, now the question is how to identify the corresponding regions to be refined such that the overall accuracy remains optimal. To answer this question, the concept of a posteriori error estimation came into play [15]. Most of the time, a priori estimators require regularity properties of the solution, which are not satisfied in the presence of singularities, and provide information on the asymptotic behavior of the error and do not help us estimate the concrete error on the current mesh. Therefore, the need for error indicators, which can be extracted a posteriori from the data and the approximate solution, was considered. By defining such an estimator, an adaptive algorithm can be designed for the h and p-adaptive finite element method by refining the cells where the a posteriori estimated error is large. In the hp-AFEM, however, a single error estimate cannot simultaneously determine whether it is better to do the refinement by h or p. Several strategies for making this determination have been proposed over the years. In [16, 17] the idea of testing the smoothness of the solution is investigated, in [18, 19] the global interpolation error is minimized, and in [20, 21, 22] local boundary value problems are solved. Historically, despite uniform refinement in FEM and its well-understood analysis using a priori error estimators, adaptive FEMs were used for more than three decades without being sure whether those methods converge and if so, do they converge at the optimal rate or not. The lack

of understanding in convergence analysis of AFEMs could be due to the fact that compared with standard FEM and the role of a priori estimates in there, the tools required to apply the convergence analysis in AFEMs are different and were not well-understood at the time. The adaptivity analysis started with the work by Dörfler [23] in 1996, where he introduced a crucial bulk marking criterion and also proved error reduction for the Poisson equation. A few years later, Morin, Nochetto, and Siebert in [24, 25] introduced the concept of data oscillation and the interior property, and they proved the convergence of AFEM. Binev et al., in 2004 [26], proved a quasi-optimal convergence rates for the AFEMs. In 2005, Mekchay and Nochetto [27] introduced the concept of *total error* and gave convergence analysis for second order elliptic problems. The proof of contraction for the total error was another major result in that paper. Stevenson in 2007 [28], constructed an AFEM for more applicable and realistic elliptic PDEs with optimal convergence rate. Cascon, Kreuzer, Nochetto, and Siebert [4], inspired by Morin's work [29] on the convergence analysis of AFEMs, provide a very comprehensive convergence analysis for linear and symmetric elliptic problems. Later on, because of its generality, the framework was applied to other problems and adaptive refinement methods. It is remarkable that in all the aforementioned results on the analysis of optimal rate for AFEM, the refinement algorithm is designed based on estimating the energy error. We also can refer to the book by Bangerth and Rannacher [30] and the article [31] as a good survey for adaptive finite element methods.

In our study of the analysis of AFEMs, we are more interested in the analysis of convergence rate in goal-oriented AFEMs, where the error estimator is not defined for the energy error, but instead is specified so as to control the error in the quantity of interest. As some early works on the goal-oriented AFEM, we can mention to [32, 33, 34, 35, 30, 36]. Even though some of these works address to the analysis of convergence, but none of them provide any proof on that regard. As some early discussions on the optimal convergence rate in the concept of goal-oriented we can mention [37]. Moon et al. in [38] imposed strong regularity assumption on the solution of primal and dual problem and then proved the convergence and optimality of the dual-weighted adaptive algorithm. In 2009, Mommer and Stevenson [39] proved the convergence and the optimality in

the context of their proposed goal-oriented refinement algorithm for the Poisson equation. In their approach, at each refinement cycle, the Dörfler marking is applied for both primal and dual estimators separately and then between these two marked sets they choose the one with the smallest cardinality. The drawback of this goal-oriented refinement algorithm is that even though the decay rate of goal-error in this algorithm has been proven to be quasi-optimal, due to the fact that at each iteration step the error reduction happens by either the primal or dual estimator, this leads to slow convergence. The weighted marking algorithm for the goal-oriented AFEM by Becker et al. in 2011 [40], overcomes the issue described in Mommer and Stevenson's work while retaining the quasi-optimality. The most recent and interesting article in this regard is the one by Feischl et al. [3]. In this work, inspired by the comprehensive paper on axioms of adaptivity [5], they proved the optimal decay rate for the product of primal and dual estimators in the Mommer-Stevenson marking strategy, and showed their convergence proof extends beyond just the Poisson equation and is applicable for any general second order elliptic PDEs. Moreover, in this recent study on the general second order linear elliptic PDEs, Feischl et al. proved the quasi-optimality in the estimators' product for the weighted marking proposed by Becker et al. in [40].

2. PRELIMINARIES

In this chapter, we will introduce function spaces that play a significant role in the theory of finite element approximation. Then we will describe the most important concepts, namely the finite element spaces and also the approximation spaces needed in the analysis of finite element methods. We also discuss interpolation operators for adaptive methods, mainly for the hp-AFEM which map functions from the L_2 and H^1 spaces into the corresponding discrete finite element spaces.

2.1 Function spaces

In this section we start with recalling the Lebesgue space, that plays a significant role in the weak or variational formulation of differential equations. We refer the interested readers for the extended view and definitions in this regard to the book by Rudin [41].

2.1.1 The Lebesgue integration theory

Lebesgue integration theory implies for any real-valued function $u : \Omega \longrightarrow \mathbb{R}$, where $\Omega \in \mathbb{R}^d, d \in \mathbb{N}$, the Lebesgue space $L^p(\Omega), p \in [1, \infty]$ is given as

$$L^p(\Omega) := \{u : \|u\|_{L^p(\Omega)} < \infty\},$$

such that the norm for $p \in [1, \infty)$ is defined

$$\|u\|_{L^p(\Omega)} := \left(\int_\Omega |u|^p \right)^{\frac{1}{p}}$$

and for the case $p = \infty$ is

$$\|u\|_{L^\infty(\Omega)} := \sup_{x \in \Omega} |u(x)|.$$

Below we mention some well-known inequalities that are widely used for functions in these spaces and so we do further on in the next chapters. The first one is the triangle inequality for L^p spaces

reads as follows:

Lemma 2.1.1 (Minkowski's Inequality)**.** *For $u, v \in L^P(\Omega)$ and $p \in [1, \infty]$ we have*

$$\|u + v\|_{L^p(\Omega)} \leqslant \|u\|_{L^p(\Omega)} + \|v\|_{L^p(\Omega)}.$$

The next inequality which has significant application in the analysis of functions in Sobolev space is the Hölder inequality, which was introduced by Hölder in 1889.

Lemma 2.1.2 (Hölder Inequality})**.** *Let $u \in L^p(\Omega)$ and $v \in L^q(\Omega)$, for $p, q \in [1, \infty]$, $\frac{1}{p} + \frac{1}{q} = 1$. Then $uv \in L^1(\Omega)$ such that*

$$\|uv\|_{L^1(\Omega)} \leqslant \|u\|_{L^p(\Omega)} \|v\|_{L^q(\Omega)},$$

for the special case when $p = q = 2$, this inequality is called the Cauchy-Schwarz inequality.

2.1.2 The Sobolev spaces

Including weak derivatives into the definition of Lebesgue norm and Lebesgue spaces we present the standard Sobolev spaces $H^\alpha, for\, \alpha \geqslant 0$. It should be noted that the L^2 spaces are the foundation of finite element analysis and the H^α spaces are subspaces of L^2 space with some additional regularity properties. Moreover, the boundary condition notations is associated with these spaces. To start, we give the definition of weak derivatives which are significant in the theory of Sobolev spaces [42]:

Definition 2.1.3 (Weak Derivative)**.** *Let $u \in L^1_{\boldsymbol{loc}}(\Omega)$ and $n \in \mathbb{N}_0^d$, where d is the space dimension. Then the weak derivative $\partial^n u$ is defined*

$$\int_\Omega \partial^n uv = (-1)^{|n|} \int_\Omega \frac{d^n v}{dx^n} u, \qquad \forall v \in C_c^\infty(\Omega).$$

The standard Sobolev space H^α for $\alpha \geqslant 0$ and $u \in L^2(\Omega)$ is given as

$$H^\alpha(\Omega) := \{u \in L^2(\Omega) : \|u\|_{H^\alpha(\Omega)} < \infty\}$$

where

$$\|u\|_{H^\alpha}(\Omega) := \left\{ \sum_{|k|_1 \leqslant \alpha} \|\partial^k u\|^2_{L^2(\Omega)} + \sum_{|k|_1=\alpha} \int_\Omega \int_\Omega \frac{|\partial^k u(x) - \partial^k u(y)|}{|x-y|^{d+2(\alpha-\lfloor\alpha\rfloor)}} dxdy \right\}^{\frac{1}{2}}.$$

2.1.3 Basic concepts of finite element spaces

In this section we define the finite element space which we mainly use in the next chapters, the H^1 conforming spaces.

Definition 2.1.4 (H^1-Conforming Finite Element Spaces)**.** *The H^1-conforming finite elements that are often called continuous Galerkin finite elements provide continuity across cell boundaries.*

All the basic notions to construct meshes, approximation spaces, and introducing the shape functions as the basis for the polynomial space can be found in [43, 42, 44, 45, 46, 11].

2.2 Stokes model problem and basic assumptions

Let $\Omega \in \mathbb{R}^2$ be an open and connected domain with smooth boundary Γ such that it satisfies a Lipschitz condition. $u(\mathrm{x})$ is the velocity and $\varrho(\mathrm{x})$ be the pressure of the fluid at some point $\mathrm{x} \in \Omega$, respectively. Given body force $f \in L^2(\Omega)^2$ and the constant viscosity parameter $\nu > 0$, consider stationary incompressible fluid flows as our model problem: For the Stokes equations as described below we are interested in finding $u : \Omega \to \mathbb{R}^2$ and $\varrho : \Omega \to \mathbb{R}$ such that

$$\begin{aligned} -\nu\Delta u + \nabla\varrho &= f \qquad \text{in} \quad \Omega, \\ -\nabla \cdot u &= 0 \qquad \text{in} \quad \Omega, \\ u &= 0 \qquad \text{on} \quad \Gamma. \end{aligned} \tag{2.1}$$

Since similar results are valid for other type of boundary conditions, here we made the choice of homogeneous boundary condition for the ease of presentation. As shown here, we impose the *no slip* boundary condition on the velocity field, and to ensure uniqueness of solution, we apply the *vanishing mean* for pressure field such that $\int_\Omega \varrho = 0$. Because the solution of Stokes, namely

the velocity and pressure have different regularity properties, we will approximate them in two different finite element spaces.

We denote the standard Sobolev spaces by $H^m(\Omega)$ for $m \in \mathbb{N}_0$. In particular, the norm and the scalar product of $L^2(\Omega) = H^0(\Omega)$ are denoted by $\|\cdot\|_\Omega$ and $(\cdot,\cdot)_\Omega$, respectively. To account for homogeneous Dirichlet boundary conditions, we set

$$H_0^1(\Omega) := \{v \in H^1(\Omega) : \varphi = 0 \text{ on } \Gamma\}.$$

Further, we denote the space containing all functions from $L^2(\Omega)$ with zero mean value by

$$L_0^2(\Omega) := \{v \in L^2(\Omega) : (\varphi, 1)_\Omega = 0\}$$

and define

$$\mathcal{H}(\Omega) := H_0^1(\Omega)^2 \times L_0^2(\Omega).$$

Then, we introduce the bilinear form $\mathcal{L} : \mathcal{H}(\Omega) \times \mathcal{H}(\Omega) \to \mathbb{R}$ by

$$\mathcal{L}([u,\varrho];[v,q]) := (\nu\nabla u, \nabla v)_\Omega - (\varrho, \nabla\cdot v)_\Omega - (\nabla\cdot u, q)_\Omega. \tag{2.2}$$

The standard weak formulation of problem (2.1) is: Seek $[u,\varrho] \in \mathcal{H}$ such that

$$\mathcal{L}([u,\varrho];[v,q]) = (f,v)_\Omega \qquad \forall [v,q] \in \mathcal{H}(\Omega). \tag{2.3}$$

Due to the continuous $\inf$-$\sup$ condition

$$\inf_{[u,\varrho]\in\mathcal{H}} \sup_{[v,q]\in\mathcal{H}} \frac{\mathcal{L}([u,\varrho];[v,q])}{(\|\nabla u\|_\Omega + \|\varrho\|_\Omega)\,(\|\nabla v\|_\Omega + \|q\|_\Omega)} \geq \kappa > 0,$$

where κ is the $\inf$-$\sup$ constant depending only on Ω, the weak problem is well-posed and has a unique solution, see [47] and [48] for more details on the solution of the Stokes equations. Now,

assume $\mathcal{T} = \{K\}$ is a triangulation of domain Ω. For each element K, we associate an element map $T_K : \hat{K} \to K$ where $K \in \mathcal{T}$ is the image of the reference element $\hat{K}$ where $\hat{K} = [0,1]^2$. Further, we define the mesh size vector $h := (h_K)_{K\in\mathcal{T}}$, where $h_K := \operatorname{diam}(K)$. With each element $K \in \mathcal{T}$, we associate a polynomial degree $p_K \in \mathbb{N}$ and collect them in a polynomial degree vector $p := (p_K)_{K\in\mathcal{T}}$. Throughout this work, we assume that the discretization $(\mathcal{T}, p)$ of Ω is (γ_h, γ_p)-regular [11].

Definition 2.2.1 ((γ_h, γ_p)-Regularity)**.** *A sequence of meshes $(\mathcal{T}, p)$ is called (γ_h, γ_p)-regular if and only if there exist constants $\gamma_h, \gamma_p > 0$ such that for all $K, K' \in \mathcal{T}$ with $K \cap K' \neq \emptyset$ it holds*

$$\gamma_h^{-1} h_K \leq h_{K'} \leq \gamma_h h_K \tag{2.4}$$

and

$$\gamma_p^{-1} p_K \leq p'_K \leq \gamma_p p_K. \tag{2.5}$$

The aforementioned regularity implies the element sizes and also the polynomial degrees of neighboring elements are comparable for every mesh in the sequence.

To define the discrete solution space, for arbitrary element $K \in \mathcal{T}$ we denote $\mathcal{F}(K)$ as the set of all interior faces of cell K. Then, $h_f := \operatorname{diam}(f)$ is the diameter of face $f \in \mathcal{F}(\mathcal{K})$ and its polynomial degree p_f is given by $p_f := \min\{p_K, p_{K'}\}$ for $K, K' \in \mathcal{T}$ with $f = K \cap K'$. Further, the problem is discretized by the standard (p_k, p_{k-1}) Taylor-Hood finite element. The corresponding spaces for velocity and pressure are as follows,

$$V_u^p(\mathcal{T})^2 := \left\{ u \in H_0^1(\Omega)^2 : \;\; u|_K \circ T_K \in \mathcal{Q}_{p_K}^2\left(\hat{K}\right) \text{ for all } K \in \mathcal{T} \right\}, \tag{2.6}$$

and

$$V_\varrho^p(\mathcal{T}) := \left\{ \varrho \in L_0^2(\Omega) : \;\; \varrho|_K \circ T_K \in \mathcal{Q}_{p_K-1}\left(\hat{K}\right) \text{ for all } K \in \mathcal{T} \right\}. \tag{2.7}$$

Here, $\mathcal{Q}_r$ is the tensor-product polynomial space of complete degree at most $r \in \mathbb{N}_0$ defined on

the quadrilateral reference cell $\hat{K}$,

$$Q_r = \text{span}\Big\{ \prod_{i=1}^{2} x_i^j, 0 \leq j \leq r \Big\}. \tag{2.8}$$

To simplify notations, we set

$$\mathcal{V}^p(\mathcal{T}) := V_u^p(\mathcal{T})^2 \times V_\varrho^p(\mathcal{T}) \subseteq \mathcal{H}(\Omega). \tag{2.9}$$

Then, the discrete approximation to (2.3) consists of seeking $[u_{\text{FE}}, \varrho_{\text{FE}}] \in \mathcal{V}^p(\mathcal{T})$ such that

$$\mathcal{L}\left([u_{\text{FE}}, \varrho_{\text{FE}}]\,; [v_{\text{FE}}, q_{\text{FE}}]\right) = \left(f, v_{\text{FE}}\right)_\Omega \qquad \forall\, [v_{\text{FE}}, q_{\text{FE}}] \in \mathcal{V}^p(\mathcal{T}). \tag{2.10}$$

From [49], due to using stable Taylor-Hood finite elements, the discrete space satisfies the Babuska-Brezzi condition, which implies that the following discrete $\inf$-$\sup$ inequality holds

$$\inf_{[u_h, \varrho_h] \in \mathcal{H}} \sup_{[v_h, q_h] \in \mathcal{H}} \frac{\mathcal{L}([u_h, \varrho_h]; [v_h, q_h])}{\left(\|\nabla u_h\| + \|\varrho_h\|\right)\left(\|\nabla v_h\| + \|q_h\|\right)} \geq \kappa_d > 0,$$

where the constant κ_d is independent of cell size h and polynomial degree p. It also can be shown that the following Galerkin orthogonality holds:

Lemma 2.2.2 (Galerkin Orthogonality)**.** *Let $[u, \varrho] \in \mathcal{H}$ be the solution of (2.3) and $[u_{FE}, \varrho_{FE}] \in \mathcal{V}^p(\mathcal{T})$ be the solution of (2.10). Then, the following holds*

$$\mathcal{L}\left([u - u_{FE}, \varrho - \varrho_{FE}]\,; [v_{FE}, q_{FE}]\right) = 0 \qquad \forall\, [v_{FE}, q_{FE}] \in \mathcal{V}^p(\mathcal{T}). \tag{2.11}$$

2.2.1 Interpolation

The approximability property or the the interpolation capability of the finite elements is one of the main factors in the efficiency of the finite element method. In this section we discuss some interpolation operators used in the analysis of our h and hp- adaptive finite element method. Essen-

tially, the interpolation operators map the continuous space, in our application the H^1-conforming, into the corresponding space of continuous Galerkin finite elements. The different mapping methods between the continuous and the discrete space produce different interpolation methods. In some situations that functions are not regular enough to be in the domain of nodal-based or the Lagrange interpolation operator, the local averaging operators such as Clément or Scott-Zhang type of interpolation operators introduced [50, 51] are applicable; for example when interpolating discontinuous functions in $H^1(\Omega)$ or $L^2(\Omega)$-conforming for $\Omega \in \mathbb{R}^d,\ d \geqslant 2$. Moreover, in [52, 53] the projection-based interpolations introduced, where some local minimization problems are solved to evaluate the function in degrees of freedom. In our work, we limit ourself to just the H^1-conforming interpolation operators.

2.2.1.1 H^1-conforming finite element interpolation

A Clément-type interpolation is a H^1-conforming interpolation operator which replaces the point evaluation of the interpolated function by some local average [50]. This procedure does not require the extra regularity of the point evaluation, and is consequently well-defined for functions from the space $H^1(\Omega)$. In [51], this interpolation operator was modified in such a way that it also preserves polynomial boundary conditions. In [54], Melenk extended this H^1-conforming interpolation to the context of hp-adaptive finite element spaces. In our definition of hp-Clément interpolation operators, we consider $\mathcal{T}$ as a (γ_h, γ_p)-regular triangulation of $\mathbb{R}^{\mathrm{d}}$, such that $\mathcal{T}|_\Omega$ is a triangulation of Ω. Moreover, we require our triangulation be compatible with the Dirichlet boundary Γ_D, so that we can represent the collection of all faces of $\mathcal{T}$ as $\cup_{K\in\mathcal{T}}\partial K \cap \bar{\Gamma}_D$. For some arbitrary cell $K \in \mathcal{T}$ and for all faces $f \in \mathcal{F}(K)$ we define the patch sets

$$\omega_K := \bigcup \{K \cup L \in \mathcal{T} : K \text{ and } L \text{ share a common edge}\}, \tag{2.12}$$

$$\omega_f := \bigcup \{\tilde{K} \cup K \in \mathcal{T};\ \text{such that}\, K \cap \tilde{K} = f; \text{where } f \text{ is a face of } K\}. \tag{2.13}$$

The following result from [2], gives us an estimate for the interpolation error in terms of the gradient of the interpolated function.

Theorem 2.2.3 (H^1-Conforming Interpolation)**.** *Let $\mathcal{T}$ be (γ_h, γ_p)-regular sequence of meshes and $K \in \mathcal{T}$ be arbitrary. Then, there exists a bounded linear operator $\Pi^{hp} : H_0^1(\Omega)^2 \to \mathcal{V}^p(\mathcal{T})$, and a constant $C > 0$ independent of mesh size h and polynomial degree p such that,*

$$\left\|u - \Pi^{hp} u\right\|_K \leq C \frac{h_K}{p_K} \|\nabla u\|_{\omega_K} \tag{2.14}$$

and

$$\left\|u - \Pi^{hp} u\right\|_f \leq C \sqrt{\frac{h_f}{p_f}} \|\nabla u\|_{\omega_f} \tag{2.15}$$

for all $u \in H_0^1(\Omega)$ and all $f \in \mathcal{F}(K)$.

Proof. Following the lines of [11], one can find proofs for 2D in [54, Theorem 3.3], and for 3D in [55, Theorem 2]. □

Remark 2.2.4. *If the polynomial degrees are fixed, then the above results on H^1-conforming finite elements stay valid for the h-adaptive finite element, as well.*

2.2.2 Auxiliary notations and results

We provide some auxiliary results that we use later in this work. Now, we want to present some polynomial smoothing estimates, which are widely used in the error estimator analysis of many numerical methods for partial differential equations and integral equations [56, 2]. Here we require them in proving the upper and the lower bounds of our error estimator.

We define the smoothing weight functions $\Phi_K : K \subset \mathbb{R}^2 \to \mathbb{R}^+$ and $\Phi_{\omega_f} : \omega_f \subset \mathbb{R}^2 \to \mathbb{R}^+$ by

$$\Phi_K(x) := \frac{1}{h_K} \operatorname{dist}(x, \partial K) \tag{2.16}$$

and

$$\Phi_{\omega_f}(x) := \frac{1}{\operatorname{diam}(\omega_f)} \operatorname{dist}(x, \partial \omega_f), \tag{2.17}$$

Lemma 2.2.5. *Let $\delta \in [0, 1]$, $a, b \in \mathbb{R}$ such that $-1 \leq a \leq b$, and consider Φ_K as the smoothing function given in (2.16). Then, for any $\pi_p \in \mathcal{Q}_p(K)$, there exists some constant $C > 0$ independent*

of mesh size vector h and polynomial vector $p \in \mathbb{N}$ such that

$$\|\pi_p \left(\Phi_K\right)^a \|_{L^2(K)} \leq C(a,b) p^{(b-a)} \|\pi_p \left(\Phi_K\right)^b \|_{L^2(K)} \tag{2.18}$$

and

$$\|\nabla \pi_p \left(\Phi_K\right)^\delta \|_{L^2(K)} \leq \frac{C(\delta) p^{(2-\delta)}}{h_K} \|\pi_p \left(\Phi_K\right)^{\frac{\delta}{2}} \|_{L^2(K)} \tag{2.19}$$

Proof. The proofs of these estimates for one-dimensional case on the reference cell $\hat{K}$ are given in [56, Lemmas 4, 5]. Following the lines of [2, Lemma 2.5], applying a map from reference cell $\hat{K}$ to the cell K, and using (γ_h, γ_p)-regularity assumptions (2.4) and (2.5) we find the desired results for the two and three dimension cases. □

The next lemma gives some results for the extension of a polynomial from an edge to a domain. These estimates are used in the efficiency analysis of our error estimator.

Lemma 2.2.6. *Let $f \in \partial K$ be a face of cell $K \in \mathcal{T}$, Φ_{ω_f} be the smoothing function from (2.17) and $\alpha \in \left(\frac{1}{2}, 1\right)$. Then, for any $\pi_{p_f} \in \mathcal{Q}_p(f)$ from (2.8) and every $\delta \in (0,1]$, there exists some extension $v_f \in H_0^1(\omega_f)$ and constants $C_{tr} > 0$ and $C_{inv} > 0$ independent of mesh size vector h, and polynomial degree vector $p \in \mathbb{N}$ such that:*

(i) $v|_f = \pi_p \Phi_f^\alpha$;

(ii) $\|v_f\|_{\omega_f}^2 \leq C_{tr} \frac{h_f}{p^2} \|\pi_p \Phi_f^\alpha\|_f^2$;

(iii) $\|\nabla v_f\|_{\omega_f}^2 \leq C_{inv} \frac{(p^{2(2-\alpha)} + \delta^{-1})}{h_f} \left\|\pi_p \phi_f^\alpha\right\|_f^2$

Proof. See [2, Lemma 2.6]. □

3. A RESIDUAL BASED A POSTERIORI ERROR ESTIMATOR IN HP-AFEM FOR THE STOKES EQUATION

3.1 Introduction

h-adaptive finite element methods in which the mesh size is adjusted to resolve features of the solution, have been known to be efficient tools for solving partial differential equations since the late 1970s [7, 8]. The development of practical and efficient estimators of the local error over the past 25 years [57, 30, 15] has made them a standard tool in the finite element analysis of many equations.

On the other hand, the p or hp versions of adaptive finite element methods – in which one adjusts either the polynomial degree of the approximation on every cell, or both the polynomial degree and the mesh size – has seen much less practical attention. Originally, introduced in [10, 9, 58], it is known that the hp-adaptive FEM can achieve exponential rates of convergence with respect to the number of degrees of freedom [59, 60, 14, 12, 13, 11]. However, it is technically much more complicated to derive reliable and efficient estimates of the error for hp approximations. Furthermore, even if estimates for the error on each cell are available, one is faced with the decision whether increasing the polynomial degree p of the approximation or reducing the mesh size h is more likely to reduce the error, measured with regard to the computational cost of the two possible resulting meshes (e.g., see [20, 21, 18, 16, 22, 19, 17]). Finally, the implementation of algorithms and data structures for conforming hp finite element methods is complex in practice [61].

Because of these difficulties, much less is known about efficient ways to derive hp adaptive finite element methods. Moreover, despite its known superiority in terms of computational efficiency, its practical impact has not been add profound as h-adaptive refinements. In particular, published theoretical considerations of error estimates and optimality of refinement strategies are largely confined to the Laplace equation.

In this contribution, we advance the state of the art by deriving residual-based a posteriori estimates for conforming hp discretization of the Stokes equation. This work is inspired by previous work for the Laplace equation [21, 62, 2]. However, it has to address the key difficulty of the Stokes equation that the solution is not the unconstrained minimizer of an energy. Therefore, the Stokes operator is not positive definite, so that working with it is not as straightforward as for example the elliptic operators with their implied coercivity condition.

In particular, we present the following results:

- We derive estimates for the error between the finite-dimensional hp approximation and the continuous solution of the Stokes equation.

- As in similar approaches for the Laplace equation, it is not easily possible to show that these estimates are reliable and efficient, i.e., that the true error is bounded from above and below by our estimator up to a constant that does not depend on h or p. This is so because the inverse estimates that are used to derive reliability and efficiency statements typically involve the polynomial degree p. To overcome this deficiency, we instead introduce a whole *family* of estimates η_α parameterized by an index $\alpha \in [0, 1]$. For a fixed α, we can not show that an estimator is both efficient and reliable; on the other hand, we can show that for some members of this family, either one or the other property hold. We demonstrate through numerical experiments that the estimator η_0 is, in practice, both reliable and efficient.

- Based on the idea proposed for 1D problems in [23], we devise a strategy to mark cells for either h or p refinement based on criteria for a systematic reduction of the error.

- Although we make no claims about the optimality of this strategy – i.e., we can not prove that among all strategies it leads to the greatest error reduction – we show numerical results that suggest that the strategy can achieve the desired exponential convergence rate for the hp-adaptive refinement.

To the best of our knowledge, none of these properties have previously been derived or demonstrated for the Stokes equation using continuous hp- adaptive finite element method.

3.1.1 Outline

The remainder of this chapter is organized as follows. First in section 3.2 the required definitions and corresponding literature review on the error estimator is given. Residual-based a posteriori error estimator and its analysis on the proof of reliability and efficiency is presented in 3.2.3. The hp-adaptive refinement algorithm and the related discussion on h- or p-marking criterion is given in section 3.3. Finally section 3.4 contains the numerical results to illustrate the performance of our hp-estimator.

3.2 Error estimation

3.2.1 A priori error estimation

Since the inception of theoretical study of finite element methods in the late 1960's and early 1970's a priori estimators have been studied and established for a wide range of problems and methods. A priori error estimates give estimation of the finite element error in terms of the unknown solution u and the mesh parameter h or p. A very standard information that one can get from a priori error estimates is the expected convergence rate for solutions that are regular enough on a smooth domain, for example

$$\|u - u_h\|_{H_0^1(\Omega)} \leqslant C\, h^r |u|_{H^{r+1}(\Omega)}.$$

3.2.2 A posteriori error estimation

The idea behind a posteriori error estimation is to assess the error between the exact solution, in our case for the Stokes problem, $[u, \varrho] \in \mathcal{H}$ and its finite element approximation $[u_{\text{FE}}, \varrho_{\text{FE}}] \in \mathcal{V}^p(\mathcal{T})$ only in terms of known quantities [63, 46, 64], such as problem data, the approximate solution, mesh, and the finite element space. As an early study of a posteriori error estimation we can mention to the work by Babuska and Rheinboldt [7]. Many innovations and improvements occurred in this regard over the years. Meanwhile, the adaptivity based on the a posteriori error estimation was developed by Babuska and Vogelius [65], where they provided a convergence analysis of adaptive

FEM for one-dimensional problems. The article by Dörfler in 1996 [23] was one of the major works by that time to reveal and present the most critical ideas for the rigorous study of adaptive finite element method. In 2004, Binev, Dahmen, and Devore [26], starting from ideas of nonlinear approximation theory, provide a very fundamental notion on the concept of optimality in adaptive finite element method. There is a variety of methods proposed to a posteriori estimating of the energy error. Here we name the most frequent useful ones. Explicit estimators [66, 67, 68], only require the evaluation of an explicit formula involving the approximate solution. Another type of a posteriori error estimator is the implicit error estimators [69, 70, 7] that require some auxiliary boundary value problems be solved. To formulate the equilibrated a posteriori error estimators we need to solve the adjoint of the problem [71, 72]. These are the major types of a posteriori error estimators for the energy error. Of course for the case that some specific physical quantity is of interest, then one can estimate and refine based on those quantities of interest, not just the energy error [36, 73, 74, 33]. It should be noted that all a posteriori error estimators can be formulated for the hp-adaptive refinement methods. However, for our hp-AFEM algorithm we stick with the explicit hp-residual based a posteriori error estimation.

Definition 3.2.1 (A Posteriori Error Estimator)**.** *A functional $\eta\left(u_{FE}, \varrho_{FE}, f\right)$ is called an a posteriori error estimator for the Stokes equation, if and only if there exists a constant $C > 0$ such that*

$$\|\nabla\left(u - u_{FE}\right)\|_{\Omega} + \|\varrho - \varrho_{FE}\|_{\Omega} \leq C\eta\left(u_{FE}, \varrho_{FE}, f\right). \tag{3.1}$$

Furthermore, if $\eta\left(u_{FE}, \varrho_{FE}, f\right)$ can be decomposed into localized quantities $\eta_K\left(u_{FE}, \varrho_{FE}, f\right)$, $K \in \mathcal{T}$, such that

$$\eta(u_{FE}, \varrho_{FE}, f)^2 = \sum_{K \in \mathcal{T}} \eta_K\left(u_{FE}, \varrho_{FE}, f\right)^2, \tag{3.2}$$

then $\eta_K\left(u_{FE}, \varrho_{FE}, f\right)$ is called local error indicator.

Estimate (3.1) is usually called a reliability estimate, since it guarantees that the error of the finite element approximation $[u_{\mathrm{FE}}, \varrho_{\mathrm{FE}}]$ in the natural energy norm is controlled by the error estimator $\eta\left(u_{\mathrm{FE}}, \varrho_{\mathrm{FE}}, f\right)$ up to a constant independent of mesh size h and polynomial degree p. Further,

the local error indicators $\eta_K\left(u_{\text{FE}}, \varrho_{\text{FE}}, f\right)$ given in identity (3.2) provide the most important tool for adaptive mesh refinement by identifying those cells $K \in \mathcal{T}$ where the error is large and consequently, the mesh has to be refined locally. This procedure can be repeated several times until the error estimator $\eta\left(u_{\text{FE}}, \varrho_{\text{FE}}, f\right)$ is smaller than a prescribed tolerance.

Obviously, computational efficiency requires that the local error estimators also satisfy some efficiency property guaranteeing that the upper bound (3.1) is sharp enough and does not overestimate the true error. To this end, we would like to derive a local lower bound for the energy error

$$\eta_K\left(u_{\text{FE}}, \varrho_{\text{FE}}, f\right) \leq C\left(\left\|\nabla\left(u-u_{\text{FE}}\right)\right\|_{\omega_K}+\left\|\varrho-\varrho_{\text{FE}}\right\|_{\omega_K}\right) \qquad \forall K \in \mathcal{T}. \tag{3.3}$$

The *Effectivity Index* is a tool to show the quality of the proposed error estimator η, given as

$$\textit{Eff. Index} := \frac{\text{error estimator}}{\text{energy error}} = \frac{\eta\left(u_{\text{FE}}, \varrho_{\text{FE}}, f\right)}{\left\|\nabla\left(u-u_{\text{FE}}\right)\right\|_{\Omega}+\left\|\varrho-\varrho_{\text{FE}}\right\|_{\Omega}}. \tag{3.4}$$

Ideally we want to have *Eff. Index* $= 1$, however in practice will only happen as *Eff. Index* $\longrightarrow 1$, while $h \longrightarrow 0$. Other error estimators guarantee that $C_1 \leqslant$ *Eff. Index* $\leqslant C_2$ for some $C_1, C_2 > 0$.

3.2.3 Residual-based a posteriori error estimator and error analysis

In this section, we define a residual-based a posteriori error estimator for the Stokes problem (2.1) and derive upper and lower bounds for this error estimator in terms of the energy error of the approximated solution. Following the steps of [2], we define a family of error estimators η_α for $\alpha \in [0,1]$. In the analysis of hp a posteriori error estimator, neither an upper nor a lower bound can be proved for any fixed $\alpha \in [0,1]$. As given in identity (3.2), the a posteriori error estimator η_α shall be the sum of local error indicators $\eta_{\alpha,K}$:

$$\eta_\alpha^2 := \sum_{K \in \mathcal{T}} \eta_{\alpha;K}^2$$

for $\alpha \in [0,1]$. The local error indicator $\eta_{\alpha;K}$ can be decomposed into a cell and interface contribution:

$$\eta_{\alpha;K}^2 := \eta_{\alpha;K;R}^2 + \eta_{\alpha;K;B}^2, \tag{3.5}$$

where $\eta_{\alpha;K;R}$ denotes the residual-based term and $\eta_{\alpha;K;B}$ indicates the jump-based term. These terms are defined as

$$\eta_{\alpha;K;R}^2 := \frac{h_K^2}{p_K^2} \left\| \left(I_{p_K}^K f + \nu \Delta u_{\mathrm{FE}} - \nabla \varrho_{\mathrm{FE}} \right) \Phi_K^{\frac{\alpha}{2}} \right\|_K^2 + \left\| \left(\nabla \cdot u_{\mathrm{FE}} \right) \Phi_K^{\frac{\alpha}{2}} \right\|_K^2 \tag{3.6}$$

where $I_{p_K}^K f$ denotes the local L^2-projection of f into the space of piecewise vector-valued polynomials of degree less or equal than p_K, and

$$\eta_{\alpha;K;B}^2 := \sum_{f \in \mathcal{F}(\mathcal{K})} \frac{h_f}{2p_f} \left\| \left[\nu \frac{\partial u_{\mathrm{FE}}}{\partial n_K} \right] \Phi_{\omega_f}^{\frac{\alpha}{2}} \right\|_f^2. \tag{3.7}$$

Here h_f, is the length of face f and for every two cells K, K' which share face f, let $p_f := \min(p_K, p_{K'})$. The $[\cdot]$ notation is the jump across the edge and n_K is the outward pointing unit normal vector of cell K for each face f. The interface contribution of error estimator in (3.7) is the summation over all faces of K that are not on the domain boundary $\partial\Omega$. Now, let us begin with the error analysis of the a posteriori error estimator η_α. First, we derive an upper bound for the energy error, that is the reliability estimate.

Theorem 3.2.2 (Reliability)**.** *Let $[u_{FE}, \varrho_{FE}] \in \mathcal{V}^p(\mathcal{T})$ be the solution of discrete problem (2.10) and $[u, \varrho] \in \mathcal{H}$ be solution of weak problem (2.3). Further, let $\alpha \in [0,1]$ and assume that triangulation $\mathcal{T}$ is (γ_h, γ_p)-regular. Then, there exists some constant $C_{rel} > 0$ independent of mesh size vector h and polynomial degree vector p such that*

$$\|\nabla (u - u_{FE})\|_\Omega^2 + \|\varrho - \varrho_{FE}\|_\Omega^2 \leq C_{rel} \sum_{K \in \mathcal{T}} \left(p_K^{2\alpha} \eta_{\alpha;K}^2 + \frac{h_K^2}{p_K^2} \left\| I_{p_K}^K f - f \right\|_K^2 \right).$$

Proof. Set $e_{\mathrm{FE}} := u - u_{\mathrm{FE}}$ and $\epsilon_{\mathrm{FE}} := \varrho - \varrho_{\mathrm{FE}}$. From Lemma 2.2.2, we have

$$\begin{aligned}\mathcal{L}\left([e_{\mathrm{FE}}, \epsilon_{\mathrm{FE}}]\,;[v,q]\right) &= \left(\nu\nabla e_{\mathrm{FE}}, \nabla\left(v - \Pi^{hp}v\right)\right)_\Omega - \left(\epsilon_{\mathrm{FE}}, \nabla\cdot\left(v - \Pi^{hp}v\right)\right)_\Omega \\ &\quad - \left(\nabla\cdot e_{\mathrm{FE}}, q\right)_\Omega \\ &= \sum_{K\in\mathcal{T}}\Bigg(\left(\nu\nabla e_{\mathrm{FE}}, \nabla\left(v - \Pi^{hp}v\right)\right)_K - \left(\epsilon_{\mathrm{FE}}, \nabla\cdot\left(v - \Pi^{hp}v\right)\right)_K \\ &\quad - \left(\nabla\cdot e_{\mathrm{FE}}, q\right)_K\Bigg),\end{aligned}$$

where $\Pi^{hp} : H_0^1(\Omega)^2 \to \mathcal{V}^p(\mathcal{T})$ denotes the H^1-conforming interpolation operator from Theorem 2.2.3. Using integration by parts and also the incompressibility condition $\nabla\cdot u = 0$ yields

$$\begin{aligned}\mathcal{L}\left([e_{\mathrm{FE}}, \epsilon_{\mathrm{FE}}]\,;[v,q]\right) = \sum_{K\in\mathcal{T}}\Bigg(&\left(f + \nu\Delta u_{\mathrm{FE}} - \nabla\varrho_{\mathrm{FE}}, v - \Pi^{hp}v\right)_K - \left(\nabla\cdot u_{\mathrm{FE}}, q\right)_K \\ &+ \sum_{f\in\mathcal{F}(\mathcal{K})}\left(\left[\nu\frac{\partial u_{\mathrm{FE}}}{\partial n}\right], v - \Pi^{hp}v\right)_f\Bigg)\end{aligned}$$

and by applying the continuous Cauchy-Schwarz inequality, we have

$$\begin{aligned}\mathcal{L}\left([e_{\mathrm{FE}}, \epsilon_{\mathrm{FE}}]\,;[v,q]\right) \le \sum_{K\in\mathcal{T}}\Bigg(&\left\|I_{p_K}^K f + \nu\Delta u_{\mathrm{FE}} - \nabla\varrho_{\mathrm{FE}}\right\|_K \left\|v - \Pi^{hp}v\right\|_K \\ &+ \left\|\nabla\cdot u_{\mathrm{FE}}\right\|_K \|q\|_K \quad + \left\|f - I_{p_K}^K f\right\|_K \left\|v - \Pi^{hp}v\right\|_K \\ &+ \sum_{f\in\mathcal{F}(\mathcal{K})}\left\|\left[\nu\frac{\partial u_{\mathrm{FE}}}{\partial n_K}\right]\right\|_f \left\|v - \Pi^{hp}v\right\|_f\Bigg).\end{aligned}$$

With Theorem 2.2.3, we obtain

$$\begin{aligned}\mathcal{L}\left([e_{\mathrm{FE}}, \epsilon_{\mathrm{FE}}]\,;[v,q]\right) \le C\sum_{K\in\mathcal{T}}\Bigg(&\frac{h_K}{p_K}\left\|I_{p_K}^K f + \nu\Delta u_{\mathrm{FE}} - \nabla\varrho_{\mathrm{FE}}\right\|_K \\ &+ \left\|\nabla\cdot u_{\mathrm{FE}}\right\|_K + \frac{h_K}{p_K}\left\|f - I_{p_K}^K f\right\|_K \\ &+ \sum_{f\in\mathcal{F}(\mathcal{K})}\sqrt{\frac{h_f}{p_f}}\left\|\left[\nu\frac{\partial u_{\mathrm{FE}}}{\partial n_K}\right]\right\|_f\Bigg)\left(\|\nabla v\|_{\omega_K} + \|q\|_K\right)\end{aligned}$$

and, with the discrete Cauchy-Schwarz inequality, this implies

$$\begin{aligned}\mathcal{L}\left([e_{\text{FE}}, \epsilon_{\text{FE}}]\,;[v,q]\right) &\leq C\left(\sum_{K\in\mathcal{T}}\left(\eta_{0;K}^2 + \frac{h_K^2}{p_K^2}\left\|f - I_{p_K}^K f\right\|_K^2\right)\right)^{\frac{1}{2}}\left(\|\nabla v\|_\Omega^2 + \|q\|_\Omega^2\right)^{\frac{1}{2}}\\ &\leq C\left(\sum_{K\in\mathcal{T}}\left(\eta_{0;K}^2 + \frac{h_K^2}{p_K^2}\left\|f - I_{p_K}^K f\right\|_K^2\right)\right)^{\frac{1}{2}}\left(\|\nabla v\|_\Omega^2 + \|q\|_\Omega^2\right)^{\frac{1}{2}}\end{aligned}$$

for some constant $C > 0$ independent of mesh size vector h and polynomial degree vector p. Moreover, for $(e_{\text{FE}}, \varepsilon_{\text{FE}}) \in \mathcal{H}$ we have

$$\left(\|\nabla e_{\text{FE}}\|_\Omega^2 + \|\epsilon_{\text{FE}}\|_\Omega^2\right)^{\frac{1}{2}} \leq C \sup_{[v,q]\in\mathcal{H}} \frac{\mathcal{L}\left([e_{\text{FE}}, \epsilon_{\text{FE}}]\,;[v,q]\right)}{\left(\|\nabla v\|_\Omega^2 + \|q\|_\Omega^2\right)^{\frac{1}{2}}},$$

for some constant $C > 0$. The result follows for $\alpha = 0$. Using the inverse estimates given in Lemma 2.2.5, we can bound $\eta_{0;K}$ in terms of $\eta_{\alpha;K}$ for $\alpha \in (0, 1]$ from above. Therefore, set $a := 0$ and $b := \alpha$ in Lemma 2.2.5 and we get

$$\left(\|\nabla e_{\text{FE}}\|_\Omega^2 + \|\epsilon_{\text{FE}}\|_\Omega^2\right)^{\frac{1}{2}} \leq C_{rel}\left(\sum_{K\in\mathcal{T}}\left(p_K^{2\alpha}\eta_{\alpha;K}^2 + \frac{h_K^2}{p_K^2}\left\|f - I_{p_K}^K f\right\|_K^2\right)\right)^{\frac{1}{2}}$$

which concludes the proof. □

Next, we derive an upper bound for the a posteriori error estimator $\eta_{\alpha;K}$ in terms of the energy error $\|\nabla\left(u - u_{\text{FE}}\right)\|_{\omega_K}^2 + \|\varrho - \varrho_{\text{FE}}\|_{\omega_K}^2$ defined on the patch ω_K around cell K. Therefore, we consider the residual-based term $\eta_{\alpha;K;R}$ and the jump-based term $\eta_{\alpha;K;B}$ separately and combine the derived efficiency estimates later to obtain an upper bound for the residual-based a posteriori error estimator in equation (3.5).

Note that for $\alpha = 1$, the following lemma provides a p-independent upper bound in terms of the finite element energy error for the residual part of estimator $\eta_{\alpha;K;R}$.

Lemma 3.2.3. *Let $[u, \varrho] \in \mathcal{H}$ be the solution of weak problem (2.3) and $[u_{FE}, \varrho_{FE}] \in \mathcal{V}^p(\mathcal{T})$ be the solution of the discrete problem (2.10). Further, we assume that sequence of meshes in*

triangulation $\mathcal{T}$ be (γ_h, γ_p)-regular and let $\alpha \in [0,1]$ be arbitrary. Then, there exists some constant $C > 0$ independent of the mesh size vector h and polynomial degree vector p such that

$$\eta^2_{\alpha;K;R} \leq C\Bigg(p_K^{2(1-\alpha)} \left(\nu^2 \left\| \nabla \left(u - u_{FE} \right) \right\|^2_K + \left\| \varrho - \varrho_{FE} \right\|^2_K \right) + \frac{h_K^{2+\frac{\alpha}{2}}}{p_K^{1+\alpha}} \left\| f - I^K_{p_K} f \right\|^2_K \Bigg).$$

Proof. For simplicity, we can write the residual-based term $\eta_{\alpha;K;R}$ as

$$\eta^2_{\alpha;K;R} = \eta^2_{\alpha;K;R_1} + \eta^2_{\alpha;K;R_2},$$

where $\eta_{\alpha;K;R;1}$ and $\eta_{\alpha;K;R;2}$ are defined as follows:

$$\begin{aligned} \eta^2_{\alpha;K;R_1} &:= \frac{h_K^2}{p_K^2} \left\| \left(I^K_{p_K} f + \nu \Delta u_{\text{FE}} - \nabla \varrho_{\text{FE}} \right) \Phi_K^{\frac{\alpha}{2}} \right\|^2_K, \\ \eta^2_{\alpha;K;R_2} &:= \left\| \nabla \cdot u_{\text{FE}} \Phi_K^{\frac{\alpha}{2}} \right\|^2_K. \end{aligned} \tag{3.8}$$

Using the idea in [15] and [2] to build the test functions, for $0 < \alpha \leq 1$, we define the cell residual term R_K as, $R_K := \left(I^K_{p_K} f + \nu \Delta u_{\text{FE}} - \nabla \varrho_{\text{FE}} \right) \Phi_K^{\alpha} \in H^1_0(K)$ and obtain

$$\left\| R_K \Phi_K^{-\frac{\alpha}{2}} \right\|^2_K = \left(f + \nu \Delta u_{\text{FE}} - \nabla \varrho_{\text{FE}}, R_K \right)_K + \left(I^K_{p_K} f - f, R_K \right)_K. \tag{3.9}$$

With equation (2.3) and applying integration by parts, the first term reads

$$\left(f + \nu \Delta u_{\text{FE}} - \nabla \varrho_{\text{FE}}, R_K \right)_K = \left(\nu \nabla \left(u - u_{\text{FE}} \right), \nabla R_K \right)_K - \left(\varrho - \varrho_{\text{FE}}, \nabla \cdot R_K \right)_K - \left(\nabla \cdot u, q \right)_K$$

and inserting into (3.9) and using the incompressibility condition $\nabla \cdot u = 0$, implies

$$\left\| R_K \Phi_K^{-\frac{\alpha}{2}} \right\|^2_K = \left(\nu \nabla \left(u - u_{\text{FE}} \right), \nabla R_K \right)_K - \left(\varrho - \varrho_{\text{FE}}, \nabla \cdot R_K \right)_K + \left(I^K_{p_K} f - f, R_K \right)_K.$$

Then, by using the Cauchy-Schwarz inequality, we get

$$\begin{aligned}\left\|R_K\Phi_K^{-\frac{\alpha}{2}}\right\|_K^2 \leq &\left(\nu\left\|\nabla\left(u-u_{\mathrm{FE}}\right)\right\|_K+\left\|\varrho-\varrho_{\mathrm{FE}}\right\|_K\right)\left\|\nabla R_K\right\|_K\\ &+\left\|\left(I_{p_K}^K f-f\right)\Phi_K^{\frac{\alpha}{2}}\right\|_K\left\|R_K\Phi_K^{-\frac{\alpha}{2}}\right\|_K.\end{aligned} \tag{3.10}$$

Now, let us derive an upper bound for the H^1-seminorm of R_K. Using equations (2.18) and (2.19) in Lemma 2.2.5, we can see

$$\begin{aligned}\left\|\nabla R_K\right\|_K^2 &= \left\|\nabla\left(\left(I_{p_K}^K f+\nu\Delta u_{\mathrm{FE}}-\nabla\varrho_{\mathrm{FE}}\right)\Phi_K^\alpha\right)\right\|_K^2\\ &\leq 2\left\|\nabla\left(I_{p_K}^K f+\nu\Delta u_{\mathrm{FE}}-\nabla\varrho_{\mathrm{FE}}\right)\Phi_K^\alpha\right\|_K^2\\ &\quad+2\left\|\left(I_{p_K}^K f+\nu\Delta u_{\mathrm{FE}}-\nabla\varrho_{\mathrm{FE}}\right)\Phi_K^{\alpha-1}\nabla\Phi_K\right\|_K^2\\ &\leq C\Bigg(\frac{p_K^{2(2-\alpha)}}{h_K^2}\left\|R_K\Phi_K^{-\frac{\alpha}{2}}\right\|_K^2\\ &\quad+\frac{C}{h_K^2}\left\|\left(I_{p_K}^K f+\nu\Delta u_{\mathrm{FE}}-\nabla\varrho_{\mathrm{FE}}\right)^2\Phi_K^{2(\alpha-1)}\right\|_K\Bigg),\end{aligned}$$

where $C>0$ denotes some constant independent of mesh size vector h and polynomial degree vector p. For the second term, we have to distinguish between two cases. Assuming $\alpha>\frac{1}{2}$, we set $a:=2(\alpha-1)$ and $b:=\alpha$ in Lemma 2.2.5 to get

$$\left\|\left(I_{p_K}^K f+\nu\Delta u_{\mathrm{FE}}-\nabla\varrho_{\mathrm{FE}}\right)\Phi_K^{\alpha-1}\right\|_K \leq C p_K^{1-\frac{\alpha}{2}}\left\|R_K\Phi_K^{-\frac{\alpha}{2}}\right\|_K$$

and inserting into the estimate above yields

$$\left\|\nabla R_K\right\|_K \leq C\frac{p_K^{2-\alpha}}{h_K}\left\|R_K\Phi_K^{-\frac{\alpha}{2}}\right\|_K. \tag{3.11}$$

Inequality (3.10) then reads as

$$\left\|R_K\Phi_K^{-\frac{\alpha}{2}}\right\|_K \leq C\frac{p_K^{2-\alpha}}{h_K}\left(\nu\left\|\nabla\left(u-u_{\mathrm{FE}}\right)\right\|_K+\left\|\varrho-\varrho_{\mathrm{FE}}\right\|_K\right)+h_K^{\frac{\alpha}{2}}\left\|I_{p_K}^K f-f\right\|_K,$$

and, after multiplying both sides by $\frac{h_K}{p_K}$ and using definition (3.8), we have

$$\eta_{\alpha;K;R_1} \leq C p_K^{1-\alpha}\left(\nu \left\|\nabla\left(u-u_{\text{FE}}\right)\right\|_K + \left\|\varrho-\varrho_{\text{FE}}\right\|_K\right) + \frac{h_K^{1+\frac{\alpha}{2}}}{p_K}\left\|I_{p_K}^K f - f\right\|_K. \tag{3.12}$$

Now, let us consider the case $0 \leq \alpha \leq \frac{1}{2}$. Therefore, let $\beta := \frac{1+\alpha}{2}$. Again, using the smoothing estimates given in Lemma 2.2.5 and considering the fact that $\beta > \alpha$, we find

$$\begin{aligned}\left\|R_K \Phi_K^{-\frac{\alpha}{2}}\right\|_K &\leq C p_K^{\beta-\alpha}\left\|\left(I_p^K f + \nu\Delta u_{\text{FE}} - \nabla\varrho_{\text{FE}}\right)\Phi_K^{\frac{\beta}{2}}\right\|_K \\ &= C\frac{p_K^{1+\beta-\alpha}}{h_K}\eta_{\beta;K;R_1}\end{aligned}$$

and estimate (3.12) implies

$$\begin{aligned}\left\|R_K \Phi_K^{-\frac{\alpha}{2}}\right\|_K \leq C\Bigg(&\frac{p_K^{2-\alpha}}{h_K}\left(\nu\left\|\nabla\left(u-u_{\text{FE}}\right)\right\|_K + \left\|\varrho-\varrho_{\text{FE}}\right\|_K\right) \\ &+ \frac{h_K^{\frac{\beta}{2}}}{p_K^{\alpha-\beta}}\left\|I_{p_K}^K f - f\right\|_K\Bigg).\end{aligned}$$

Then, the definition of β yields

$$\begin{aligned}\eta_{\alpha;K;R_1} \leq C\Bigg(&p_K^{1-\alpha}\left(\nu\left\|\nabla\left(u-u_{\text{FE}}\right)\right\|_K + \left\|\varrho-\varrho_{\text{FE}}\right\|_K\right) \\ &+ \frac{h_K^{\frac{5+\alpha}{4}}}{p_K^{\frac{1+\alpha}{2}}}\left\|I_{p_K}^K f - f\right\|_K\Bigg).\end{aligned} \tag{3.13}$$

To obtain the upper bound for $\eta_{\alpha;K;R_2}^2$, we observe

$$\eta_{\alpha;K;R_2} = \left\|(\nabla\cdot u_{\text{FE}})\Phi_K^{\frac{\alpha}{2}}\right\|_K \leq h_K^{\frac{\alpha}{2}}\left\|\nabla\cdot u_{\text{FE}}\right\|_K.$$

Since $\nabla\cdot u = 0$, we have $\nabla\cdot u_{\text{FE}} = \nabla\cdot\left(u-u_{\text{FE}}\right)$ and, hence,

$$\eta_{\alpha;K;R_2} \leq h_K^{\frac{\alpha}{2}}\left\|\nabla\left(u-u_{\text{FE}}\right)\right\|_K. \tag{3.14}$$

Finally, combining estimates (3.12)-(3.14) gives the desired result. □

Now, let us consider the jump-based term $\eta_{\alpha;K;B}$ from equation (3.7). In order to derive an upper bound for this term, we use the same ideas as in Lemma 3.2.3.

Lemma 3.2.4. *Let $[u, \varrho] \in \mathcal{H}$ be the solution of weak problem (2.3) and $[u_{FE}, \varrho_{FE}] \in \mathcal{V}^p(\mathcal{T})$ be the solution of discrete problem (2.10). Further, we assume that the family of triangulation $\mathcal{T}$ is (γ_h, γ_p)-regular. Then, there exists some constant $C > 0$ independent of mesh size vector h and polynomial degree vector p such that*

$$\eta^2_{\alpha;K;B} \leq C\Bigg(\frac{}{p_K^{\frac{3-\alpha}{2}}}\left(\nu^2 \left\|\nabla\left(u - u_{FE}\right)\right\|^2_{\omega_K} + \left\|\varrho - \varrho_{FE}\right\|^2_{\omega_K}\right) + \frac{h_K^2}{p_K^{\frac{3+\alpha}{2}}}\left\|I^K_{p_K} f - f\right\|^2_{\omega_K}\Bigg)$$

for all $\alpha \in [0, 1]$.

Proof. For given element $K \in \mathcal{T}$ and interior face $f \in \mathcal{F}(\mathcal{K})$, there exists some $K_1 \in \mathcal{T}$ such that $f = \partial K \cap \partial K_1$; For each face f, we then consider the face patch set ω_f given in (2.13). Moreover, by Lemma 2.2.5 there exists an extension function $R_f \in H^1_0(\omega_f)$ such that $R_f|_f = \left[\nu \frac{\partial u_{\text{FE}}}{\partial n}\right] \Phi^{\alpha}_{\omega_f}$. The unit normal vector n and the jump term $[.]$ are the same as in (3.7). R_f is continuous on K and vanishes on $\partial\omega_f$. We can extend R_f by zero to $\Omega\backslash\omega_f$ which gives us $R_f \in H^1_0(\Omega)$. Now, to derive an upper bound for the jump-based term $\eta^2_{\alpha;K;B}$, we use integration by parts to get

$$\left\|R_f \Phi^{-\frac{\alpha}{2}}_{\omega_f}\right\|^2_e = (\nu\Delta u_{\text{FE}}, R_f)_{\omega_f} + (\nu\nabla u_{\text{FE}}, \nabla R_f)_{\omega_f},$$

and, from the weak formulation (2.3), we have

$$\begin{aligned}\left\|R_f\Phi_{\omega_f}^{-\frac{\alpha}{2}}\right\|_f^2 &= (\nu\Delta u_{\text{FE}}, R_f)_{\omega_f} - (\nu\nabla\left(u-u_{\text{FE}}\right), \nabla R_f)_{\omega_f} + (f, R_f)_{\omega_f} \\ &\quad + (\varrho, \nabla\cdot R_f)_{\omega_f} + (\nabla\cdot u, R_f)_{\omega_f} \\ &= (\nu\Delta u_{\text{FE}}, R_f)_{\omega_f} - (\nu\nabla\left(u-u_{\text{FE}}\right), \nabla R_f)_{\omega_f} + (f, R_f)_{\omega_f} \\ &\quad + (\varrho_{\text{FE}}, \nabla\cdot R_f)_{\omega_f} + (\varrho-\varrho_{\text{FE}}, \nabla\cdot R_f)_{\omega_f}\end{aligned}$$

by incompressibility condition $\nabla\cdot u = 0$. Then, performing integration by parts gives

$$\begin{aligned}\left\|R_f\Phi_{\omega_f}^{-\frac{\alpha}{2}}\right\|_f^2 &= \left(I_{p_K}^K f + \nu\Delta u_{\text{FE}} - \nabla\varrho_{\text{FE}}, R_f\right)_{\omega_f} - (\nu\nabla(u-u_{\text{FE}}), \nabla R_e)_{K_e} \\ &\quad + (\varrho-\varrho_{\text{FE}}, \nabla\cdot R_f)_{\omega_f} + \left(f - I_{p_K}^K f, R_f\right)_{\omega_f}\end{aligned}$$

and applying the Cauchy-Schwarz inequality yields

$$\begin{aligned}\left\|R_f\Phi_{\omega_f}^{-\frac{\alpha}{2}}\right\|_f^2 &\le \left(\left\|I_{p_K}^K f + \nu\Delta u_{\text{FE}} - \nabla\varrho_{\text{FE}}\right\|_{\omega_f} + \left\|f - I_{p_K}^K f\right\|_{\omega_f}\right)\|R_e\|_{\omega_f} \\ &\quad + \nu\left\|\nabla(u-u_{\text{FE}})\right\|_{\omega_f}\left\|\nabla R_f\right\|_{\omega_f} + \left\|\varrho-\varrho_{\text{FE}}\right\|_{\omega_f}\left\|\nabla\cdot R_e\right\|_{\omega_f}.\end{aligned} \tag{3.15}$$

Now, we have to distinguish between two cases. First, let us assume $\alpha > \frac{1}{2}$ and use Lemma 2.2.6, we obtain the following upper bounds for $\|R_f\|_{\omega_f}$ and $\|\nabla R_f\|_{\omega_f}$ on face f:

$$\begin{aligned}\|\nabla R_f\|_{\omega_f}^2 &\le C\frac{\delta p_K^{(2(2-\alpha))} + \delta^{-1}}{h_K}\left\|\left[\nu\frac{\partial u_{\text{FE}}}{\partial n}\right]\Phi_{\omega_f}^{\frac{\alpha}{2}}\right\|_f^2, \\ \|R_f\|_{\omega_f}^2 &\le C\delta h_K\left\|\left[\nu\frac{\partial u_{\text{FE}}}{\partial n}\right]\Phi_{\omega_f}^{\frac{\alpha}{2}}\right\|_f^2.\end{aligned}$$

Knowing that $\|\nabla \cdot R_f\|_{\omega_f} \leq \|\nabla R_f\|_{\omega_f}$, estimate (3.15) yields

$$\begin{aligned}\left\| \left[\nu \frac{\partial u_{\mathrm{FE}}}{\partial n} \right] \Phi_{\omega_f}^{\frac{\alpha}{2}} \right\|_f \leq & C \Bigg((\delta h_K)^{\frac{1}{2}} \left(\left\| I_{p_K}^K f + \nu \Delta u_{\mathrm{FE}} - \nabla \varrho_{\mathrm{FE}} \right\|_{\omega_f} \right. \\ & \left. + \left\| f - I_{p_K}^K f \right\|_{\omega_f} \right) \\ & + \sqrt{\frac{\delta p_K^{2(2-\alpha)} + \delta^{-1}}{h_K}} \Big(\nu \left\| \nabla \left(u - u_{\mathrm{FE}} \right) \right\|_{\omega_f} \\ & + \left\| \varrho - \varrho_{\mathrm{FE}} \right\|_{\omega_f} \Big) \Bigg)\end{aligned}$$

and it follows that

$$\begin{aligned}\left\| \left[\nu \frac{\partial u_{\mathrm{FE}}}{\partial n} \right] \Phi_{\omega_f}^{\frac{\alpha}{2}} \right\|_f \leq & C \Bigg((\delta h_K)^{\frac{1}{2}} \left(\frac{p_K^2}{h_K} \Big(\nu \left\| \nabla \left(u - u_{\mathrm{FE}} \right) \right\|_{\omega_f} \right. \right. \\ & \left. \left. + \left\| \varrho - \varrho_{\mathrm{FE}} \right\|_{\omega_f} \Big) + p_K^{\frac{1}{2}} \left\| f - I_{p_K}^K f \right\|_{\omega_f} \right) \\ & + \sqrt{\frac{\delta p_K^{2(2-\alpha)} + \delta^{-1}}{h_K}} \Big(\nu \left\| \nabla \left(u - u_{\mathrm{FE}} \right) \right\|_{\omega_f} \\ & + \left\| \varrho - \varrho_{\mathrm{FE}} \right\|_{\omega_f} \Big) \Bigg)\end{aligned}$$

with Lemma 3.2.3. By squaring both sides and summing over all edges $f \in \mathcal{F}(\mathcal{K})$, we get

$$\begin{aligned}\eta_{\alpha;K;B}^2 \leq C \Bigg(& \delta \left(p_K^3 \left(\nu^2 \left\| \nabla \left(u - u_{\mathrm{FE}} \right) \right\|_{\omega_f}^2 + \left\| \varrho - \varrho_{\mathrm{FE}} \right\|_{\omega_f}^2 \right) + h_K^2 \left\| f - I_{p_K}^K f \right\|_{\omega_f}^2 \right) \\ & + \frac{\delta p_K^{2(2-\alpha)} + \delta^{-1}}{p_K} \left(\nu^2 \left\| \nabla \left(u - u_{\mathrm{FE}} \right) \right\|_{\omega_f}^2 + \left\| \varrho - \varrho_{\mathrm{FE}} \right\|_{\omega_f}^2 \right) \Bigg)\end{aligned} \tag{3.16}$$

and setting $\delta := p_K^{-2}$ gives the desired result.

Now, let $0 \leq \alpha \leq \frac{1}{2}$. Similar to the proof of Lemma 3.2.3, we set $\beta := \frac{1+\alpha}{2}$ and apply Lemma

2.2.5 to get $\eta_{\alpha;K;B} \leq p_K^{\beta-\alpha}\eta_{\beta;K;B}$. Then, using estimate (3.16) gives

$$\eta_{\alpha;K;B}^2 \leq C\Bigg(\delta\Bigg(p_K^{\frac{\gamma-\alpha}{2}}\left(\nu^2\left\|\nabla\left(u-u_{\text{FE}}\right)\right\|_{\omega_f}^2+\left\|\varrho-\varrho_{\text{FE}}\right\|_{\omega_f}^2\right) + \frac{h_K^2}{p_K^{\frac{\alpha-1}{2}}}\left\|f-I_{p_K}^K f\right\|_{\omega_f}^2\Bigg) + \frac{\delta p_K^{2(2-\alpha)}+\delta^{-1}}{p_K^{\frac{1+\alpha}{2}}}\left(\nu^2\left\|\nabla\left(u-u_{\text{FE}}\right)\right\|_{\omega_f}^2+\left\|\varrho-\varrho_{\text{FE}}\right\|_{\omega_f}^2\right)\Bigg)$$

and setting $\delta := p_K^{-2}$ concludes the proof. □

By combining the results from Lemmas 3.2.3 and 3.2.4, we can derive an upper bound for the residual-based a posteriori error estimator η in terms of the quasi-local energy error.

Theorem 3.2.5. *Let $[u_{FE}, \varrho_{FE}] \in \mathcal{V}^p(\mathcal{T})$ be the solution of discrete problem (2.10) and $[u, \varrho] \in \mathcal{H}$ be solution of weak problem (2.3). Further, we assume that the triangulation $\mathcal{T}$ is (γ_h, γ_p)-regular and let $\alpha \in [0, 1]$ be arbitrary. Then, there exists some constant $C_{\mathit{eff}} > 0$ independent of mesh size vector h and polynomial degree vector p such that*

$$\eta_{\alpha;K}^2 \leq C_{\mathit{eff}}\Bigg(p_K^k\left(\nu^2\left\|\nabla\left(u-u_{FE}\right)\right\|_{\omega_K}^2+\left\|\varrho-\varrho_{FE}\right\|_{\omega_K}^2\right) + \frac{h_K^2}{p_K^{1+\alpha}}\left\|I_{p_K}^K f-f\right\|_{\omega_K}^2\Bigg)$$

for all $K \in \mathcal{T}$, where $k := \max\left\{2(1-\alpha), \frac{3-\alpha}{2}\right\}$.

Proof. The result follows from Definition 2.2.1 and Lemmas 3.2.3 and 3.2.4. □

3.3 hp-Adaptive refinement

The fully automatic hp-AFEM proposed here is based on the residual type estimator introduced in section 3.1, and consists of standard adaptive loops of the form

$$\text{SOLVE} \longrightarrow \text{ESTIMATE} \longrightarrow \text{MARK} \longrightarrow \text{REFINE}. \tag{3.17}$$

The procedures SOLVE and REFINE are essentially the same in all AFEM algorithms. Therefore, the distinction between different adaptive approaches comes from the procedures ESTIMATE and MARK. Our automatic hp-AFEM strategy follows from [55, 21].

In Section 3, a reliable and efficient residual based a posteriori error estimator has been developed. Module ESTIMATE computes the accuracy of the finite element solution obtained from module SOLVE. In order to enhance the finite element space, a local procedure called adaptive refinement is applied. In module estimate, in order to compare the error estimations for each cell K we apply h and p-refinement and then we calculate the error estimate for both refinements. In h-adaptive refinement, we use equal size bisection in each coordinate direction. Through this procedure we need to make sure that no new hanging nodes appear at the edge of the refined cell. If the current cell already has a hanging node, we have to consider all the neighboring cells, namely patch cells ω_K around the cell K, and refine all of them. For the quadrilateral cells this refinement pattern on patch ω_K is shown in Fig. 3.1, left. Similarly, for p-refinement we want to assure that no new constrained degrees of freedom are created due to enriching the polynomial degrees on the current cell K. The right graph in Fig. 3.1 shows we increase the polynomial degrees corresponding to all neighboring cells in patch ω_K. Module MARK determines which cells are the best candidates for h- or p-refinement. Unlike the pure h- or p-refinement, for the hp-refinements, the information given from ESTIMATE is not sufficient to choose the cells with the biggest error contribution to be refined. The reason comes from the fact that in hp-refinements, one also needs to determine which refinement patterns should be applied on the selected cells. Therefore, besides the error estimator given from ESTIMATE, some extra indicators have to be defined to determine the best refinement strategy on the candidate refined cells. We will develop that in the next section.

3.3.1 Convergence indicator

Let $j \in \{1, 2, \cdots, n\}$, where n indicates the number of different h and p refinement patterns, and consider $K \in \mathcal{T}_N$ be an arbitrary cell during the N-th cycle of refinement. Following the idea of [62] we define a quantity named the "convergence indicator" $k_{K,j} \in \mathbb{R}^+$ that shows the error reduction of cell K refined by refinement pattern j. For the Stokes problem similar to [57],

we establish an equivalent norm for the energy norm defined on the space $\mathcal{H}$ in domain ω_K. Let $e := u - u_{\text{FE}}$ and $E := \varrho - \varrho_{\text{FE}}$ such that $(e, E) \in \mathcal{H}$. Considering the residual of the Stokes problem on the local patch domain ω_K and the bilinear notation from (2.2), $\forall (v, q) \in \mathcal{H}$ we have:

$$\int_{\omega_K} vf - \int_{\omega_K} \nabla v : \nabla u_{\text{FE}} + \int_{\omega_K} (\nabla \cdot v)\varrho_{\text{FE}} + \int_{\omega_K} q \nabla \cdot u_{\text{FE}} = \mathcal{L}([v, q]; [e, E])_{\omega_K}.$$

Integration by parts gives:

$$\int_{\omega_K} v\left(f + \nu \Delta u_{\text{FE}} - \nabla \varrho_{\text{FE}}\right) - \int_{\omega_K} q\left(\nabla \cdot u_{\text{FE}}\right) = \mathcal{L}([v, q]; [e, E])_{\omega_K}.$$

The pair $(w_u, w_\varrho) \in \mathcal{H}$ is defined to be the Ritz projection of the residual, as follows:

$$(\nabla v, \nabla(w_u))_{\omega_K} + (q, w_\varrho)_{\omega_K} = \mathcal{L}([v, q]; [e, E])_{\omega_K}, \qquad \forall (v, q) \in \mathcal{H}. \tag{3.18}$$

The existence and uniqueness of the pair (w_u, w_ϱ) is concluded from the continuity of the operators in the definition of the bilinear form (2.2). In particular, this pair of functions can of course not be found analytically. Consequently, we approximate it by solving a discrete problem using either a finite element space with a higher polynomial degree, or a finer mesh. The energy norm of errors can be defined as

$$|||(e, E)|||^2_{\omega_K} = \|\nabla(w_u)\|^2_{\omega_K} + \|w_\varrho\|^2_{\omega_K}. \tag{3.19}$$

For cell K refined by pattern j, we combine the idea of the convergence estimator in [62] and the above discussion on the Ritz representation of the residual (3.18) and get the following definition:

$$k_{K,j} = \frac{1}{\eta_K(u_{\text{FE}}, \varrho_{\text{FE}})} \left(\left\| \nabla w_u^j \right\|^2_{\omega_K} + \left\| w_\varrho^j \right\|^2_{\omega_K} \right)^{\frac{1}{2}}. \tag{3.20}$$

The convergence estimator $k_{K,j}$ as defined in (3.20), indicates which refinement pattern $j \in \{1, 2, \cdots, n\}$ provides the biggest error reduction on every cell. In order to choose the most efficient refinement pattern, we would like to define another parameter namely the workload number

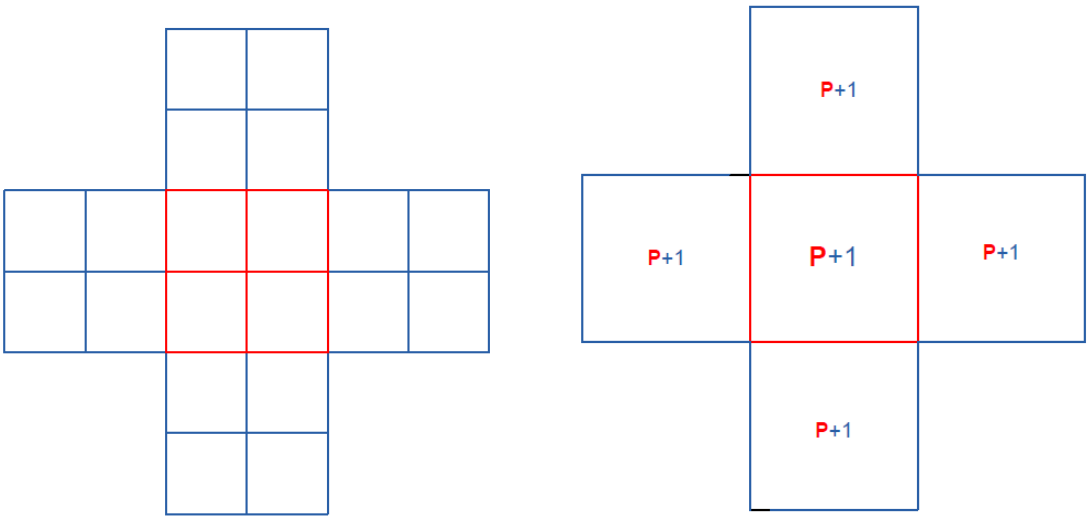

Figure 3.1: Classical h- and p-refinement in 2-dimensions for patch cells corresponding to the marked cell K shown in red.

$\varpi_{K,j} \in \mathbb{R}^+$. This parameter indicates the required work for the achieved error reduction $k_{K,j}$ on cell K. Different definitions of the workload number are possible. Here, we take it as the number of degrees of freedom in the local finite element space $\mathcal{V}^p_{K,j}(\mathcal{T}_N|_{\omega_K})$. The advantage of locally defined convergence indicators is that they can be computed in parallel. In calculating convergence indicators on the patch cells ω_K, associated with each cell K, there are number of local variational equations that can be treated as independent tasks. In such cases in our implementation using deal.II, we use the software design pattern called the WorkStream [75].

3.3.2 Marking

In our hp-adaptive finite element method, we decide between two refinement patterns, $j \in \{1, 2\}$: the classical h-refinement, where one does equal weight bisection, and the classical p-refinement, where one increases the polynomial degree on the marked cell by one. Figure 3.1 shows the graphical representation of the classical h- and p-refinement for the patch cells corresponding to marked cell K in $d = 2$.

With the aforementioned two quantities, namely the error reduction $k_{K,j}$ and the workload number $\varpi_{K,j}$, we can mark cells for h- or p-refinement by exploring a solution $(\mathcal{M}, (j_K)_{K\in\mathcal{M}})$

where $\mathcal{M} \subseteq \mathcal{T}$ comes from the following constraint setting. For every cell K we assign integer $j_K \in \{1, 2, \cdots, n\}$ such that

$$\frac{k_{K,j_K}}{\varpi_{K,j_K}} = \max_{j \in \{1,2,\cdots,n\}} \frac{k_{K,j}}{\varpi_{K,j}} \tag{3.21}$$

under the constraint

$$\sum_{K \in \mathcal{M}} k_{K,j_k}^2 \eta_K^2 \geq \theta^2 \eta^2 \tag{3.22}$$

where $\mathcal{M} \subseteq \mathcal{T}$ is a set with minimal cardinality. Before we go to the next section and discuss numerical results, it is important to mention the criterion on choosing the parameter $\theta \in (0, 1]$ in Dörfler marking in equation (3.22). Dörfler and Heuveline in [62] provided some results indicating that it might not be guaranteed that the above constraint maximization problems (3.21) and (3.22) has a solution for any chosen $\theta \in (0, 1]$. As they discussed in the section 3.6 of that paper, if the parameter θ is chosen such that it always is in the interval

$$\theta \in (0, \min_{K \in \mathcal{T}_N} k_{K,j_K}), \tag{3.23}$$

then they showed that the constraint maximization problem (3.21) is solvable.

Algorithm 1 Adaptive hp-refinement

- **Initialization**: Set N $= 0$, a coarse mesh $\mathcal{T}_0$, $\theta \in (0, 1]$ and also tolerance TOL.
- **SOLVE**: Find the solution $(u_{\text{FE}}, \varrho_{\text{FE}})$ of discrete problem (2.10).
- **ESTIMATE**: Compute a posteriori error estimation given by equation (3.5), if $\eta_K <$ TOL then STOP the algorithm.
- **MARK**: For all cells $K \in \mathcal{T}_N$ and all refinement patterns $j \in \{1, 2, \cdots, n\}$, compute the convergence estimator $k_{K,j}$ and the work-load number $\varpi_{K,j}$. Then approximate the solution of constraint maximization problem given in equations (3.21) and (3.22)
- **REFINE**: Given $(\mathcal{M}_N, (j_K)_{K \in \mathcal{M}_N})$, we refine the cells contained in set $\mathcal{M}_N$ with refinement patterns j_K corresponding to each cell. Then set $N = N + 1$ and go to step SOLVE.

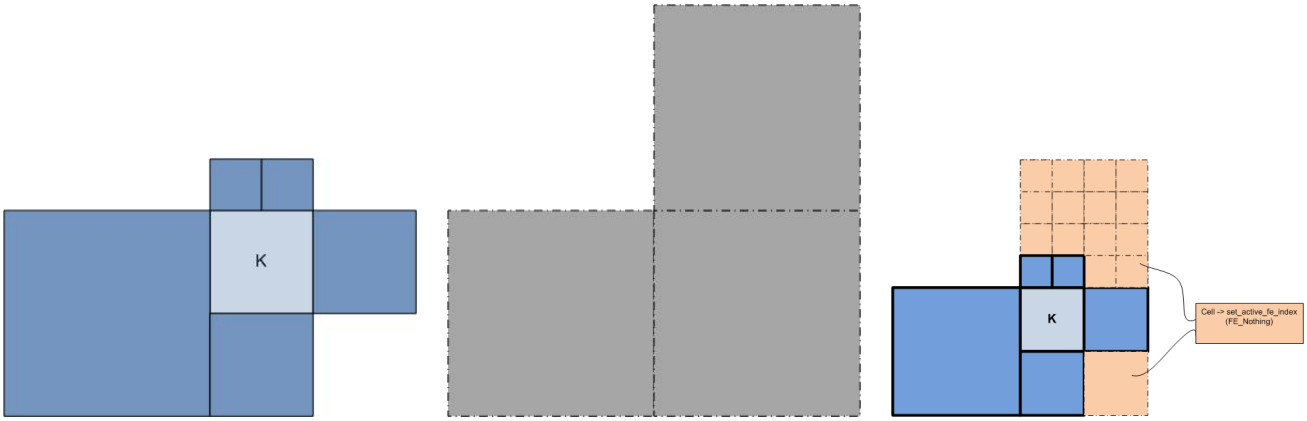

Figure 3.2: Graphical illustration of building triangulation from an irregular patch cells. (Left) patch ω_K; (Middle) extension of ω_K to the coarsest common level of refinement with no hanging node; (Right) retrieve again patch ω_K from the created triangulation as shown in blue, and assign *FE-Nothing* to the rest of this triangulation.

3.4 Numerical results

The numerical implementation is performed in the differential equation analysis library, deal.II, [76]. As presented in sections 3.3.1 and 3.3.2, in order to implement our proposed refinement strategy, for each cell K, we need to solve some local variational problems on the patch ω_K corresponding to that cell. For that reason, first of all we need to build a triangulation out of each patch. This task for the patches with no hanging node is straight forward and easy to implement. However, for the cases in which the patch cells around cell K are not at the same refinement level, we need to design an algorithm to handle this situation. Figure 3.2 graphically visualizes how we used the existing tools in the deal.II library, namely FE-Nothing and Material-Id, in order to build a triangulation for any given patch of cells.

In this section, we try to illustrate the computational performance of our hp residual-based a posteriori error estimator. In order to have an appropriate observation for the proposed estimator, within the automatic hp-adaptive refinement Algorithm 1, we consider some test cases in two dimensions. The important thing is that we want to keep track of the reduction rate in our proposed residual based estimator and demonstrate that it decreases with the same asymptotic rate as the actual error in the energy norm on a sequence of non-uniform hp-adaptive refined cells. Moreover,

Figure 3.3: Example-1, Analytical solution to the y-component of the vector valued velocity field, V_y.

the effectivity index, which is defined as the ratio of the residual a posteriori error estimator and the energy error, remains bounded around a constant number.

3.4.1 Example-1

Let $\Omega \in \mathbb{R}^2$ be L-shaped domain,

$$\Omega = (-1,1)^2 \backslash ([0,1] \times [-1,0]).$$

We enforce appropriate inhomogeneous Dirichlet boundary conditions for velocity u on Γ such that the analytical solution $u : \overline{\Omega} \to \mathbb{R}^2$ and $\varrho : \Omega \to \mathbb{R}$ are given as in [77].

$$u = \begin{bmatrix} -e^x(y\cos(y) + \sin(y)) \\ e^x y \sin(y) \end{bmatrix}, \qquad \varrho = 2e^x \sin(y) - (2(1-e)(\cos(1)-1))/3.$$

The right hand side $f(x,y)$ is set such that the Stoke equation 2.1 holds. We set the initial

Figure 3.4: Example-1. (Left) Final mesh generated after 11 hp-adaptive refinement steps (Right) Mesh generated after 7 h-adaptive refinement steps.

Table 3.1: Example 1. Number of h and p refined cells per refinement level.

refinement level	# cells	$\#h$	$\#p$
0	12	0	8
1	12	0	6
2	12	0	5
3	12	0	7
4	12	0	6
5	12	0	4
6	12	0	3
7	12	0	4
8	12	0	6
9	12	0	3
10	12	0	7
11	12	0	5

triangulation $\mathcal{T}_0$ to consist of 12 uniform cells, the initial polynomial degree $p_3 - p_2$, and $\theta = 0.75$. In order to get an idea about how the exact solution looks like, the y-component of vector valued velocity field is presented in Figure 3.3. Figure 3.4 shows the h- and hp-adaptive refined meshes with almost the same number of degrees of freedom generated using our hp and h residual based estimator. Table 3.1 presents the history of mesh and polynomial refinements in our hp-refinement algorithm. As we can see in this example, based on the marking decision algorithm described in detail in Section 3.3.2, the hp-adaptive algorithm chooses p-refinements over the h-refinement and for this example performs as adaptive p-refinement. The convergence graph in Figure 3.5a presents the decay rate in the energy error and the hp residual based a posteriori error estimator as a function of number of degrees of freedom. The graph indicates the exponential convergence rate and also shows the hp-error estimator as a sharp upper bound for the energy error which validates this as an efficient and reliable a posteriori error estimator. From Figure 3.5b we observe that the effectivity indices remains bounded between the range $5.4 \leqslant$ Eff. Indices $\leqslant 8.1$. We present the comparison between the energy norm of the error for both h- and hp-adaptive refinement in Figure 3.6. This convergence plot clearly shows the superiority of hp-AFEM over the h-AFEM. As we can observe from this plot, with the same number of degrees of freedom, the energy norm of the error using the hp-refinement is over 8 order of magnitude smaller than the energy norm of the error in the h-refinement for the same number of unknowns.

3.4.2 Example 2

In this example we consider a singular solution for Stokes problem in two dimensions in a L-shaped domain

$$\Omega := (-1, 1)^2 \backslash ([0, 1] \times [-1, 0]).$$

The exact velocity u and pressure ϱ are given in polar coordinates as in [78]:

$$u(r, \varphi) = r^{\alpha} \begin{bmatrix} \cos(\varphi)\psi^{'}(\varphi) + (1 + \alpha)\sin(\varphi)\psi(\varphi) \\ \sin(\varphi)\psi^{'}(\varphi) - (1 - \alpha)\cos(\varphi)\psi(\varphi) \end{bmatrix},$$

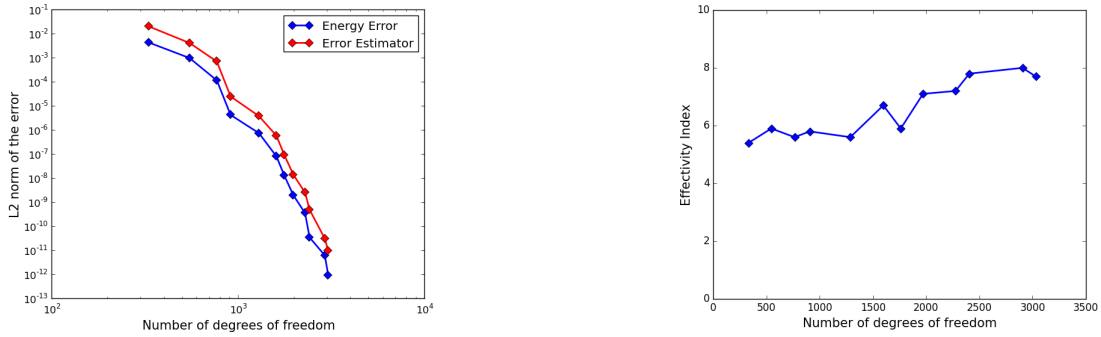

(a) (b)

Figure 3.5: Example 1. (Left) Comparison of the energy error and the error estimator, (Right) Effectivity indices.

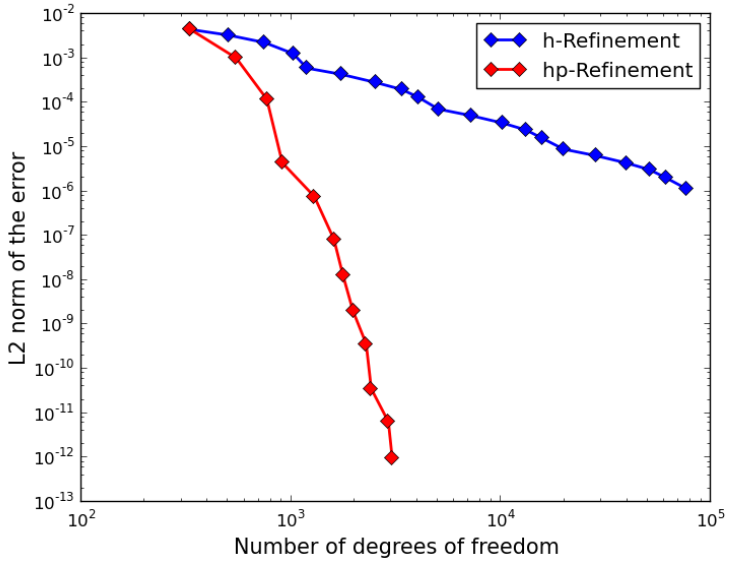

Figure 3.6: Example 1. Comparison between the actual energy error in h- and hp- adaptive mesh refinements.

and

$$\varrho(r,\varphi) = -r^{\alpha-1}\frac{(1+\alpha)^2\psi'(\varphi)+\psi'''(\phi)}{1-\alpha},$$

where $\psi(\varphi)$ is as follows:

$$\begin{aligned}\psi(\varphi) =& \frac{\sin((1+\alpha)\varphi)\cos(\alpha\omega)}{1+\alpha} - \cos((1+\alpha)\varphi) \\ & - \frac{\sin((1-\alpha)\varphi)\cos(\alpha\omega)}{1-\alpha} + \cos((1-\alpha)\varphi), \\ \omega =& \frac{3\pi}{2}.\end{aligned}$$

Here α is the smallest positive solution of

$$\sin(\alpha\omega) + \alpha\sin(\omega) = 0, \qquad \alpha \approx 0.54448373678246.$$

We set the initial triangulation $\mathcal{T}_0$ to consist of 12 uniform cells, the initial polynomial degree $p_2 - p_1$, and $\theta = 0.85$. The pressure is shown in Figure 3.7. This example is a typical test case for the Stokes problem where the solution (u, ϱ) is analytic in Ω, but the gradient of the velocity, ∇u, and the pressure ϱ itself are both singular at the re-entrant corner $(0, 0)$. In our computational results, we will see the singular behavior of the solution in the vicinity of the re-entrant corner. Figure 3.8 shows h and also the hp-adaptive refined mesh generated by our residual based estimator. As we can see the h-refinement algorithm does largely refinement around the origin and the area adjacent of this re-entrant corner. The hp-refined mesh on the other hand, shows how the algorithm performs in both capturing the singularity around the re-entrant corner by applying the h-refinement, and the polynomial enrichment happens for the cells away from the origin and the areas that the underlying solution is smooth. Table 3.2 presents the history of our hp-refinement algorithm. The comparison of the energy error and the proposed residual based a posteriori error estimator is shown in Figure 3.9a. In the right 3.9b, we can see that the effectivity indices oscillate from one hp refinement cycle to another, but these indices remain bounded around the range $1.2 \leqslant$ Eff. Indices $\leqslant 2.2$. Figure 3.10 presents the comparison between the energy norm

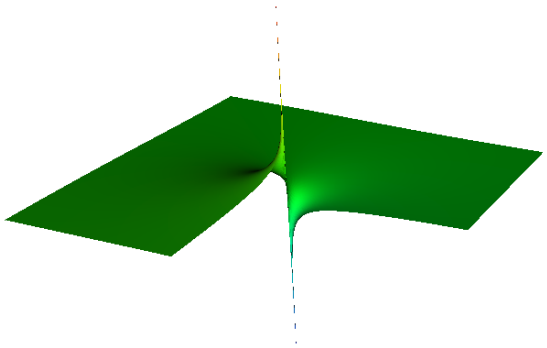

Figure 3.7: Example 2. Analytic solution corresponding to the pressure.

of the error for h- and hp-adaptive refinements.

3.4.3 Example 3

Let $\Omega = (-1, 1) \times (-1, 1)$ be a square domain and the velocity field u and pressure ϱ be given [79] by

$$u = \begin{bmatrix} 2y\cos(x^2 + y^2) \\ -2x\cos(x^2 + y^2) \end{bmatrix}, \qquad \varrho = e^{-10(x^2+y^2)} - p_m$$

where the quantity p_m is such that $\int_\Omega \varrho = 0$, and the data is computed as $f = -\Delta u + \nabla\varrho$. We set the initial triangulation $\mathcal{T}_0$ to consist of 16 uniform cells, the initial polynomial degree $p_3 - p_2$, and $\theta = 0.85$. Figure 3.11, shows the exact pressure solution. The hp and also the h-adaptive refined mesh generated by our residual based estimator is shown in Figure 3.12. Table 3.3 presents the history of our hp-refinement algorithm. As we can see due to the smoothness of solution on a regular square domain Ω, at each refinement step, the hp-adaptive refinement algorithm between h-refinement and p-enrichment chooses to increase the polynomial degree. The

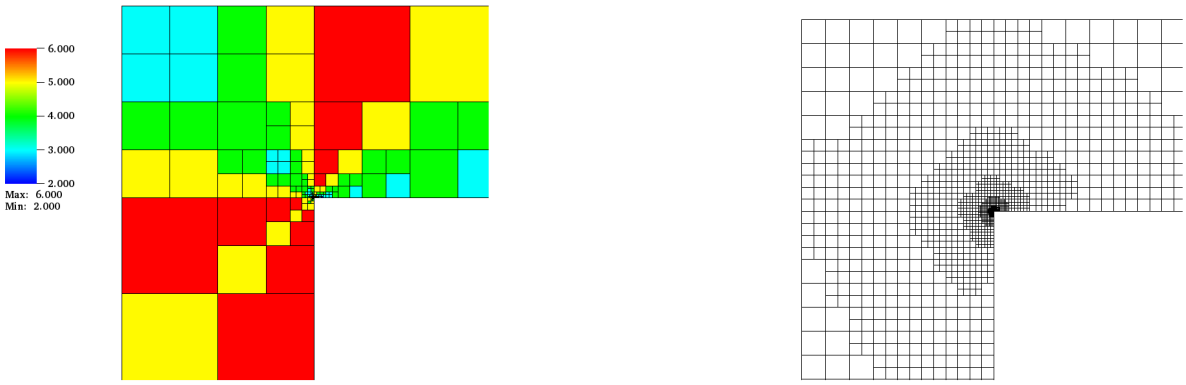

Figure 3.8: Example 2. (Left) Mesh generated after 10 hp-adaptive refinement steps; (Right) Mesh generated after 12 h-adaptive refinement steps.

Table 3.2: Example 2. Number of h and p refined cells per refinement level.

refinement level	# cells	$\#h$	$\#p$
0	12	6	2
1	30	6	7
2	48	20	25
3	108	15	31
4	153	14	21
5	195	23	33
6	264	16	42
7	312	16	15
8	360	19	32
9	417	28	39
10	501	30	12

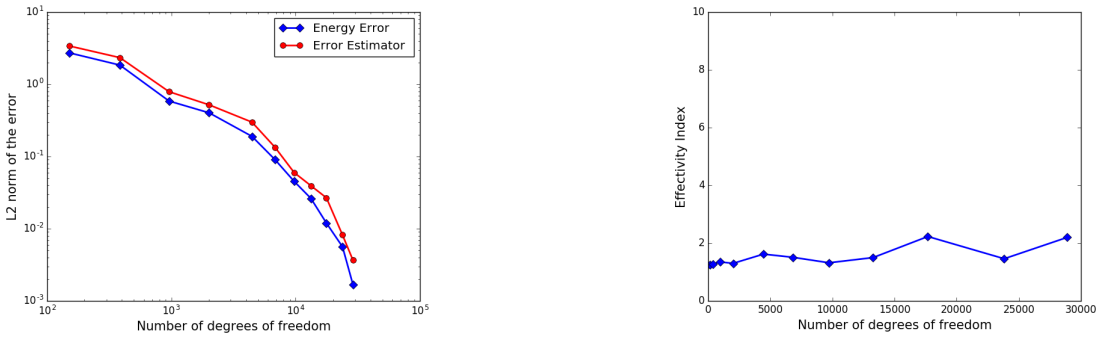

(a) (b)

Figure 3.9: Example 2. (Left) Comparison of the energy error and the error estimator, (Right) Effectivity Indices.

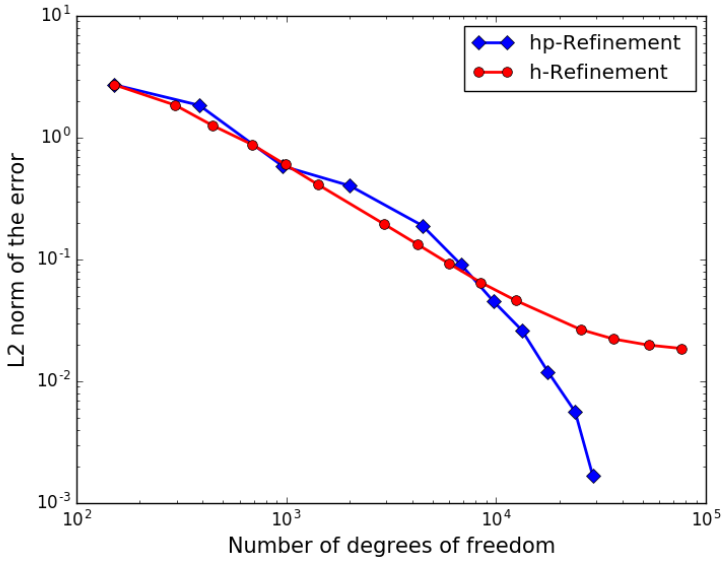

Figure 3.10: Example 2. Comparison between the actual energy error in h- and hp- adaptive mesh refinements.

exponential convergence rate, the comparison of the energy error and the proposed residual based a posteriori error estimator are shown in Figure 3.13. On the right, the effectivity indices are shown which remain bounded around $6.0 \leqslant$ Eff. Indices $\leqslant 10.1$. Figure 3.14 shows the comparison between the energy norm of the error for both h- and hp-adaptive refinement.

3.4.4 Example 4

For the last example, we consider the Stokes fluid flows through a pipe with a bend. We prescribe the homogeneous Dirichlet boundary condition on the walls. For the inlet and outlet we set parabolic boundary condition. The exact solution of the problem is not in hand. However, the solution on a very fine grid is given in Figure 3.15. In our h- and hp-adaptive algorithms we set $\theta = 0.75$ and we start with 28 equally sized cells. The meshes generated by h-adaptive refinement are shown in Figure 3.16. As the h-adaptive refinement shows in this figure, more local h-refinement happens in the vicinity of the re-entrant corners, where the solution gets larger residual values. Figure 3.17 presents the triangulation and the corresponding polynomial degree distribution for the hp-adaptive refinement strategy. The history of the hp-refinement is given in

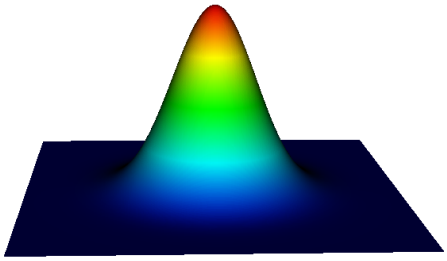

Figure 3.11: Example 3. Analytic solution corresponding to the third component of solution (pressure).

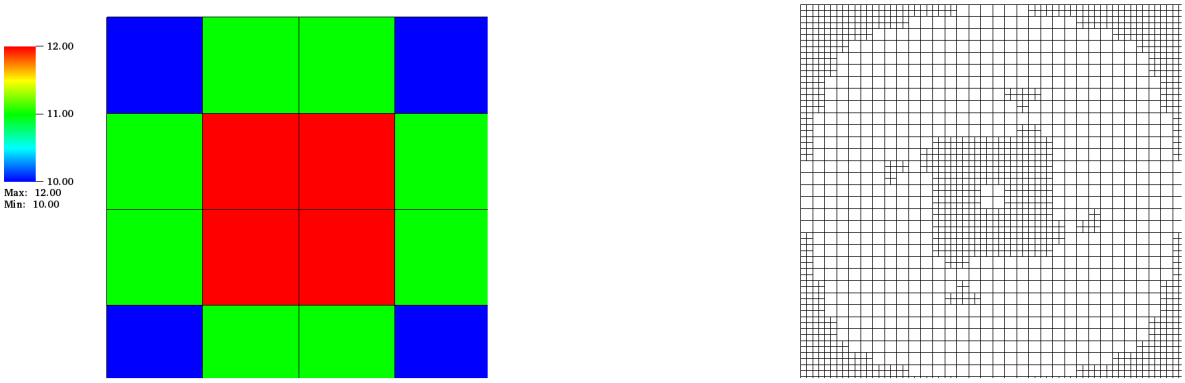

Figure 3.12: Example 3. (Left) Mesh generated after 7 hp-adaptive refinement steps; (Right) Mesh generated after 8 h-adaptive refinement steps

Table 3.3: Example 3. Number of h and p refined cells per refinement level.

refinement level	# cells	$\#h$	$\#p$
0	4	0	4
1	4	0	4
2	4	0	4
3	4	0	3
4	4	4	0
5	16	0	10
6	16	0	9
7	16	0	12
8	16	0	11

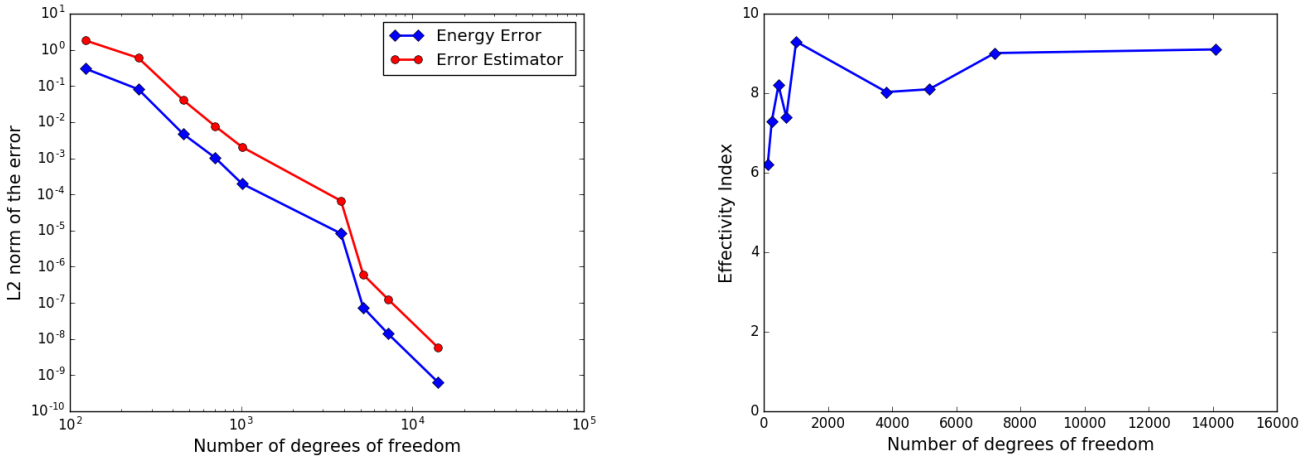

Figure 3.13: Example 3. (Left) Comparison of the energy error and the error estimator, (Right) Effectivity Indices

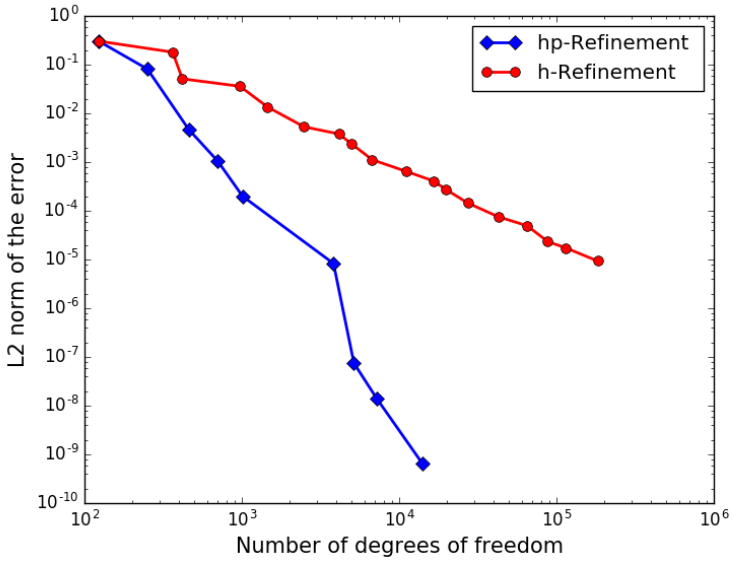

Figure 3.14: Example 3. Comparison of the actual error with h- and hp- adaptive mesh refinement

Table 3.4. Finally, we present comparison plots between the energy estimators for both h- and hp-refinement in Figure 3.18.

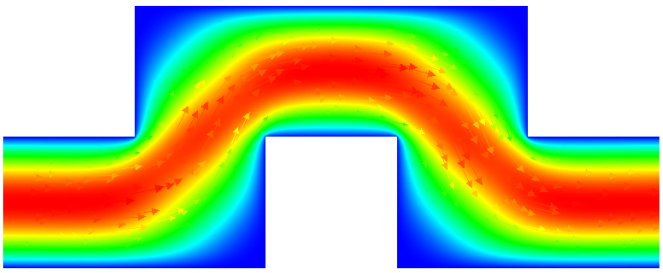

Figure 3.15: Example 4. Analytic solution corresponding to the velocity components

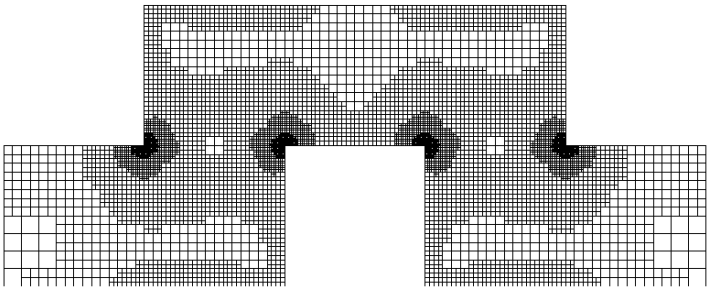

Figure 3.16: Example 4. Mesh generated after 12 h-adaptive refinement steps

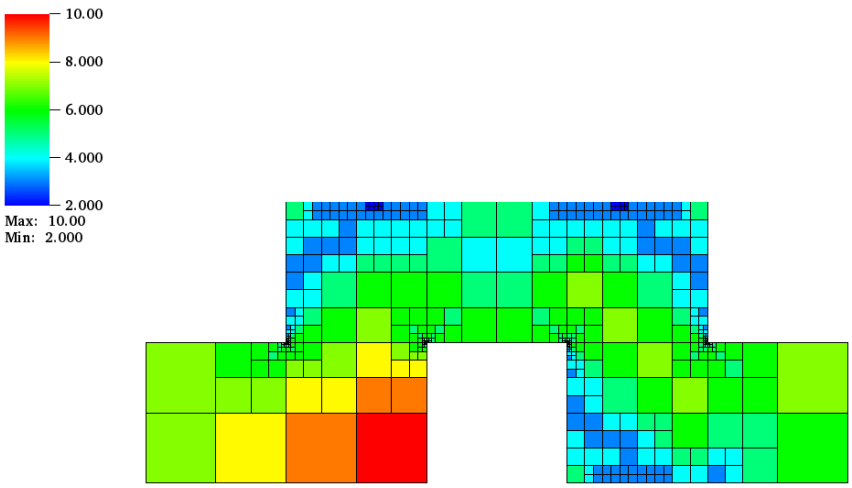

Figure 3.17: Example 4. Mesh generated after 16 hp-adaptive steps

Table 3.4: Example 4. Number of h and p refined cells per refinement level.

refinement level	# cells	$\#h$	$\#p$
0	28	15	1
1	91	15	3
2	141	15	11
3	181	15	23
4	226	35	47
5	352	15	66
6	397	14	73
7	442	22	101
8	505	27	101
9	592	16	117
10	637	18	129
11	697	21	147
12	745	26	103
13	811	19	157
14	868	18	135
15	929	17	156

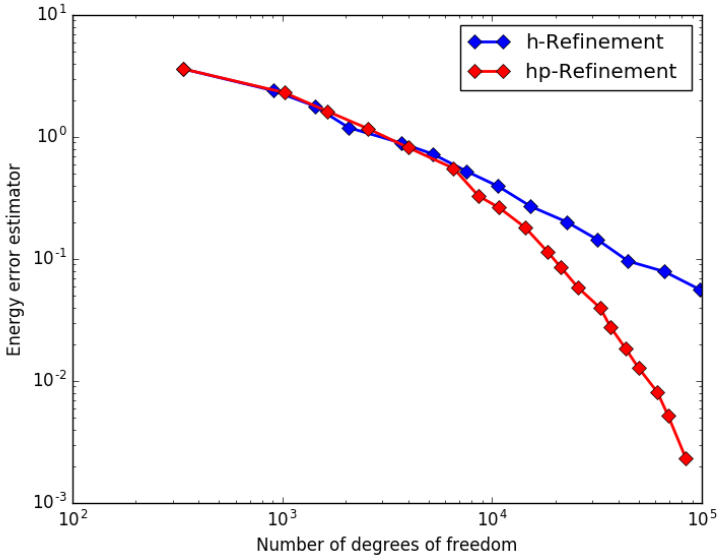

Figure 3.18: Example 4. Comparison of the energy error estimator with h- and hp-adaptive mesh refinement.

4. DUAL-WEIGHTED GOAL-ORIENTED A POSTERIORI ERROR ESTIMATION IN H- AND HP-ADAPTIVE FEM FOR THE STOKES PROBLEM

4.1 Introduction

When one has a specific goal in mind, such as evaluating the stress, the pressure, or temperature at a given critical point in the domain, then the energy norm of the error itself brings very little relevant information about the accuracy of the prescribed quantity of interest. Therefore, the adaptive refinement strategy must be defined in a way that captures the error for that feature of solutions. The goal-oriented adaptive refinement is an approach to deal with the described situation. The aforementioned quantity of interest, which represents physical or practical meaning for engineers, can be expressed in terms of some functional of the solution and the whole idea of goal-oriented adaptivity is based on minimizing the error in that *quantity of interest* [80, 34, 81, 39]. Additionally, the main concept in the definition of goal-oriented estimators is creating a relation between the residual, which is considered the source of the error, and the error in the *quantity of interest*. This requires finding the solution of the adjoint of the primal problem, which indicates how the information from the residual as a source of error propagates to the error in the prescribed *quantity of interest*. Therefore, the error in the functional of interest can be considered as a product of residual of the primal problem and the solution of the corresponding adjoint problem. Knowing this fact, the idea of dual-weighted a posteriori error estimates was used in earlier works in [80, 34, 32, 81] and later on was successfully applied to a variety of problems [82, 83] with computationally efficient and accurate results. Before the work in [38] by Moon, the analysis and the convergence rate of goal-oriented adaptivity was not proven. In that paper, convergence and optimality of the adaptive algorithm were proven by making strong smoothness assumptions about the solution of the primal and adjoint problem. Later on, Mommer and Stevenson [39] considered the scaled Poisson problem as their model problem, and for that they proved convergence of their proposed goal-oriented adaptive algorithm. Moreover, they provide a reasonable upper bound for

the convergence rate of their GOAFEM strategy. Using the contraction framework described in [4], Holst et al. [84] proved the convergence of their proposed goal-oriented adaptive algorithm applied to nonsymmetric elliptic problems. [85, 86] are examples of h-adaptive goal-oriented adaptivity for the Stokes problem. Their numerical results and the comparison plots confirm the efficiency of applying the goal-oriented error estimator in controlling the error in the quantity of interest rather than standard h-adaptive refinement.

4.1.1 Outline

Our study in this chapter continues as follows. First, the primary tools, namely the primal and dual contributions of the goal estimator, are presented in section 4.2. In section 4.3, in continuation of earlier work on goal-oriented error estimators for elliptic problems [1], we study a locally defined dual-weighted goal-oriented error estimator for the Stokes problem. The error in the functional of interest is estimated as a sum of errors for each cell, which are defined as the product of primal and dual error contributions. Despite the energy error in the quantity of interest, there are no complete two-sided upper and lower bounds. Knowing this, we prove that our proposed h and hp dual-weighted goal-oriented estimator is an upper bound of the error in the functional of interest. Then we show that the goal-estimator is a lower bound for the product of energy errors in both primal and dual problems. The goal-oriented h- and hp-AFEM refinement algorithms are presented in section 4.4. Finally, in section 4.5 the implementation is tested on a couple of standard benchmark numerical problems. We demonstrate the exponential convergence rate of the hp goal-oriented adaptivity and compare it with the h goal-oriented estimator. Moreover, the close-to-optimal expected convergence rate in the h-AFEM goal-oriented algorithm is observed in our numerical test cases.

4.2 Primal and dual contributions of the goal estimator

Given $j \in H^{-1}(\Omega)$ as a goal functional defined on the velocity space, the corresponding adjoint problem for the primal equation (2.1) consists of seeking $(z_u, z_\varrho) \in \mathcal{H}(\Omega)$ such that

$$\begin{aligned} -\Delta z_u + \nabla z_\varrho &= j \qquad \text{in} \quad \Omega, \\ -\nabla \cdot z_u &= 0 \qquad \text{in} \quad \Omega, \\ z_u &= 0 \qquad \text{on} \quad \Gamma. \end{aligned} \tag{4.1}$$

The standard weak formulation of equation (4.1) is: find $[z_u, z_\varrho] \in \mathcal{H}(\Omega)$ such that

$$\mathcal{L}([\varphi, q]; [z_u, z_\varrho])_\Omega = (\varphi, j)_\Omega \qquad \forall [\varphi, q] \in \mathcal{H}(\Omega), \tag{4.2}$$

where the bilinear form $\mathcal{L} : \mathcal{H}(\Omega) \times \mathcal{H}(\Omega) \to \mathbb{R}$ is defined as

$$\mathcal{L}([\varphi, q]; [z_u, z_\varrho])_\Omega := (\nabla\varphi, \nabla z_u)_\Omega - (\nabla \cdot \varphi, z_\varrho)_\Omega - (q, \nabla \cdot z_u)_\Omega. \tag{4.3}$$

The discrete approximation to (4.2) is obtained by finding $[z_{u_{\text{FE}}}, z_{\varrho_{\text{FE}}}] \in \mathcal{V}^p(\mathcal{T})$ such that

$$\mathcal{L}\left([\varphi_{\text{FE}}, q_{\text{FE}}]; [z_{u_{\text{FE}}}, z_{\varrho_{\text{FE}}}]\right)_\Omega = (\varphi_{\text{FE}}, j)_\Omega \qquad \forall\, [\varphi_{\text{FE}}, q_{\text{FE}}] \in \mathcal{V}^p(\mathcal{T}), \tag{4.4}$$

where $\mathcal{T}$ is a triangulation of Ω.

Note that the dual problem (4.1) is simply the same Stokes problem as (2.1) except for the different right hand side. Therefore, existence and uniqueness in solution of the dual problem follows directly from the same properties of the primal setting. Since the system matrix for the dual problem is identical to the system matrix for the primal problem, the dual can be solved almost for free if the matrix is factorized or a good preconditioner is available when solving the original problem.

This section relies on the general idea of goal oriented error estimation, which implies to de-

fine a dual-weighted residual estimator as being the product of local error indicators for primal and adjoint problem. The definition of goal-oriented error estimator for the Stokes model problem is initiated by the goal-oriented estimator introduced in [1] for the Poisson problem, that itself is a combination of the ideas of weighted a posteriori error in [87] and the hp-adaptive refinement algorithm based on the energy norm for the Poisson problem [21]. In section 4.2.1, first we introduce the residual weight which comes from the primal problem for the Stokes equation, and which is used in the definition of our goal-oriented estimator. Then in section 4.2.2, we discuss how to derive the dual weight term. Finally, the primal and dual weights introduced in these two sections will be used further in section 4.3 to formulate our locally defined dual-weighted h and hp goal-oriented a posteriori error estimator.

4.2.1 Residual-based a posteriori error estimator (primal weight)

In this section we consider some other auxiliary results that we need to formulate our goal-oriented a posteriori error estimator. First, we define the residual-based a posteriori error estimator for the Stokes problem (2.1) in hp-adaptive finite element method. This estimator η, is decomposed into a sum of local error indicators η_K:

$$\eta^2 := \sum_{K \in \mathcal{T}} \eta_K^2.$$

The local error indicator η_K can be decomposed into a cell and an interface contribution, as follows:

$$\eta_K^2 := \eta_{K;R}^2 + \eta_{K;B}^2, \tag{4.5}$$

where $\eta_{K;R}$ denotes the residual-based term and $\eta_{K;B}$ indicates the jump-based term. These terms are defined by

$$\eta_{K;R}^2 := \frac{h_K^2}{p_K^2} \left\| \left(I_{p_K}^K f + \Delta u_{\text{FE}} - \nabla \varrho_{\text{FE}} \right) \right\|_K^2 + \left\| (\nabla \cdot u_{\text{FE}}) \right\|_K^2 , \tag{4.6}$$

and

$$\eta_{K;B}^2 := \sum_{e \in \mathcal{E}(K)} \frac{h_e}{2p_e} \left\| \left[\frac{\partial u_{\text{FE}}}{\partial n_K} \right] \right\|_e^2. \tag{4.7}$$

Here, $I_{p_K}^K f$ denotes the local L^2-projection of f onto the space of vector-valued polynomials of degree less or equal than p_K. Here h_e, is the length of edge e and for every two cells K, K' which share edge e, let $p_e := \min(p_K, p_{K'})$. The $[\cdot]$ notation is the jump across the edge and n_K is the outward pointing unit normal vector of cell K for each edge e. The interface contribution of the error estimator in (4.7) is the summation over all edges of K that are not on the domain boundary $\partial\Omega$. We derive an upper bound and a lower bound for the energy error, i.e. reliability and efficiency estimates, respectively.

Theorem 4.2.1 (Reliability & Efficiency)**.** *Let $[u_{FE}, \varrho_{FE}] \in \mathcal{V}^p(\mathcal{T})$ be the solution of discrete problem (2.10) and $[u, \varrho] \in \mathcal{H}$ be solution of weak problem (2.3). Further, assume that triangulation $\mathcal{T}$ is (γ_h, γ_p)-regular then:*

- *there exists some constant $C_{rel} > 0$ independent of mesh size vector h and polynomial degree vector p such that*

$$\|\nabla (u - u_{FE})\|_\Omega^2 + \|\varrho - \varrho_{FE}\|_\Omega^2 \leq C_{rel} \sum_{K \in \mathcal{T}} \left(\eta_K^2 + \frac{h_K^2}{p_K^2} \left\| I_{p_K}^K f - f \right\|_K^2 \right). \tag{4.8}$$

- *there exists some constant $C_{eff} > 0$ independent of mesh size vector h and polynomial degree vector p such that*

$$\begin{aligned} \eta_K^2 \leq C_{eff} \Bigg(& p_K^2 \left(\|\nabla (u - u_{FE})\|_{\omega_K}^2 + \|\varrho - \varrho_{FE}\|_{\omega_K}^2 \right) \\ & + \frac{h_K^2}{p_K} \left\| I_{p_K}^K f - f \right\|_{\omega_K}^2 \Bigg), \end{aligned} \tag{4.9}$$

  for all $K \in \mathcal{T}$.

Proof. The proof is given in Theorems 3.2.2 and 3.2.5. □

4.2.2 A posteriori error estimator for the local patch problems (dual weight)

In the goal-oriented adaptive refinement, we try to formalize the estimator in such a way that it takes into account the impact of the introduced functional of interest $J \in L^2(\Omega)'$. In this method, we want to assess the accuracy of the finite element solution $(u_{\text{FE}}, \varrho_{\text{FE}}) \in \mathcal{V}^p(\mathcal{T})$ in measure of some quantity of interest other than the classical energy norm of the error itself. Before we propose the formulation for the goal-oriented a posteriori error estimator, we need some preliminary results. Let $(e^d, E^d) \in \mathcal{V}^p(\mathcal{T})$ be the error of the solution of the adjoint problem (4.4) where $e^d := z_u - z_{u_{\text{FE}}}$ and $E^d := z_\varrho - z_{\varrho_{\text{FE}}}$. Considering the residual of the dual problem on the local patch $\omega_{K,2}$ and the bilinear notation introduced in (4.3), we have

$$\begin{aligned}\int_{\omega_{K,2}} \phi j - \int_{\omega_{K,2}} \nabla\phi \nabla z_{u_{\text{FE}}} + \int_{\omega_{K,2}} (\nabla\cdot\phi) z_{\varrho_{\text{FE}}} \\ + \int_{\omega_{K,2}} q(\nabla\cdot z_{u_{\text{FE}}}) = \mathcal{L}([\phi,q];[e^d,E^d])_{\omega_{K,2}}.\end{aligned} \tag{4.10}$$

Integration by parts gives:

$$\int_{\omega_{K,2}} \phi\,(j + \Delta z_{u_{\text{FE}}} - \nabla z_{\varrho_{\text{FE}}}) + \int_{\omega_{K,2}} q\,(\nabla\cdot z_{u_{\text{FE}}}) = \mathcal{L}([\phi,q];[e^d,E^d])_{\omega_{K,2}}. \tag{4.11}$$

such that $\phi \in H_0^1(\omega_{K,2})$ and $q \in L^2(\omega_{K,2})$, where $\omega_{K,2}$ is a two layer patch around cell K. The pair $(w_u, w_\varrho) \in \mathcal{H}(\omega_{K,2})$ is defined to be the Ritz representation of the residual, as follows:

$$(\nabla\phi, \nabla(w_u))_{\omega_{K,2}} + (q, w_\varrho)_{\omega_{K,2}} = \mathcal{L}([\phi,q];[e^d,E^d])_{\omega_{K,2}},\ \ \forall(\phi,q) \in \mathcal{H}(\omega_{K,2}). \tag{4.12}$$

Therefore we may define the energy norm of errors in the solution of the dual problem as

$$|||(e^d,E^d)|||^2_{\omega_{K,2}} = \|\nabla w_u\|^2_{\omega_{K,2}} + \|w_\varrho\|^2_{\omega_{K,2}}. \tag{4.13}$$

To obtain $(w_{u_{\text{FE}}}, w_{\varrho_{\text{FE}}})$ as the solution of discrete system of equations, we solve equation (4.12) with a higher order space. We seek for $(w_{u_{\text{FE}}}, w_{\varrho_{\text{FE}}}) \in \mathcal{V}^{p+1}(\mathcal{T}_{\omega_{K,2}})$ such that

$$(\nabla\phi, \nabla w_{u_{\text{FE}}})_{\omega_{K,2}} + (q, w_{\varrho_{\text{FE}}})_{\omega_{K,2}} = \mathcal{L}([\phi, q]; [e^d, E^d])_{\omega_{K,2}}, \ \ \forall (\phi, q) \in \mathcal{V}^{p+1}(\mathcal{T}_{\omega_{K,2}}). \tag{4.14}$$

The energy error corresponding to the above variational equations can be estimated by a residual based a posteriori error estimation, as follows in the next definition.

Definition 4.2.2 (A Posteriori Error Estimation on patch $\omega_{K,2}$)**.** *Let $K \in \mathcal{T}$ be an arbitrary cell. Further assume $(w_{u_{FE}}, w_{\varrho_{FE}}) \in \mathcal{V}^{p+1}(\omega_{K,2})$ be a solution of (4.14) and $(z_{u_{FE}}, z_{\varrho_{FE}}) \in \mathcal{V}^{p}(\mathcal{T})$ be the solution of (4.4). Then the residual based a posteriori error estimator for local patch problems on $\omega_{K,2}$ is given by*

$$\tilde{\eta}(K)^2 := \sum_{L \in \mathcal{T}_{\omega_{K,2}}} \tilde{\eta}_L(K)^2,$$

where the local estimator $\tilde{\eta}_L$ is expressed as

$$\tilde{\eta}_L^2 = \tilde{\eta}_{R,L}^2 + \tilde{\eta}_{B,L}^2 \quad \forall L \in \mathcal{T}_{\omega_{K,2}} \tag{4.15}$$

In (4.15), the residual based term $\tilde{\eta}_{R,L}$ is defined as

$$\tilde{\eta}_{R,L}^2(K) := \frac{h_L^2}{p_L^2} \left\| I_{p_L}^L j + \Delta z_{u_{FE}} - \nabla z_{\varrho_{FE}} + \Delta w_{u_{FE}} \right\|_L^2 + \| \nabla \cdot z_{u_{FE}} - w_{\varrho_{FE}} \|_L^2, \tag{4.16}$$

and the jump based term $\tilde{\eta}_{B,L}$ as

$$\tilde{\eta}_{B,L}^2 := \sum_{e \in \mathcal{E}(\omega_{K,2} \cap L)} \frac{h_e}{2p_e} \left\| \left[\frac{\partial z_{u_{FE}} + \partial w_{u_{FE}}}{\partial n_L} \right] \right\|_e^2. \tag{4.17}$$

Here $I_{p_L}^L j$ is the L^2-projection of functional j into the finite element space, and h_e, is the length of edge e. For every two cells L, L' which share edge e, let $p_e := \min(p_L, p_{L'})$. The $[\cdot]$ notation is the jump across the edge and n_L is the outward pointing unit normal vector of cell L for each edge e.

Now, we provide the efficiency of the above residual estimator. First we find an upper bound for the residual based term $\tilde{\eta}^2_{R,L}(K)$ given in (4.16).

Lemma 4.2.3 (Efficiency-Dual-1)**.** *Let $(z_{u_{FE}}, z_{\varrho_{FE}}) \in \mathcal{V}^p(\mathcal{T})$ be the solution of (4.4), $K \in \mathcal{T}$ and $L \in \omega_{K,2}$ be arbitrary. Moreover assume $(w_u, w_\varrho) \in \mathcal{H}(\omega_{K,2})$ be the solution of* (4.12) *and $(w_{u_{FE}}, w_{\varrho_{FE}}) \in \mathcal{V}^{p+1}(\omega_{K,2})$ be the solution of (4.14). Then for all $\delta \in (0,3)$ there exists some constant $C(\delta) > 0$ independent of mesh size h_L and polynomial degree p_L such that:*

$$\tilde{\eta}^2_{R,L}(K) \leq C p_L^{\frac{3-\delta}{2}} \left(\|\nabla(w_u - w_{u_{FE}})\|^2_L + \|w_\varrho - w_{\varrho_{FE}}\|^2_L + \frac{h_L^2}{p_L^2} \|j - I^L_{p_L} j\|^2_L \right).$$

Proof.

$$\tilde{\eta}^2_{R,L}(K) := \tilde{\eta}^2_{R_1,L}(K) + \tilde{\eta}^2_{R_2,L}(K), \tag{4.18}$$

where

$$\tilde{\eta}^2_{R_1,L}(K) = \frac{h_L^2}{p_L^2} \left\| I^L_{p_L} j + \Delta z_{u_{\text{FE}}} - \nabla z_{\varrho_{\text{FE}}} + \Delta w_{u_{\text{FE}}} \right\|^2_L, \tag{4.19}$$

and

$$\tilde{\eta}^2_{R_2,L}(K) = \|\nabla \cdot z_{u_{\text{FE}}} - w_{\varrho_{\text{FE}}}\|^2_L. \tag{4.20}$$

Let $res_1 := I^L_{p_L} j + \Delta z_{u_{\text{FE}}} - \nabla z_{\varrho_{\text{FE}}} + \Delta w_{u_{\text{FE}}}$. By equation (2.18) of Lemma 2.2.5 we get

$$\|res_1\|_L \leq C_1 p_L^{\frac{1+\delta}{4}} \|\Phi_L^{\frac{1+\delta}{4}} res_1\|_L, \quad \delta > 0. \tag{4.21}$$

Then we define a function

$$w^*_{L,1} : \omega_{K,2} \longrightarrow \mathbb{R}, \text{ as } w^*_{L,1} := \begin{cases} \Phi_L^{\frac{1+\delta}{2}} res_1 & in\, L, \\ 0 & otherwise. \end{cases}.$$

Here Φ_L is the smoothing weight function as defined in equation (2.16). With the usage of the standard polynomial inverse estimate introduced in lemma 2.2.5, knowing that the smoothing functions Φ_L are bounded, and also the fact that $\|\nabla \Phi_L\|_L \leq \frac{C}{h_L}$, for some $C > 0$, it follows $w^*_{L,1} \in H^1_0(L)$.

Integration by parts and using (4.12) and (4.14) gives

$$\begin{aligned}\|\Phi_L^{\frac{1+\delta}{4}} res_1\|_L^2 &= \int_L w_{L,1}^* res_1 = \int_L w_{L,1}^* j + \int_L w_{L,1}^*(j - I_{p_L}^L j) \\ &+ \int_L w_{L,1}^*(\Delta z_{u_{\text{FE}}} + \Delta w_{u_{\text{FE}}}) - \int_L w_{L,1}^* \nabla z_{\varrho_{\text{FE}}} \\ &= \int_L w_{L,1}^*(j - I_{p_L}^L j) + \int_L w_{L,1}^*(j + \Delta z_{u_{\text{FE}}} - \nabla z_{\varrho_{\text{FE}}}) - \int_L \nabla w_{L,1}^* \nabla w_{u_{\text{FE}}} \\ &= \int_L w_{L,1}^*(j - I_{p_L}^L j) + \int_L \nabla w_{L,1}^* \nabla (w_u - w_{u_{\text{FE}}}).\end{aligned} \tag{4.22}$$

Using the L^2 property of projection operator $I_{p_L}^L$, where Π^{hp} is the Scott-Zhang interpolation operator $\Pi^{hp} : \mathcal{H}(\omega_{K,2}) \longrightarrow \mathcal{V}^p(\mathcal{T} \cap \omega_{K,2})$

$$\int_L w_{L,1}^*(j - I_{p_L}^L j) = \int_L (w_{L,1}^* - \Pi^{hp} w_{L,1}^*)(j - I_{p_L}^L j).$$

For the first term on the right-hand-side of equation (4.22), using the Cauchy-Schwartz inequality and also the approximation results given in Theorem 2.2.3 gives

$$\begin{aligned}\left| \int_L w_{L,1}^*(j - I_{p_L}^L j) \right| &\leq \|w_{L,1}^* - \Pi^{hp} w_{L,1}^*\|_L \|j - I_{p_L}^L j\|_L \\ &\leq C_{SZ} \frac{h_L}{p_L} \|\nabla w_{L,1}^*\|_L \|j - I_{p_L}^L j\|_L.\end{aligned} \tag{4.23}$$

For the second term on the right-hand-side of equation (4.22), using Young's inequality, and also inverse estimates (2.18) and (2.19) given in Lemma 2.2.5, we have

$$\begin{aligned}\|\nabla w_{L,1}^*\|_L^2 &= \left\| \nabla \left(\Phi_L^{\frac{1+\delta}{2}} \left(I_{p_L}^L j + \Delta z_{u_{\text{FE}}} - \nabla z_{\varrho_{\text{FE}}} + \Delta w_{u_{\text{FE}}} \right) \right) \right\|_L^2 \\ &\leq 2 \int_L \Phi_L^{1+\delta} |\nabla (res_1)|^2 + 2 \int_L |\nabla \Phi_L^{\frac{1+\delta}{2}}|^2 |res_1|^2 \\ &\leq C \left(\frac{p_L^{3+\delta}}{h_L^2} \int_L \Phi_L^{\frac{1+\delta}{2}} res_1^2 \right).\end{aligned} \tag{4.24}$$

By (4.23) and (4.24), equation (4.22) reads as

$$\begin{aligned}\|\Phi_L^{\frac{1+\delta}{4}} res_1\|_L^2 \leq & C_{SZ}\frac{h_L}{p_L}\|j - I_{p_L}^L j\|_L \cdot \frac{p_L^{\frac{3+\delta}{2}}}{h_L}\|\Phi_L^{\frac{1+\delta}{4}} res_1\|_L \\ & + \|\nabla(w_u - w_{u_{\text{FE}}})\|_L \cdot C\frac{p_L^{\frac{3+\delta}{2}}}{h_L}\|\Phi_L^{\frac{1+\delta}{4}} res_1\|_L.\end{aligned} \tag{4.25}$$

From (4.21), multiply by $p_L^{\frac{1+\delta}{4}}$ for $\delta > 0$

$$\begin{aligned}\|res_1\|_L \leq p_L^{\frac{1+\delta}{4}}(\|\Phi_L^{\frac{1+\delta}{4}} res_1\|_L) \leq & CC_{SZ}p_L^{\frac{1+\delta}{4}} p_L^{\frac{1+\delta}{2}}\|j - I_{p_L}^L j\|_L \\ & + p_L^{\frac{1+\delta}{4}} C\frac{p_L^{\frac{3+\delta}{2}}}{h_L}\|\nabla(w_u - w_{u_{\text{FE}}})\|_L\end{aligned} \tag{4.26}$$

Let $C_{max} = \max(CC_{SZ}, C)$, then by equation (4.19)

$$\tilde{\eta}_{R_1,L}^2(K) = \frac{h_L^2}{p_L^2} res_1^2 \leq \tilde{C}_{max} p_L^{\frac{3+\delta}{2}}\left(\|\nabla(w_u - w_{u_{\text{FE}}})\|_L^2 + \frac{h_L^2}{p_L^2}\|j - I_{p_L}^L j\|_L^2\right). \tag{4.27}$$

Now let $res_2 := \nabla \cdot z_{u_{\text{FE}}} - w_{\varrho_{\text{FE}}}$. Similarly, by lemma 2.2.5 we get

$$\|res_2\|_L \leq C_2 p_L^{\frac{1+\delta}{4}}\|\Phi_L^{\frac{1+\delta}{4}} res_2\|_L, \quad \delta > 0. \tag{4.28}$$

Then we define a function $w_{L,2}^* : \omega_{K,2} \longrightarrow \mathbb{R}$ as $w_{L,2}^* := \begin{cases} \Phi_L^{\frac{1+\delta}{2}} res_2 & in\, L \\ 0 & otherwise \end{cases}$. By equation (4.12)

$$\begin{aligned}\|\Phi_L^{\frac{1+\delta}{4}} res_2\|_L^2 &= \int_L w_{L,2}^* res_2 = \int_L w_{L,2}^* \nabla \cdot z_{u_{\text{FE}}} - \int_L w_{L,2}^* w_{\varrho_{\text{FE}}} \\ &= \int_L w_{L,2}^* w_\varrho - \int_L w_{L,2}^* w_{\varrho_{\text{FE}}} = \int_L w_{L,2}^*(w_{\varrho_{\text{FE}}} - w_\varrho).\end{aligned} \tag{4.29}$$

Therefore, after cancellation from both sides, we will get

$$\|\Phi_{L,2}^{\frac{1+\epsilon}{4}} res_2\|_L \leq \|w_\varrho - w_{\varrho_{\text{FE}}}\|_L, \tag{4.30}$$

multiply by $p_L^{\frac{1+\delta}{4}}$ and taking square of both sides

$$\tilde{\eta}^2_{R_2,L}(K) \leq C p_L^{\frac{1+\delta}{2}} \|w_\varrho - w_{\varrho_{\text{FE}}}\|^2_L, \tag{4.31}$$

adding up the results in (4.27) and (4.31) gives

$$\tilde{\eta}^2_{R,L}(K) \leq p_L^{\frac{3+\delta}{2}} \left(\|\nabla(w_u - w_{u_{\text{FE}}})\|^2_L + \|w_\varrho - w_{\varrho,\text{FE}}\|^2_L \right) + \frac{h_L^2}{p_L^2} \|j - I^L_{p_L} j\|^2_L. \tag{4.32}$$

□

Lemma 4.2.4 (Efficiency-Dual-2)**.** *Let* $(z_{u_{FE}}, z_{\varrho_{FE}}) \in \mathcal{V}^p(\mathcal{T})$ *be solution of (4.4),* $K \in \mathcal{T}$ *and* $L \in \omega_{K,2}$ *be arbitrary. Moreover assume* $(w_u, w_\varrho) \in \mathcal{H}(\omega_{K,2})$ *be the solution of* (4.12) *and* $(w_{u_{FE}}, w_{\varrho_{FE}}) \in \mathcal{V}^{p+1}(\omega_{K,2})$ *be solution of* (4.14)*. Then for all* $\delta \in (0,3)$ *there exists some constant* $C > 0$ *independent of mesh size* h_L *and polynomial degree* p_L *such that*

$$\tilde{\eta}^2_{B,L}(K) \leq C p_L^{\frac{3+\delta}{2}} \left(\|\nabla(w_u - w_{u_{FE}})\|^2_{\omega_{L,1}} + \|w_\varrho - w_{\varrho_{FE}}\|^2_{\omega_{L,1}} \right) + \frac{h_L^2}{p_L^{\frac{5-\delta}{2}}} \|j - I^L_{p_L} j\|^2_{\omega_{L,1}}.$$

Proof. First set the jump term as

$$J := \left[\frac{\partial}{\partial n_L} (z_{u_{\text{FE}}} + w_{u_{\text{FE}}}) \right].$$

Again using Lemma $2.2.5$ gives

$$\sum_{e \in \mathcal{E}(\omega_{K,2})} \frac{h_e}{2p_e} \|J\|^2_e \leq C \sum_{e \in \mathcal{E}(\omega_{K,2})} \frac{h_e}{2p_e^{\frac{1-\delta}{2}}} \|J\, \Phi_e^{\frac{1+\delta}{4}}\|^2_e. \tag{4.33}$$

For any arbitrary edge $e \in \mathcal{E}(\omega_{K,2}) \cap L$ there exists some cell $\tilde{L} \in \omega_{K,2}$ such that $e = L \cap \tilde{L}$. $v_u^e \in H_0^1(\omega_{K,2})^2$ is defined as $v_u^e = \Phi_e^{\frac{1+\delta}{2}} J$ on edge e. Moreover, the function $\tilde{v}_u^e : \omega_{K,2} \longrightarrow \mathbb{R}$ can

be set as

$$\tilde{v}_u^e := \begin{cases} v_u^e & in\, L \cup \tilde{L} \\ 0 & otherwise \end{cases}.$$

In order to make an upper bound for right hand side of equation (4.33), with integration by parts we get

$$\begin{aligned} \|\Phi_e^{\frac{1+\epsilon}{4}} J\|_e^2 &= \int_e \tilde{v}_u^e \Big(\nabla(z_{u_{\text{FE}}} + w_{u_{\text{FE}}})|_L - \nabla(z_{u_{\text{FE}}} + w_{u_{\text{FE}}})|_{\tilde{L}} \Big) n_L \\ &= \int_{L\cup\tilde{L}} \tilde{v}_u^e (\Delta z_{u_{\text{FE}}} + \Delta w_{u_{\text{FE}}}) + \int_{L\cup\tilde{L}} \nabla \tilde{v}_u^e (\nabla z_{u_{\text{FE}}} + \nabla w_{u_{\text{FE}}}). \end{aligned}$$

The fact that $(w_u, w_\varrho) \in \mathcal{H}(\omega_{K,2})$ is solution of equation (4.12) implies

$$\begin{aligned} \|\Phi_e^{\frac{1+\epsilon}{4}} J\|_e^2 &= \int_{L\cup\tilde{L}} (I_{p_L}^L j + \Delta z_{u_{\text{FE}}} + \Delta w_{u_{\text{FE}}}) \tilde{v}_u^e + \int_{L\cup\tilde{L}} \nabla \tilde{v}_u^e \cdot \nabla w_{u_{\text{FE}}} \\ &\quad - \int_{L\cup\tilde{L}} \nabla z_{\varrho_{\text{FE}}} \tilde{v}_u^e + \int_{L\cup\tilde{L}} (j - I_{p_L}^L j) \tilde{v}_u^e \\ &= \int_{L\cup\tilde{L}} (I_{p_L}^L j + \Delta z_{u_{\text{FE}}} + \Delta w_{u_{\text{FE}}} - \nabla z_{\varrho_{\text{FE}}}) \tilde{v}_u^e \\ &\quad - \int_{L\cup\tilde{L}} \nabla w_u \nabla \tilde{v}_u^e + \int_{L\cup\tilde{L}} \nabla w_{u_{\text{FE}}} \nabla \tilde{v}_u^e + \int_{L\cup\tilde{L}} (j - I_{p_L}^L j) \tilde{v}_u^e \end{aligned} \tag{4.34}$$

In order to derive an upper bound for the equation (4.34) we categorize the above obtained terms as follows and work on them separately. First,

$$I := \Big| \int_{L\cup\tilde{L}} (I_{p_L}^L j + \Delta z_{u_{\text{FE}}} + \Delta w_{u_{\text{FE}}} - \nabla z_{\varrho_{\text{FE}}}) \tilde{v}_e \Big|.$$

Then, using the Cauchy-Schwarz inequality, trace inequality, and then using the equation (4.24) from Lemma $4.2.3$ implies

$$\begin{aligned} |I| &\leq \|I_{p_L}^L j + \Delta z_{u_{\text{FE}}} + \Delta w_{u_{\text{FE}}} - \nabla z_{\varrho_{\text{FE}}}\|_{(L\cup\tilde{L})} \|\tilde{v}_e\|_{L^2(L\cup\tilde{L})} \\ &\leq C_{\mathbf{tr}} \frac{\sqrt{h_e}}{p_e} \|I_{p_L}^L j + \Delta z_{u_{\text{FE}}} + \Delta w_{u_{\text{FE}}} - \nabla z_{\varrho_{\text{FE}}}\|_{(L\cup\tilde{L})} \|\Phi_e^{\frac{1+\delta}{4}} J\|_e \end{aligned} \tag{4.35}$$

To continue, we let

$$|II| := |\int_{L\cup\tilde{L}} \nabla(w_u - w_{u_{\text{FE}}})\nabla\tilde{v}_e|.$$

Again by using the Cauchy-Schwartz, Lemma 4.2.3 and the trace inequality we will get

$$|II| \leq C_{tr}\frac{p_e}{\sqrt{h_e}}\|\nabla(w_u - w_{u_{\text{FE}}})\|_{L\cup\tilde{L}}\|\Phi_e^{\frac{1+\delta}{4}}J\|_e \tag{4.36}$$

Finally, we set

$$III := \int_{L\cup\tilde{L}} (I_{p_L}^L j - j)\tilde{v}_e.$$

The L^2 property, and again Cauchy-Schwartz, Lemma 4.2.3 and the trace inequality gives

$$\begin{aligned} |III| &= \int_{L\cup\tilde{L}} (I_{p_L}^L j - j)(\tilde{v}_e + \Pi^{hp}\tilde{v}_e) \\ &\leq \tilde{C}_{tr}\frac{\sqrt{h_e}}{p_e}\|I_{p_L}^L j - j\|_{L\cup\tilde{L}}\|\Phi_e^{\frac{1+\delta}{4}}J\|_e. \end{aligned} \tag{4.37}$$

Adding up equations (4.35), (4.36) and (4.37), we have

$$\|\Phi_e^{\frac{1+\delta}{4}}J\|_e \leq \tilde{C}_{tr}\left(\sqrt{\frac{p_L}{h_L}}\|\nabla(w_u - w_{u_{\text{FE}}})\|_{L\cup\tilde{L}}\right). \tag{4.38}$$

Using the result derived in equation (4.33) we have

$$\begin{aligned} \tilde{\eta}_{B,L}^2(K) &\leq C\sum_{e\in\mathcal{E}(\omega_{K,2})}\frac{h_e}{2p_e^{\frac{1-\delta}{2}}}\left(\frac{p_L}{h_L}\|\nabla(w_u - w_{u_{\text{FE}}})\|_{L\cup\tilde{L}}^2\right. \\ &\quad \left. + \frac{h_L}{p_L}\|I_{p_L}^L j - j\|_{L\cup\tilde{L}}^2\right) \\ &\leq CP_L^{\frac{3}{2}+\frac{\delta}{2}}\left(\|\nabla(w_u - w_{u_{\text{FE}}})\|_{\omega_L}^2 + \|w_\varrho - w_{\varrho_{\text{FE}}}\|_{\omega_L}^2\right) \\ &\quad + \frac{h_L^2}{p_L^{\frac{5}{2}-\frac{\delta}{2}}}\|I_{p_L}^L j - j\|_{\omega_L}^2. \end{aligned} \tag{4.39}$$

□

Theorem 4.2.5 (Efficiency Dual)**.** *Let* $(z_{u_{FE}}, z_{\varrho_{FE}}) \in \mathcal{V}^p(\mathcal{T})$ *be the solution of (4.4),* $K \in \mathcal{T}$ *and*

$L \in \omega_{K,2}$ *be arbitrary. Moreover assume* $(w_u, w_\varrho) \in \mathcal{H}(\omega_{K,2})$ *be the solution of* (4.12) *and* $(w_{u_{FE}}, w_{\varrho_{FE}}) \in \mathcal{V}^{p+1}(\omega_{K,2})$ *be the solution of* (4.14). *Then for all* $\delta \in (0,3)$ *there exists some constant* $C_{eff}^{Ritz} > 0$ *independent of mesh size* h_L *and polynomial degree* p_L *such that:*

$$\begin{aligned}\tilde{\eta}_L^2(K) \leq & C_{eff}^{Ritz}\, p_L^{\frac{3+\delta}{2}} \left(\|\nabla(w_u - w_{u_{FE}})\|_{\omega_{L,1}}^2 + \|w_\varrho - w_{\varrho_{FE}}\|_{\omega_{L,1}}^2 \right) \\ & + \frac{h_L^2}{p_L^{\frac{1+\delta}{2}}} \|j - I_{p_L}^L j\|_{\omega_{L,1}}^2 .\end{aligned}$$

Proof. Proof follows directly from lemmas $4.2.3$ and $4.2.4$. □

Theorem 4.2.6 (Reliability Dual)**.** *Let* $(z_{u_{FE}}, z_{\varrho_{FE}}) \in \mathcal{V}^p(\mathcal{T})$ *be the solution of (4.4),* $K \in \mathcal{T}$ *and* $L \in \omega_{K,2}$ *be arbitrary. Moreover assume* $(w_u, w_\varrho) \in \mathcal{H}(\omega_{K,2})$ *be the solution of* (4.12) *and* $(w_{u_{FE}}, w_{\varrho_{FE}}) \in \mathcal{V}^{p+1}(\omega_{K,2})$ *be solution of (4.14). Then there exists some constant* $C_{rel}^{Ritz} > 0$ *independent of mesh size* h_L *and polynomial degree* p_L *such that:*

$$\begin{aligned}\|\nabla(w_u - w_{u_{FE}})\|_{\omega_{K,2}}^2 + \|w_{\varrho,K} - w_{\varrho_{FE},K}\|_{\omega_{K,2}}^2 \leq & C_{rel}^{Ritz} \Bigg(\tilde{\eta}_L^2(K) \\ & + \sum_{L \in \omega_{K,2}} \frac{h_L^2}{p_L^2} \|j - I_{p_L}^L j\|_L^2 \Bigg).\end{aligned}$$

Proof. First we set the error terms corresponding to the equations (4.12) and (4.14) as $e_{Ritz} := w_u - w_{u_{\text{FE}}}$ and $\epsilon_{Ritz} := w_\varrho - w_{\varrho_{\text{FE}}}$. Remember that w_u and w_ϱ are the solution of the following variational problem

$$(\nabla\phi, \nabla w_u)_{\omega_{K,2}} = (\phi, j)_{\omega_{K,2}} - \Big[(\nabla\phi, \nabla z_{u_{\text{FE}}})_{\omega_{K,2}} - (\nabla\cdot\phi, z_{\varrho_{\text{FE}}})_{\omega_{K,2}} \Big], \tag{4.40}$$

$$(q, w_\varrho)_{\omega_{K,2}} = (q, \nabla\cdot z_{u_{\text{FE}}}). \tag{4.41}$$

Let $\Pi^{hp} : H_0^1(\omega_{k,2}) \longrightarrow \mathcal{V}^{p+1}(\mathcal{T}|_{\omega_{k,2}})$ be a bounded linear interpolation operator from Theorem

2.2.3. By Galerkin-orthogonality, we get

$$\int_{\omega_{k,2}} \nabla e_{Ritz} \cdot \nabla \Pi^{hp} e_{Ritz} = 0.$$

Therefore

$$\|\nabla e_{Ritz}\|^2_{\omega_{K,2}} = \|\nabla(w_u - w_{u_{\text{FE}}})\|^2_{\omega_{K,2}} = \int_{\omega_{K,2}} \nabla e_{Ritz} \cdot \nabla(e_{Ritz} - \Pi^{hp} e_{Ritz}).$$

From (4.40) we get

$$\begin{aligned}
\|\nabla e_{Ritz}\|^2_{\omega_{K,2}} = \sum_{L \in \omega_{K,2}} \Bigg(& \Big(j, (e_{Ritz} - \Pi^{hp} e_{Ritz}) \Big)_L - \Big(\nabla z_{u_{\text{FE}}}, \nabla(e_{Ritz} - \Pi^{hp} e_{Ritz}) \Big)_L \\
& + \Big(z_{\varrho_{\text{FE}}}, \nabla \cdot (e_{Ritz} - \Pi^{hp} e_{Ritz}) \Big)_L - \Big(\nabla w_{u_{\text{FE}}}, \nabla(e_{Ritz} - \Pi^{hp} e_{Ritz}) \Big)_L \Bigg) \\
= & \sum_{L \in \omega_{K,2}} \int_L j(e_{Ritz} - \Pi^{hp} e_{Ritz}) - \int_L \nabla(z_{u_{\text{FE}}} + w_{u_{\text{FE}}}) \nabla(e_{Ritz} - \Pi^{hp} e_{Ritz}) \\
& + \int_L z_{\varrho_{\text{FE}}} \nabla \cdot (e_{Ritz} - \Pi^{hp} e_{Ritz}).
\end{aligned} \tag{4.42}$$

Using integration by parts and letting $j = j - I^L_{p_L} j + I^L_{P_L} j$ we will get

$$\begin{aligned}
\|\nabla e_{Ritz}\|^2_{\omega_{K,2}} = \sum_{L \in \omega_{K,2}} \Bigg(& \int_L (j - I^L_{p_L} j)(e_{Ritz} - \Pi^{hp} e_{Ritz}) \\
& + \int_L (I^L_{p_L} j + \Delta z_{u_{\text{FE}}} + \Delta w_{u_{\text{FE}}} - \nabla z_{\varrho_{\text{FE}}})(e_{Ritz} - \Pi^{hp} e_{Ritz}) \\
& + \frac{1}{2} \sum_{e \in (\omega_{K,2}, L)} \int_e \left(\frac{\partial w_{u_{\text{FE}}}}{\partial n_L} + \frac{\partial z_{u_{\text{FE}}}}{\partial n_L} \right) \Big(e_{Ritz} - \Pi^{hp} e_{Ritz} \Big) \Bigg).
\end{aligned} \tag{4.43}$$

To get the upper bound of (4.43) by using Theorem 2.2.3 we will get

$$|I| := \left| \int_L (j - I^L_{p_L} j)(e_{Ritz} - \Pi^{hp} e_{Ritz}) \right| \leq C_{SZ} \frac{h_L}{p_L} \left\| j - I^L_{p_L} j \right\|_L \left\| \nabla e_{Ritz} \right\|_{\omega_{L,1}}, \tag{4.44}$$

$$
\begin{aligned}
|II| &:= \left| \int_L (I_{p_L}^L j + \Delta z_{u_{\text{FE}}} + \Delta w_{u_{\text{FE}}} - \nabla z_{\varrho_{\text{FE}}})(e_{Ritz} - \Pi^{hp} e_{Ritz}) \right| \\
&\leq C_{SZ} \frac{h_L}{p_L} \left\| I_{p_L}^L j + \Delta z_{u_{\text{FE}}} + \Delta w_{u_{\text{FE}}} - \nabla z_{\varrho_{\text{FE}}} \right\|_L \left\| \nabla e_{Ritz} \right\|_{\omega_L},
\end{aligned}
\tag{4.45}
$$

$$
\begin{aligned}
\frac{1}{2}|III| &:= \frac{1}{2} \left| \sum_{e \in (\omega_{K,2}, L)} \int_e (\frac{\partial w_{u_{\text{FE}}}}{\partial n_L} + \frac{\partial z_{u_{\text{FE}}}}{\partial n_L})(e_{Ritz} - \Pi^{hp} e_{Ritz}) \right| \\
&\leq \frac{1}{2} C_{SZ} \sum_{e \in (\omega_{K,2}, L)} \sqrt{\frac{h_e}{p_e}} \left(\left\| \left[\frac{\partial w_{u_{\text{FE}}}}{\partial n_L} \right] \right\|_e + \left\| \left[\frac{\partial z_{u_{\text{FE}}}}{\partial n_L} \right] \right\|_e \right) \left\| \nabla e_{Ritz} \right\|_{\omega_L}.
\end{aligned}
\tag{4.46}
$$

Adding the above equations together and put in equation (4.43) gives

$$
\begin{aligned}
\|\nabla e_{Ritz}\|_{\omega_{K,2}}^2 \leq & C \Bigg(\frac{h_L}{p_L} \| I_{p_L}^L j + \Delta z_{u_{\text{FE}}} + \Delta w_{u_{\text{FE}}} - \nabla z_{\varrho_{\text{FE}}} \|_L \\
& + \frac{1}{2} \sum_{e \in (\omega_{K,2}, L)} \sqrt{\frac{h_e}{p_e}} \left(\left\| \left[\frac{\partial w_{u_{\text{FE}}}}{\partial n_L} \right] \right\|_e + \left\| \left[\frac{\partial z_{u_{\text{FE}}}}{\partial n_L} \right] \right\|_e \right) \\
& + \frac{h_L}{p_L} \left\| j - I_{p_L}^L j \|_L \| \nabla e_{Ritz} \|_{\omega_{L,1}} \right) \left\| \nabla e_{Ritz} \right\|_{\omega_{K,2}}.
\end{aligned}
\tag{4.47}
$$

Similarly for the second error term we have

$$
\begin{aligned}
\|\epsilon_{Ritz}\|_{\omega_{K,2}}^2 = \|w_\varrho - w_{\varrho_{\text{FE}}}\|_{\omega_{K,2}}^2 &= \left| \int_{\omega_{K,2}} \epsilon_{Ritz} \cdot \epsilon_{Ritz} \right| \\
&= \left| \int_{\omega_{K,2}} \nabla \cdot z_{u_{\text{FE}}} \epsilon_{Ritz} - w_{\varrho_{\text{FE}}} \epsilon_{Ritz} \right| \\
&= \left| \int_{\omega_{K,2}} (\nabla \cdot z_{u_{\text{FE}}} - w_{\varrho_{\text{FE}}}) \epsilon_{Ritz} \right| \\
&\leq \|\nabla \cdot z_{u_{\text{FE}}} - w_{\varrho_{\text{FE}}}\|_{\omega_{K,2}} \|\epsilon_{Ritz}\|_{\omega_{K,2}}.
\end{aligned}
\tag{4.48}
$$

Adding up equations (4.47) and (4.48) and by definition of the residual estimator

$$
\|\nabla e\|_{\omega_{K,2}}^2 + \|\epsilon\|_{\omega_{K,2}}^2 \leq C_{rel}^{Ritz} \left(\tilde{\eta}_L^2(K) + \sum_{L \in \omega_{K,2}} \frac{h_L^2}{p_L^2} \|j - \Pi j\|_{\omega_{K,2}}^2 \right).
\tag{4.49}
$$

□

4.3 Goal-oriented a posteriori error estimator

Similar to the the a posteriori error estimator for the primal problem, the goal-oriented a posteriori error estimator ζ can also be decomposed into local error estimators on each cell ζ_K:

$$\zeta^2 := \sum_{K \in \mathcal{T}} \zeta_K^2.$$

The goal-oriented local error estimators ζ_K^2 are defined as

$$\zeta_K^2 := \rho_K^2 \ \eta_K^2, \tag{4.50}$$

where the local weight ρ_K is given by

$$\rho_K^2 := \tilde{\eta}(K)^2 + \|\nabla w_{u_{\mathrm{FE}}}\|_{\omega_{K,2}}^2 + \|w_{\varrho_{\mathrm{FE}}}\|_{\omega_{K,2}}^2. \tag{4.51}$$

Here $\tilde{\eta}(K)$ is derived from variational equation (4.12), and $(\nabla w_{u_{\mathrm{FE}}}, w_{\varrho_{\mathrm{FE}}})$ are the solutions of the discrete variational equation (4.14), where we took the energy norm of those solutions. Before showing the reliability and efficiency of the proposed goal-oriented a posteriori error estimator, the following lemmas give some auxiliary results which will be used later in the proof of reliability and efficiency for the goal-oriented error and estimator.

Lemma 4.3.1. *Let $(z_{u_{FE}}, z_{\varrho_{FE}}) \in \mathcal{V}^p(\mathcal{T})$ be the solution of (4.4), $K \in \mathcal{T}$ and $L \in \omega_{K,2}$ be arbitrary. Moreover assume $(w_u, w_\varrho) \in \mathcal{H}(\omega_{K,2})$ be the solution of (4.12) and $(w_{u_{FE}}, w_{\varrho_{FE}}) \in \mathcal{V}^{p+1}(\omega_{K,2})$ be the solution of (4.14). Then there exists some constant $C > 0$ independent of mesh size h_L and polynomial degree p_L such that:*

$$\|\nabla(z_u - z_{u_{FE}})\|_{\omega_{K,1}}^2 + \|z_\varrho - z_{\varrho_{FE}}\|_{\omega_{K,1}}^2 \leq C(\|\nabla w_u\|_{\omega_{K,2}}^2 + \|w_\varrho\|_{\omega_{K,2}}^2). \tag{4.52}$$

Proof. The Proof easily follows from theorem 6.1 of [57] by Ainsworth and Oden.

□

Lemma 4.3.2. *Let $(z_{u_{FE}}, z_{\varrho_{FE}}) \in \mathcal{V}^p(\mathcal{T})$ be the solution of (4.4), $K \in \mathcal{T}$ and $L \in \omega_{K,2}$ be arbitrary. Moreover assume $(w_u, w_\varrho) \in \mathcal{H}(\omega_{K,2})$ be the solution of (4.12) and $(w_{u_{FE}}, w_{\varrho_{FE}}) \in \mathcal{V}^{p+1}(\omega_{K,2})$ be the solution of (4.14). Then there exists some constant $C > 0$ independent of mesh size h_L and polynomial degree p_L such that:*

$$\begin{aligned} \|\nabla(w_u - w_{u_{FE}})\|^2_{\omega_{K,2}} + \|\nabla w_{u_{FE}}\|^2_{\omega_{K,2}} + \|w_\varrho - w_{\varrho_{FE}}\|^2_{\omega_{K,2}} + \|w_{\varrho_{FE}}\|^2_{\omega_{K,2}} \\ \leq C\|\nabla(z_u - z_{u_{FE}})\|^2_{\omega_{K,2}} + \|z_\varrho - z_{\varrho_{FE}}\|^2_{\omega_{K,2}}. \end{aligned} \tag{4.53}$$

Proof. Consider the solution of equations (4.12) and (4.14) and using the triangle inequality, for some C_1 and $C_2 > 0$ we have

$$\|\nabla(w_u - w_{u_{\text{FE}}})\|^2_{\omega_{K,2}} \leq C_1(\|\nabla w_u\|^2_{\omega_{K,2}} + \|\nabla w_{u_{\text{FE}}}\|^2_{\omega_{K,2}}) \tag{4.54}$$

and

$$\|w_\varrho - w_{\varrho_{\text{FE}}}\|^2_{\omega_{K,2}} \leq C_2(\|w_\varrho\|^2_{\omega_{K,2}} + \|w_{\varrho_{\text{FE}}}\|^2_{\omega_{K,2}}). \tag{4.55}$$

By equation (4.13) and also from norm equivalence given in equation (6.15) of [57] we get

$$\begin{aligned} (\|\nabla w_u\|^2_{\omega_{K,2}} + \|w_\varrho\|^2_{\omega_{K,2}})^{\frac{1}{2}} &= |||(e^d, E^d)|||_{\omega_{K,2}} \\ &\leq C(\|\nabla e^d\|^2_{\omega_{K,2}} + \|E^d\|^2_{\omega_{K,2}})^{\frac{1}{2}} \\ &= C(\|\nabla(z_u - z_{u_{\text{FE}}})\|^2_{\omega_{K,2}} + \|z_\varrho - z_{\varrho_{\text{FE}}}\|^2_{\omega_{K,2}})^{\frac{1}{2}}. \end{aligned} \tag{4.56}$$

Using the results given in Theorems 3.1 and 3.2 and equations (3.14) and (3.15) of [81] we have

$$(\|\nabla w_{u_{\text{FE}}}\|^2_{\omega_{K,2}} + \|w_{\varrho_{\text{FE}}}\|^2_{\omega_{K,2}})^{\frac{1}{2}} \leq (\|\nabla(z_u - z_{u_{\text{FE}}})\|^2_{\omega_{K,2}} + \|z_\varrho - z_{\varrho_{\text{FE}}}\|^2_{\omega_{K,2}})^{\frac{1}{2}}. \tag{4.57}$$

The proof completes by combining equations (4.54)-(4.57).

□

Theorem 4.3.3 (Reliability of Goal-Oriented A posteriori Error Estimation)**.** *Let* $(u, \varrho) \in \mathcal{H}$ *be the solution of (2.3) and* $(u_{FE}, \varrho_{FE}) \in \mathcal{V}^{p+1}$ *be the solution of (2.10). Further let* $(z_u, z_\varrho) \in \mathcal{H}$ *be the solution of (4.2) and* $(z_{u_{FE}}, z_{\varrho_{FE}}) \in \mathcal{V}^p(\mathcal{T})$ *be the solution of (4.4),* $K \in \mathcal{T}$ *be arbitrary, then there exists a constant* $C > 0$ *independent of mesh size* h_K *and polynomial degree vector* p_K *such that*

$$|J(u,\varrho) - J(u_{FE},\varrho_{FE})|^2 \leq C_{rel} \sum_{K\in\mathcal{T}} \left(\eta_K^2(u_{FE},\varrho_{FE}, I_{p_K}^K f) + \frac{h_K^2}{p_K^2}\|f - I_{p_K}^K f\|_K^2 \right) \left(\rho_K^2 + \frac{h_K^2}{p_K^2}\|j - I_{p_K}^K\|_{\omega_{K,2}}^2 \right).$$

Proof. By definition given in (4.3) and (4.4)

$$J(u,\varrho)_\Omega = (\nabla u, \nabla z_u)_\Omega - (\nabla\cdot u, z_\varrho)_\Omega - (\varrho, \nabla\cdot z_u)_\Omega, \tag{4.58}$$

and

$$J(u_{\text{FE}},\varrho_{\text{FE}})_\Omega = (\nabla u_{\text{FE}}, \nabla z_u)_\Omega - (\nabla\cdot u_{\text{FE}}, z_\varrho)_\Omega - (\varrho_{\text{FE}}, \nabla\cdot z_u)_\Omega. \tag{4.59}$$

Subtracting equations (4.58) and (4.59) gives

$$\begin{aligned} J(u,\varrho)_\Omega - J(u_{\text{FE}},\varrho_{\text{FE}})_\Omega =& (\nabla(u-u_{\text{FE}}), \nabla z_u)_\Omega - (\nabla\cdot(u-u_{\text{FE}}), z_\varrho)_\Omega \\ & - (\varrho - \varrho_{\text{FE}}, \nabla\cdot z_u)_\Omega. \end{aligned} \tag{4.60}$$

The error terms corresponding to the solution of dual problem (4.2) are defined as $e^d := z_u - z_{u_{\text{FE}}}$ and $E^d := z_\varrho - z_{\varrho_{\text{FE}}}$. By Galerkin orthogonality we have

$$\mathcal{L}([u-u_{\text{FE}}, \varrho-\varrho_{\text{FE}}]; [z_{u_{\text{FE}}} - \Pi^{hp} e^d, z_{\varrho_{\text{FE}}}]) = 0. \tag{4.61}$$

Inserting (4.61) into (4.60) we will get

$$\begin{aligned} J(u,\varrho)_\Omega - J(u_{\text{FE}},\varrho_{\text{FE}})_\Omega &= (\nabla(u-u_{\text{FE}}),\nabla(e^d-\Pi^{hp}e^d))_\Omega \\ &\quad -(\nabla\cdot(u-u_{\text{FE}}),z_\varrho - z_{\varrho_{\text{FE}}})_\Omega \\ &\quad -(\varrho-\varrho_{\text{FE}},\nabla\cdot(e-\Pi^{hp}e^d))_\Omega. \end{aligned} \tag{4.62}$$

Using integration by parts gives

$$\begin{aligned} |J(u,\varrho)_\Omega - J(u_{\text{FE}},\varrho_{\text{FE}})_\Omega| \leq \sum_{K\in\mathcal{T}} \Bigg(& \int_K -\Delta(u-u_{\text{FE}})(e^d-\Pi^{hp}e^d) \\ & + \int_K \nabla(\varrho-\varrho_{\text{FE}})(e^d-\Pi^{hp}e^d) \\ & - \int_K \nabla\cdot(u-u_{\text{FE}})(z_\varrho - z_{\varrho_{\text{FE}}}) \\ & + \sum_{e\in\mathcal{E}(\mathcal{T})}\int_e \left[\frac{\partial u_{\text{FE}}}{\partial n_K}\right]\Big(e^d-\Pi^{hp}e^d\Big)\Bigg) \\ & = \sum_{K\in\mathcal{T}}\Bigg((f+\Delta u_{\text{FE}}-\nabla\varrho_{\text{FE}},e^d-\Pi^{hp}e^d)_K \\ & + (\nabla\cdot(u-u_{\text{FE}}),z_\varrho - z_{\varrho_{\text{FE}}})_K \\ & + \sum_{e\in\mathcal{E}(\mathcal{T})}\left(\left[\frac{\partial u_{\text{FE}}}{\partial n_K}\right],e^d-\Pi^{hp}e^d\right)_e\Bigg) \\ & = \sum_K\Bigg((I_K^{p_K}f+\Delta u_{\text{FE}}-\nabla\varrho_{\text{FE}},e^d-\Pi^{hp}e^d)_K \\ & + (f-I_K^{p_K}f,e^d-\Pi^{hp}e^d)_K \\ & + (\nabla\cdot(u-u_{\text{FE}}),z_\varrho - z_{\varrho_{\text{FE}}})_K \\ & + \sum_{e\in\mathcal{E}(\mathcal{T};\mathcal{K})}\left(\left[\frac{\partial u_{\text{FE}}}{\partial n_K}\right],e^d-\Pi^{hp}e^d\right)_e\Bigg). \end{aligned} \tag{4.63}$$

$$|J(u,\varrho)_\Omega - J(u_{\text{FE}},\varrho_{\text{FE}})_\Omega|^2 \leq C\sum_K (T_1^2(K)+T_2^2(K)+T_3^2(K)+T_4^2(K)). \tag{4.64}$$

Using the Cauchy-Schwarz inequality and also Scott-Zhang interpolation, Theorem 2.2.3 gives

$$\begin{aligned}|T_1^2(K)| &:= |(I_K^{p_K} f + \Delta u_{\text{FE}} - \nabla \varrho_{\text{FE}}, e^d - \Pi^{hp} e^d)_K|^2 \\ &\leq C_{SZ} \frac{h_K^2}{p_K^2} \|I_K^{p_K} f + \Delta u_{\text{FE}} - \nabla \varrho_{\text{FE}}\|_K^2 \cdot \|\nabla(z_u - z_{u_{\text{FE}}})\|_{\omega_{K,1}}^2.\end{aligned}$$

$$\begin{aligned}|T_2^2(K)| &:= |(f - I_K^{p_K} f, e^d - \Pi^{hp} e^d)_K| \\ &\leq C_{SZ} \frac{h_K^2}{p_K^2} \|f - I_K^{p_K} f\|_K^2 \|\nabla(z_u - z_{u_{\text{FE}}})\|_K^2.\end{aligned}$$

$$|T_3^2(K)| := |(\nabla \cdot (u - u_{\text{FE}}), z_\varrho - z_{\varrho_{\text{FE}}})_K| \leq \|\nabla \cdot u_{\text{FE}}\|_K^2 \|z_\varrho - z_{\varrho_{\text{FE}}}\|_K^2.$$

$$\begin{aligned}|T_4^2(K)| &:= \left| \sum_{e \in \mathcal{E}(\mathcal{T};\mathcal{K})} \left(\left[\frac{\partial u_{\text{FE}}}{\partial n_K} \right], e^d - \Pi^{hp} e^d \right)_e \right| \\ &\leq 2C_{SZ} \sum_{e \in \mathcal{E}(\mathcal{T};\mathcal{K})} \frac{h_e}{2p_e} \left\| \left[\frac{\partial u_{\text{FE}}}{\partial n_K} \right] \right\|_e^2 \|\nabla(z_u - z_{u_{\text{FE}}})\|_{\omega_{K,1}}^2.\end{aligned}$$

$$\begin{aligned}|J(u, \varrho)_\Omega - J(u_{\text{FE}}, \varrho_{\text{FE}})_\Omega|^2 \leq C &\left(\eta_{K,R}^2 + \eta_{K,B}^2 + \frac{h_K^2}{p_K^2} \|f - I_K^{p_K} f\|_K^2 \right) \\ &\left(\|\nabla(z_u - z_{u_{\text{FE}}})\|_{\omega_{K,1}}^2 + \|z_\varrho - z_{\varrho_{\text{FE}}}\|_{\omega_{K,1}}^2 \right).\end{aligned} \tag{4.65}$$

By Lemma 4.3.1, for some $C > 0$ we have

$$\|\nabla(z_u - z_{u_{\text{FE}}})\|_{\omega_{K,1}}^2 + \|z_\varrho - z_{\varrho_{\text{FE}}}\|_{\omega_{K,1}}^2 \leq C(\|\nabla w_u\|_{\omega_{K,2}}^2 + \|w_p\|_{\omega_{K,2}}^2). \tag{4.66}$$

The triangle inequality then gives

$$\begin{aligned}\|\nabla w_u\|_{\omega_{K,2}} + \|w_\varrho\|_{\omega_{K,2}} \leq &\|\nabla(w_u - w_{u_{\text{FE}}})\|_{\omega_{K,2}} + \|\nabla w_{u_{\text{FE}}}\| \\ &+ \|w_\varrho - w_{\varrho_{\text{FE}}}\|_{\omega_{K,2}} + \|w_{\varrho_{\text{FE}}}\|_{\omega_{K,2}} \\ &= (\|\nabla(w_u - w_{u_{\text{FE}}})\|_{\omega_{K,2}} + \|w_\varrho - w_{\varrho_{\text{FE}}}\|_{\omega_{K,2}}) \\ &+ (\|\nabla w_{u_{\text{FE}}}\|_{\omega_{K,2}} + \|w_{\varrho_{\text{FE}}}\|_{\omega_{K,2}}).\end{aligned}$$

By Theorem $(4.2.6)$, and equations (4.50) and (4.51) we have

$$\begin{aligned}\|\nabla w_u\|^2_{\omega_{K,2}} + \|w_\varrho\|^2_{\omega_{K,2}} \leq & C_{rel}\left(\tilde{\eta}(K)^2 + \sum_K \frac{h_K}{p_K}\|j - I_K^{p_K} j\|^2_{\omega_{K,2}}\right) \\ & + \|\nabla w_{u_{\text{FE}}}\|^2_{\omega_{K,2}} + \|w_{\varrho_{\text{FE}}}\|^2_{\omega_{K,2}} \\ & = C\left(\rho_K^2 + \frac{h_K^2}{p_K^2}\|j - I_K^{p_K} j\|^2_{\omega_{K,2}}\right).\end{aligned} \tag{4.67}$$

The final reliability result comes by letting the equation (4.67) into (4.65). □

Theorem 4.3.4 (Efficiency of Goal-Oriented A posteriori Error Estimation)**.** *Let $(u, \varrho) \in \mathcal{H}$ be the solution of (2.3) and $(u_{FE}, \varrho_{FE}) \in \mathcal{V}^{p+1}$ be the solution of (2.10). Further let $(z_u, z_\varrho) \in \mathcal{H}$ be the solution of (4.2) and $(z_{u_{FE}}, z_{\varrho_{FE}}) \in \mathcal{V}^p(\mathcal{T})$ be the solution of (4.4), $K \in \mathcal{T}$ be arbitrary, then there exists a constant $C > 0$ independent of mesh size h_K and polynomial degree vector p_K such that*

$$\begin{aligned}\xi_K^2 \leq & C_{eff}\left(p_K^2(\|\nabla(u - u_{FE})\|^2_{\omega_{K,1}} + \|\varrho - \varrho_{FE}\|^2_{\omega_{K,1}}) + \frac{h_K^2}{p_K}\|f - \Pi f\|_{\omega_{K,1}}\right)\times \\ & \left(p_K^{\frac{3+\varepsilon}{2}}(\|\nabla(z_u - z_{u_{FE}})\|^2_{\omega_{K,3}} + \|z_\varrho - z_{\varrho_{FE}}\|^2_{\omega_{K,3}}) + \frac{h_K^2}{p^{\frac{1+\varepsilon}{2}}}\|j - I_K^{p_K} j\|^2_{\omega_{K,2}}\right)\end{aligned}$$

Proof. By equation (4.50) we know that $\zeta_K^2 := \rho_K^2\ \eta_K^2$. Equation (4.9) of Lemma $4.2.1$ implies

$$\eta_K^2 \leq C_{\text{eff}}\left(p_K^2\left(\|\nabla\left(u - u_{\text{FE}}\right)\|^2_{\omega_K} + \|\varrho - \varrho_{\text{FE}}\|^2_{\omega_K}\right) + \frac{h_K^2}{p_K}\left\|I^K_{p_K} f - f\right\|^2_{\omega_K}\right), \tag{4.68}$$

also from equation (4.51) we have

$$\rho_K^2 := \tilde{\eta}(K)^2 + \|\nabla w_{u,\text{FE}}\|^2_{\omega_{K,2}} + \|w_{\varrho,\text{FE}}\|^2_{\omega_{K,2}}, \tag{4.69}$$

using the efficiency results given in Lemma 4.2.5

$$\tilde{\eta}^2(K) = \sum_{L \in \omega_{K,2}} \tilde{\eta}_L^2 \leq C_{\text{eff}}\, p_K^{\frac{3+\epsilon}{2}} \left(\|\nabla(w_u - w_{u_{\text{FE}}})\|^2_{\omega_{K,3}} + \|w_\varrho - w_{\varrho_{\text{FE}}}\|^2_{\omega_{K,3}} \right) + \frac{h_L^2}{p_L^{\frac{1+\epsilon}{2}}} \|j - I^L_{p_L} j\|^2_{\omega_{K,3}}.$$

Therefore equation (4.51) reads as

$$\begin{aligned} \rho_K^2 \leq & C^d_{eff} \Bigg(p_L^{\frac{3+\epsilon}{2}} \left(\|\nabla(w_{u,K} - w_{u_{\text{FE}},K})\|^2_{\omega_{K,3}} + \|w_{\varrho,K} - w_{\varrho_{\text{FE}},K}\|^2_{\omega_{K,3}} \right) \\ & + \|\nabla w_{u,\text{FE}}\|^2_{\omega_{K,3}} + \|w_{\varrho,\text{FE}}\|^2_{\omega_{K,3}} + \frac{h_L^2}{p_L^{\frac{1+\epsilon}{2}}} \|j - I^L_{p_L} j\|^2_{\omega_{K,3}} \Bigg). \end{aligned} \tag{4.70}$$

By Lemma 4.3.2

$$\rho_K^2 \leq C \left(p_L^{\frac{3+\epsilon}{2}} \left(\|\nabla(z_u - z_{u_{\text{FE}}})\|^2_{\omega_{K,3}} + \|z_\varrho - z_{\varrho_{\text{FE}}}\|^2_{\omega_{K,3}} \right) + \frac{h_L^2}{p_L^{\frac{1+\varepsilon}{2}}} \|j - I^L_{p_L} j\|^2_{\omega_{K,3}} \right). \tag{4.71}$$

The result immediately follows by multiplying equations (4.68) and (4.70). □

4.4 Goal-oriented h- and hp-AFEM refinement strategy

We present a fully automatic h- and hp-adaptive refinement strategy using the proposed goal-oriented error estimator. The algorithm relies on the standard adaptive refinement loop of the form

$$\text{SOLVE} \longrightarrow \text{ESTIMATE} \longrightarrow \text{MARK} \longrightarrow \text{REFINE}. \tag{4.72}$$

4.4.1 GO-h-AFEM algorithm

The fully automatic goal-oriented h-AFEM is shown in Algorithm 2.

4.4.2 GO-hp-AFEM algorithm

Algorithm 3 shows the fully automatic goal-oriented hp-AFEM as follows.

Algorithm 2 Goal-oriented h-AFEM algorithm

- **Initialization**: Set N $= 0$, a coarse mesh $\mathcal{T}_0$, $\theta \in (0, 1]$ and also tolerance TOL.
- **SOLVE primal**: Find the solution $(u_{\text{FE}}, \varrho_{\text{FE}})$ of primal problem (2.10).
- **SOLVE dual**: Find the solution $(z_{u_{\text{FE}}}, z_{\varrho_{\text{FE}}})$ of dual problem (4.4).
- **SOLVE local problems**: Find the solution $(w_{u_{\text{FE}}}, w_{\varrho_{\text{FE}}})$ of local variational problem (4.12) for each cell K.
- **ESTIMATE**: Compute goal-oriented a posteriori error estimation given by equation (4.50), if $\zeta_K <$ TOL then STOP the algorithm.
- **MARK**: Find set of marked cells $\mathcal{M} \subseteq \mathcal{T}$ with minimal cardinality such that the following fixed fraction property holds:
$$\sum_{k \in \mathcal{M}} \zeta_K^2 \geq \theta^2 \zeta^2 \tag{4.73}$$
- **REFINE** Refine the marked cells and set $N = N + 1$ and go to step **SOLVE primal**.

Algorithm 3 Goal-oriented hp-AFEM algorithm

- **Initialization**: Set N $= 0$, a coarse mesh $\mathcal{T}_0$, $\theta \in (0, 1]$ and also tolerance TOL.
- **SOLVE primal**: Find the solution $(u_{\text{FE}}, \varrho_{\text{FE}})$ of primal problem (2.10).
- **SOLVE dual**: Find the solution $(z_{u_{\text{FE}}}, z_{\varrho_{\text{FE}}})$ of dual problem (4.4).
- **SOLVE local problems**: Find the solution $(w_{u_{\text{FE}}}, w_{\varrho_{\text{FE}}})$ of local variational problem (4.12) for each cell K.
- **ESTIMATE**: Compute goal-oriented a posteriori error estimation given by equation (4.50), if $\zeta_K <$ TOL then STOP the algorithm.
- **MARK**: For each cell $K \in \mathcal{T}_{\mathcal{N}}$ and for all refinement patterns $j \in 1, 2, 3, \cdots, n$, compute the convergence indicator $k_{K,j}$ based on the formulation given in equation (3.20).
- **REFINE**: Refine set of marked cells $\mathcal{M} \subseteq \mathcal{T}$ with minimal cardinality such that the following fixed fraction property holds:
$$\sum_{k \in \mathcal{M}} k_{K,j}^2 \zeta_K^2 \geq \theta^2 \zeta^2, \tag{4.74}$$
set $N = N + 1$ and go to step **SOLVE primal**.

4.5 Numerical results

All the numerical experiments are implemented in $\mathbb{R}^2$, we also set the viscosity $\nu = 1$, and consider Taylor-Hood finite elements $p_{k+1} - p_k$. We want to illustrate the performance of our locally defined dual-weighted goal-oriented error estimator for both h- and hp-adaptive refinement strategy. Instead of newest vertex bisections, which is the ordinary mesh refinement method for triangles, we use the quadrilateral refinement strategy as its refinement rules and the computational complexity is well studied in [88]. Therefore, the initial triangulation $\mathcal{T}_0$ of $\Omega \in \mathbb{R}^2$ and its corresponding refinements are made of quadrilaterals. As implemented in deal.II [76], we let at most one hanging node per edge exists. For the marking strategy in our goal-oriented adaptive refinement we implement exactly the algorithms proposed as Algorithm 2 and Algorithm 3 for the h- and hp-refinement, respectively. In this section, all convergence plots represent the average or asymptotic convergence rates with black dashed and solid lines. As we know from a priori error analysis of finite elements, typically $\mathcal{O}(h^p)$ is the expected convergence rate in the energy norm, where h denotes the diameter of elements. Since in the error analysis of adaptive refinements one ends up to adaptive refinements with non-uniform mesh sizes, it does not make too much sense to use this notation for convergence lines. Instead, we draw the dashed lines with $\mathcal{O}(N^{-\frac{p}{d}})$, where N shows the number of degrees of freedom and d is the space dimension, in our case $d = 2$. It is also important to mention both dual and primal solutions live at the same finite element space. Therefore, it is computationally cheap to compute the solution in this finite element setting. All the implementations are done in the open source finite element library deal.II [76].

Example 1 - Smooth solution in two dimensions

Let $\Omega = (-1, 1) \times (-1, 1)$ be a square domain and the velocity field u and pressure ϱ be given [79] by

$$u = \begin{bmatrix} 2y\cos(x^2 + y^2) \\ -2x\cos(x^2 + y^2) \end{bmatrix}, \qquad \varrho = e^{-10(x^2+y^2)} - p_m,$$

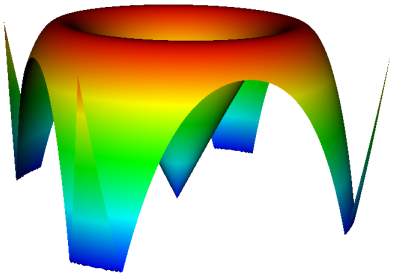

(a) Magnitude of the velocity component of the primal problem.

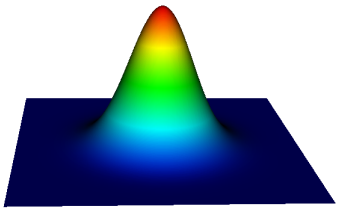

(b) Pressure component of the primal problem.

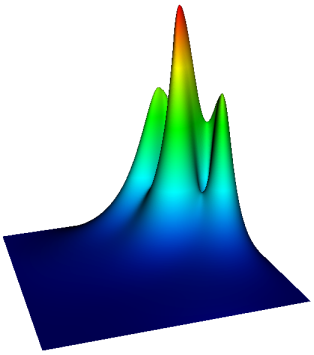

(c) Magnitude of the velocity component of the influence function associated with the average of velocity on $\Omega_1 \subset \Omega$.

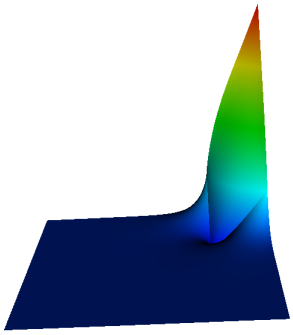

(d) Pressure component of the dual problem.

Figure 4.1: Example-1-a: velocity magnitude and pressure associated with primal and dual problems.

where p_m is defined such that $\int_\Omega \varrho = 0$, and the data is computed as $f = -\Delta u + \nabla \varrho$. In the first example, we are interested in computing two functionals as follows:

4.5.1 Example 1-a : Average of velocity values over $\Omega_1 \subset \Omega$

The first functional of interest is $J(u) = \int_{\Omega_1} (1,1) \cdot u$, where $\Omega_1 = [0.5, 1] \times [0.5, 1]$ and u denotes the velocity vector. The exact solution of primal and dual problem are shown in Figure 4.1. Figure 4.2 shows both h- and hp- adaptive meshes generated by our locally defined dual-weighted

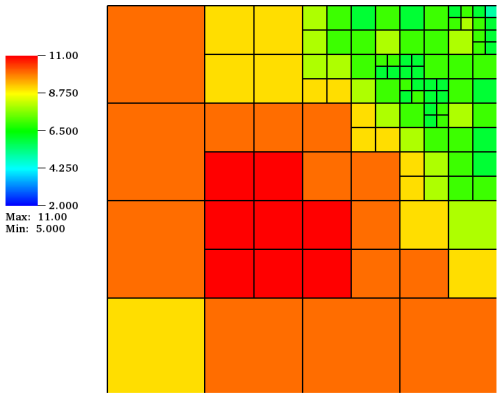

(a) Goal-oriented hp-AFEM

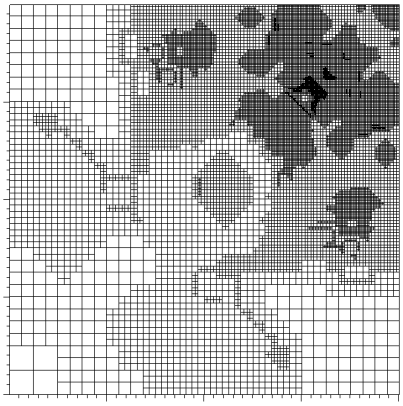

(b) Goal-oriented h-AFEM

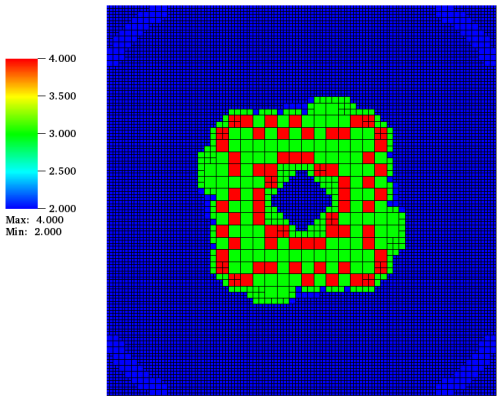

(c) hp-AFEM using Energy-estimate

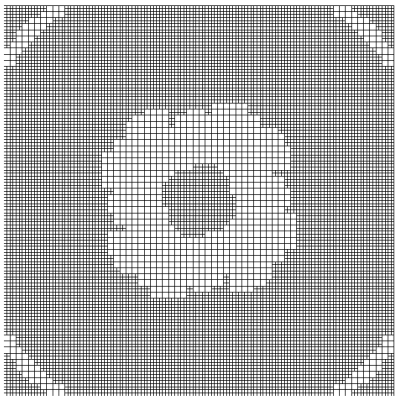

(d) h-AFEM using Energy-estimate

Figure 4.2: Example-1-a: (First row) triangulation produced by h- and hp-GO-AFEM; (Second row) h, hp-AFEM with almost the same number of degrees of freedom.

goal-oriented error estimator namely GO-AFEM and also using the energy error estimator, AFEM. As we can see in 4.2c and 4.2d for the standard AFEM triangulation, the adaptive refinements are made where the energy error estimator captures the largest error in the primal solution. Whereas, in the goal-oriented AFEM in Figures 4.2a and 4.2b, the local refinements appears in areas where the dual solution is non-smooth. For the convergence rate in h-GO-AFEM, it is important to mention that using the $p_2 - p_1$ Taylor-Hood finite elements for smooth primal and dual solutions, their solutions are in nonlinear approximation class $\mathcal{A}^{\frac{p}{d}=\frac{2}{2}}$. Therefore, we expect the decay rate in the

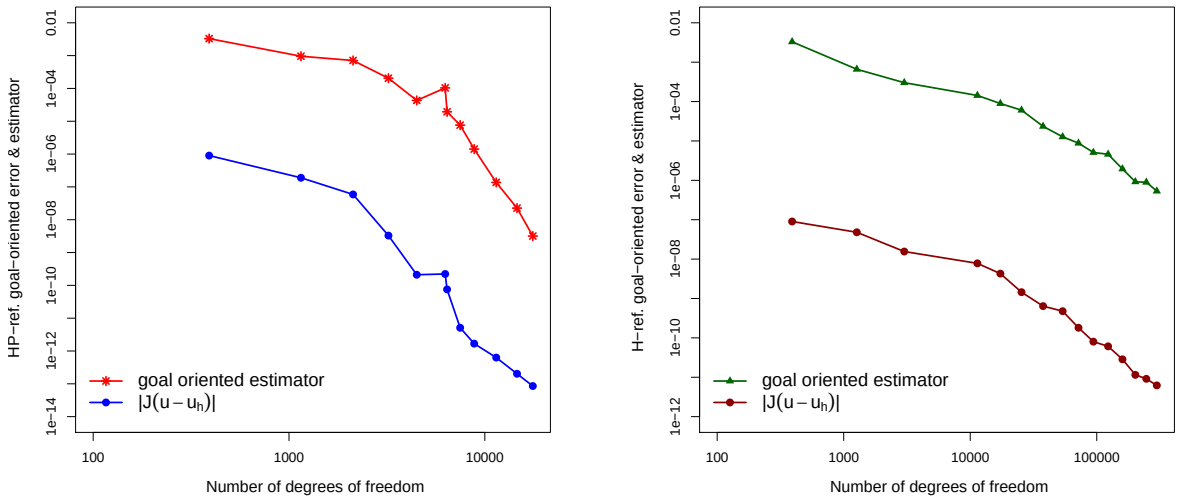

(a) hp-Goal-oriented (b) h-Goal-oriented

Figure 4.3: Example-1-a: Convergence of goal estimator and the goal-functional error for both h- and hp-GO-AFEM.

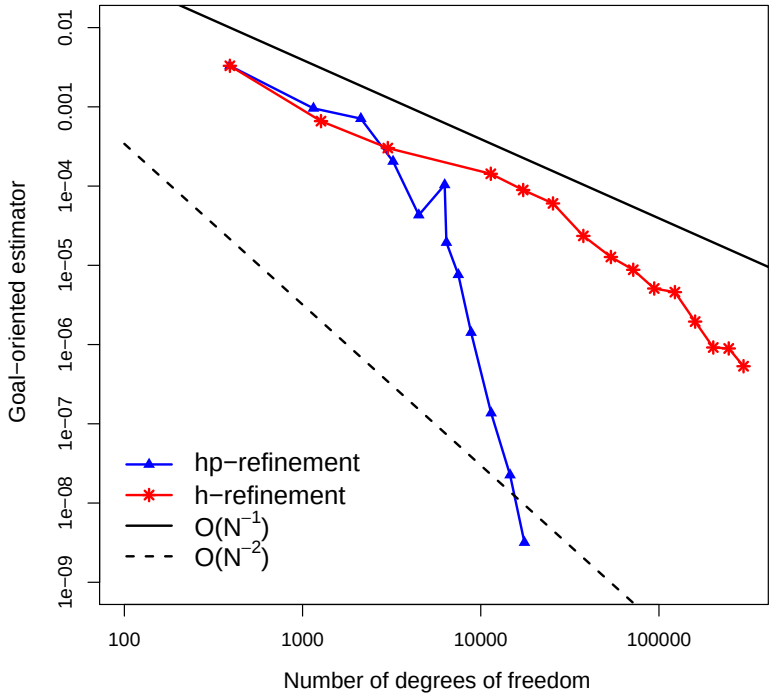

Figure 4.4: Example-1-a: Convergence rate comparison between h- and hp-GO-AFEM.

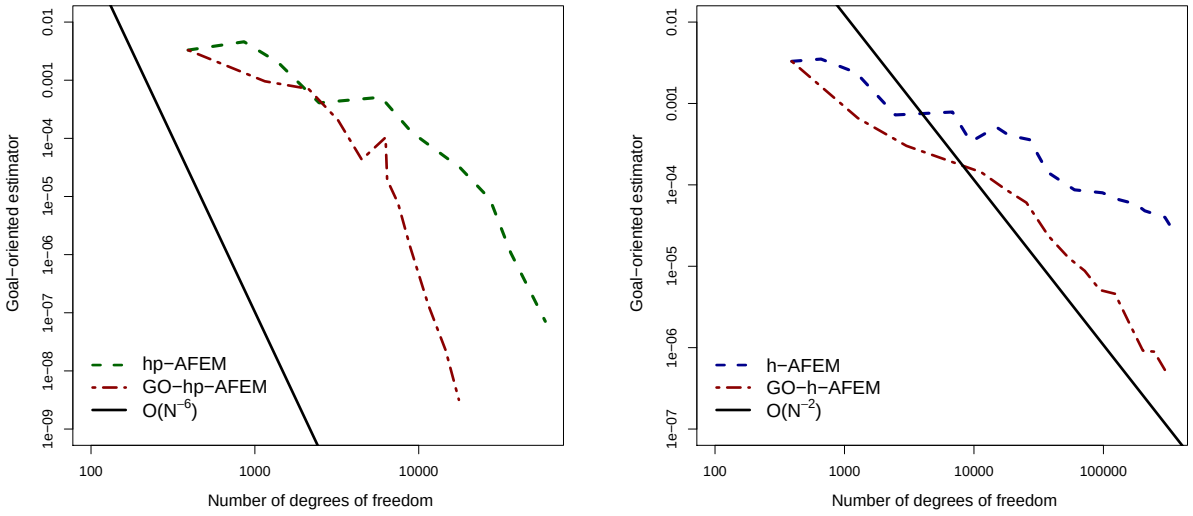

(a) GO-hp- vs. hp- error estimator

(b) GO-h- vs. h- error estimator

Figure 4.5: Example-1-a: Goal-oriented error estimator convergence rate using GO-AFEM and AFEM for both hp and h-adaptive refinement.

functional error is $\mathcal{O}\left(\#\mathcal{T} - \#\mathcal{T}_0\right)^{-2} \approx \mathcal{O}(\mathrm{N}^{-2})$, where N denotes the number of degrees of freedom. Figure 4.3 presents the convergence plots between the functional error and the goal-oriented estimator for both h- and hp-GO-AFEM. Figure 4.4 shows the convergence rate comparison between h- and hp goal-oriented adaptive refinement for the goal-oriented error estimator. We reach to the exponential convergence rate for the hp-GO-AFEM. Moreover, the refinement by h-GO-AFEM converges with expected optimal rate $\mathcal{O}(N^{-2})$. Finally, the last Figure 4.5 demonstrates the convergence rate in the goal-estimator using both goal-oriented and also the energy estimator. We give the results for both h- and hp-adaptive refinements. The solid lines corresponding to the convergence rate in Figures 4.5a and 4.5b are shown to give the measure of convergence rate in both h- and hp-GO-AFEM. Due to the knowledge we have on the convergence rate for the h-GO-AFEM we can claim that our goal-oriented AFEM converges with quasi-optimal rate as expected for the Stokes problem using $p_2 - p_1$ finite elements. From the blue line corresponding to the non goal-oriented h-AFEM in Figure 4.5b, we see its convergence rate is slower than $\mathcal{O}(N^{-2})$.

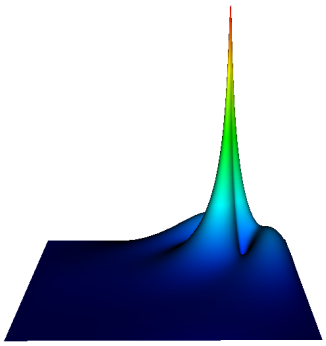

(a) Magnitude of the velocity component of the influence function associated with the point-wise error at (0.5, 0.5).

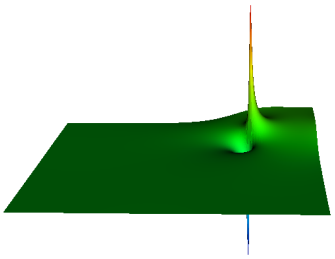

(b) Pressure component of the dual problem.

Figure 4.6: Example-1-b: Exact solutions in dual problem.

4.5.2 Example 1-b : Point-wise value

For the second case, we are interested in the point-wise error at some given point. Therefore, we set the delta function at point $(x_0, y_0) = (0.5, 0.5)$ as the right hand side of the dual problem.

$$j(x,y) = \begin{bmatrix} e^{-\mu((x-0.5)^2+(y-0.5)^2)} \\ e^{-\mu((x-0.5)^2+(y-0.5)^2)} \end{bmatrix}, \tag{4.75}$$

where $\mu = 10^{-4}$. The influence function would converge to the corresponding green's function as μ tends to zero. The goal here is to get the least possible point-wise error using both hp and h adaptive refinement strategy. The exact solutions corresponding to the dual problem are shown in Figure 4.6. Figure 4.7 shows both the h- and hp- adaptive meshes generated by using the locally defined dual-weighted goal-oriented error estimator namely the GO-AFEM. the adaptive triangulations generated by GO-AFEM confirm that the local refinements appears in areas where the dual solution is non-smooth. The convergence plots for both functional error and the goal-oriented estimator in h- and hp-refinements can be seen in Figure 4.8. As the plots in this figure show, the locally defined

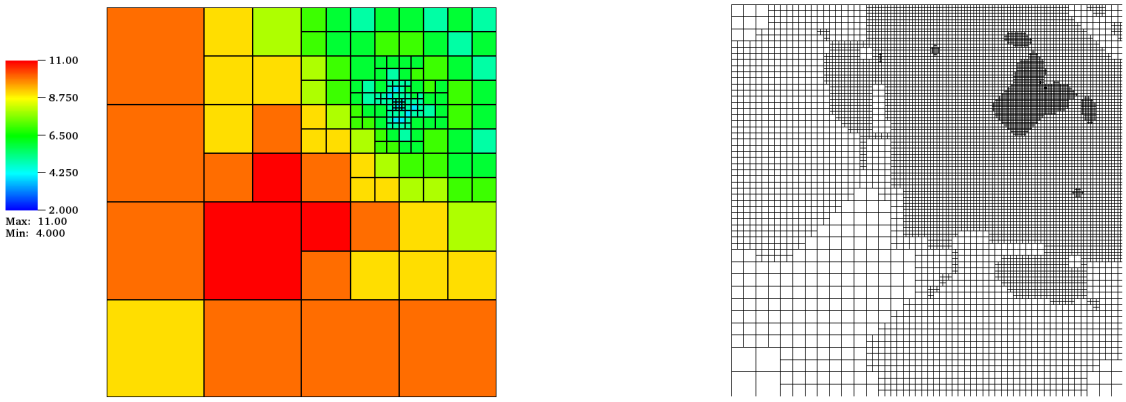

(a) Goal-oriented hp-AFEM (b) Goal-oriented h-AFEM

Figure 4.7: Example-1-b: Triangulation produced by h- and hp-GO-AFEM.

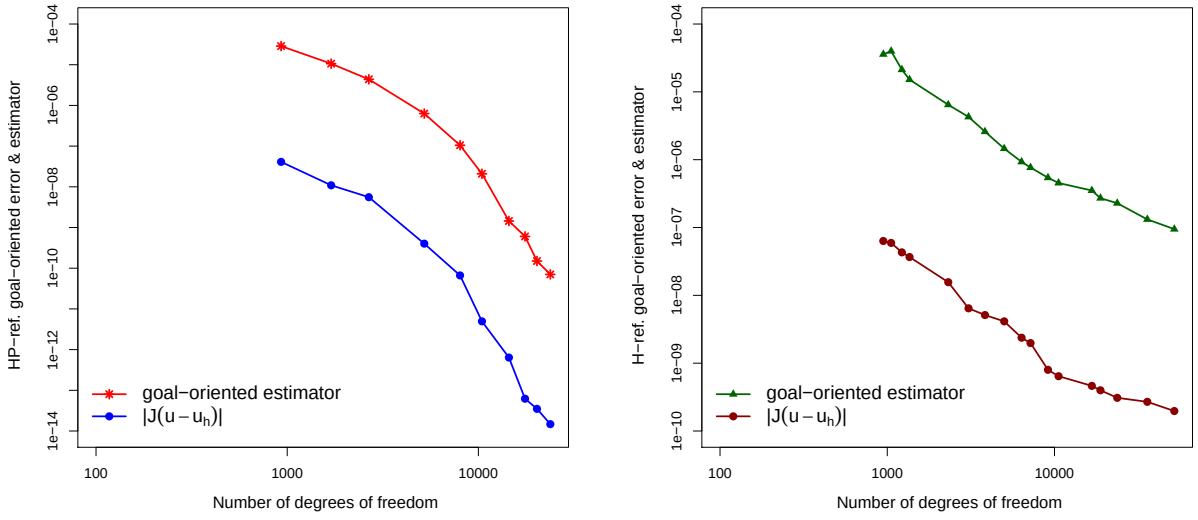

(a) hp-Goal-oriented (b) h-Goal-oriented

Figure 4.8: Example-1-b: Convergence of goal estimator and the goal-functional error for both h- and hp-GO-AFEM.

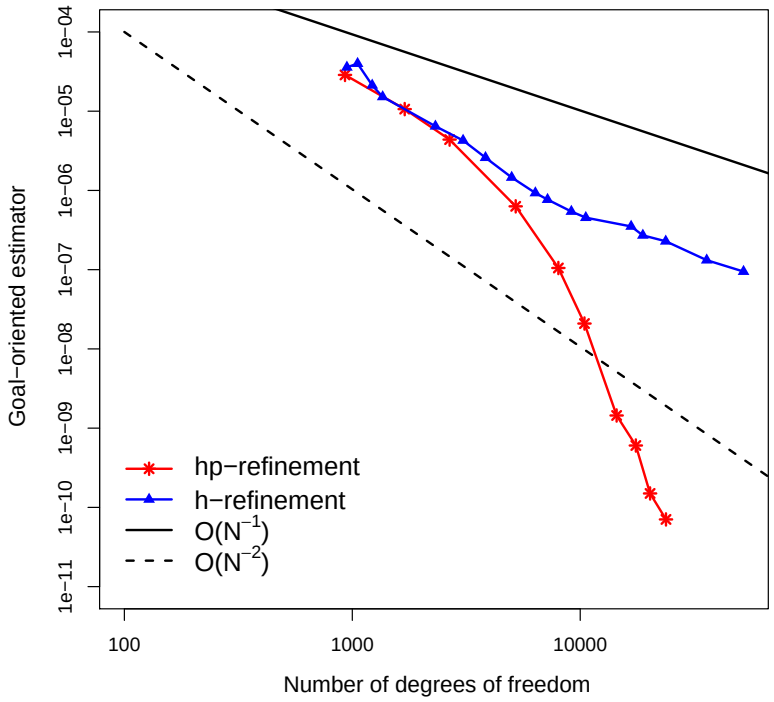

Figure 4.9: Example-1-b: Convergence rate comparison between h- and hp-GO-AFEM.

dual-weighted goal-oriented estimator for both h- and hp- is a reliable estimator for the error in the corresponding functional of interest. Figure 4.9 shows the convergence rate comparison, for the goal-oriented error estimator between h- and hp goal-oriented adaptive refinement. We observe the exponential convergence rate in the hp-GO-AFEM compared with h-GO-AFEM. It is also interesting to see the goal-estimator using h-GO-AFEM decays with the optimal rate $\mathcal{O}(N^{-2})$. The last Figure 4.10 demonstrates the convergence rate in the goal-estimator using GO-AFEM and the traditional AFEM by the energy estimator. We give the results for both h- and hp-adaptive refinements.

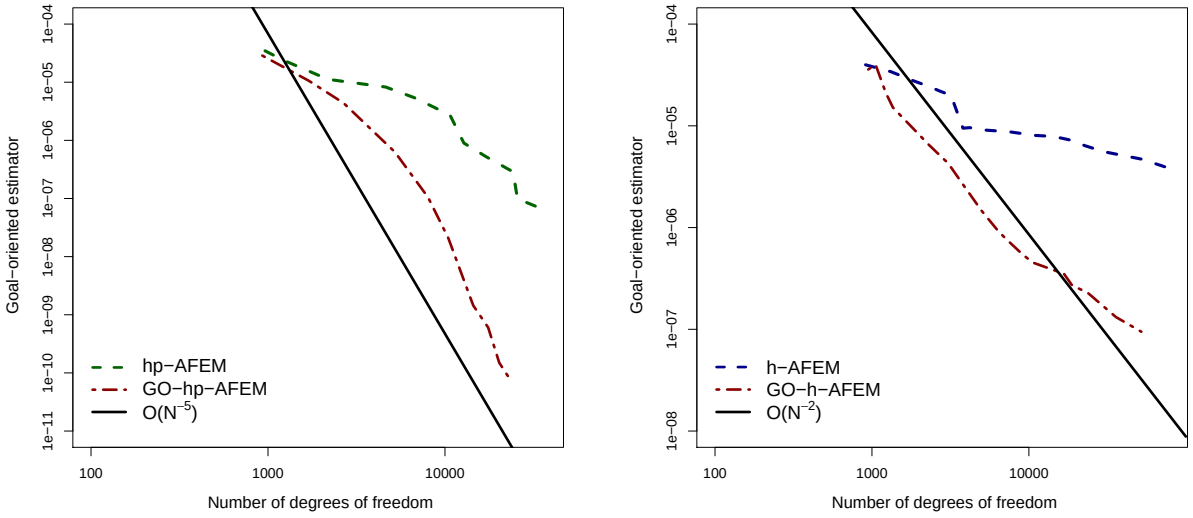

(a) GO-hp- vs. hp- error estimator

(b) GO-h- vs. h- error estimator

Figure 4.10: Example-1-b: Goal-oriented error estimator convergence rate using both GO-AFEM and AFEM.

4.5.3 Example 2 - Singular solution in two dimensions

In this example, we consider the singular solution to the Stokes problem in an L-shaped domain in two-dimensions

$$\Omega := (-1,1)^2 \backslash ([0,1] \times [-1,0]).$$

The exact velocity u and pressure ϱ are given in polar coordinates by [78, 64] as follows:

$$u(r,\varphi) = r^{\alpha} \begin{bmatrix} \cos(\varphi)\psi'(\varphi) + (1+\alpha)\sin(\varphi)\psi(\varphi) \\ \sin(\varphi)\psi'(\varphi) - (1-\alpha)\cos(\varphi)\psi(\varphi) \end{bmatrix},$$

and

$$\varrho(r,\varphi) = -r^{\alpha-1}\frac{(1+\alpha)^2\psi'(\varphi) + \psi'''(\phi)}{1-\alpha},$$

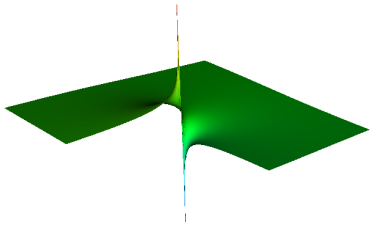

(a) Pressure component of the primal problem

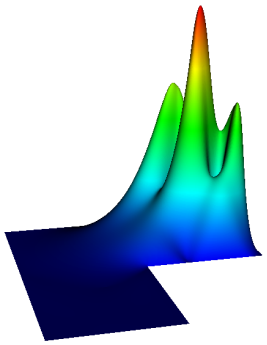

(b) Magnitude of the velocity component of the influence function associated with the average of velocity on $\Omega_1 \subset \Omega$

Figure 4.11: Example-2: Exact solution of the primal problem, and the influence function of the dual problem.

where $\psi(\varphi)$ is as follows:

$$\begin{aligned}\psi(\varphi) =& \frac{\sin((1+\alpha)\varphi)\cos(\alpha\omega)}{1+\alpha} - \cos((1+\alpha)\varphi) \\ & - \frac{\sin((1-\alpha)\varphi)\cos(\alpha\omega)}{1-\alpha} + \cos((1-\alpha)\varphi), \\ \omega =& \frac{3\pi}{2},\end{aligned}$$

and parameter α is the smallest positive solution of

$$\sin(\alpha\omega) + \alpha\sin(\omega) = 0, \qquad \alpha \approx 0.54448373678246.$$

Here we consider the quantity of interest $J(u) = \int_{\Omega_1}(1,1)\cdot u$ as the average value of velocity on Ω_1, where u denotes the vector of velocity and $\Omega_1 = [0.5, 1] \times [0.5, 1]$. The exact solution of primal and dual problem that we are interested in, both are shown in Figure 4.11. Figure 4.12 shows both h- and the hp- adaptive refinements generated by using locally defined dual-weighted goal-oriented error estimator namely GO-AFEM and also using the energy error estimator in AFEM. As the

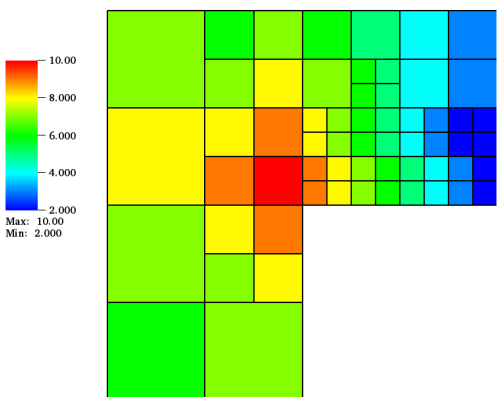

(a) Goal-oriented hp-AFEM

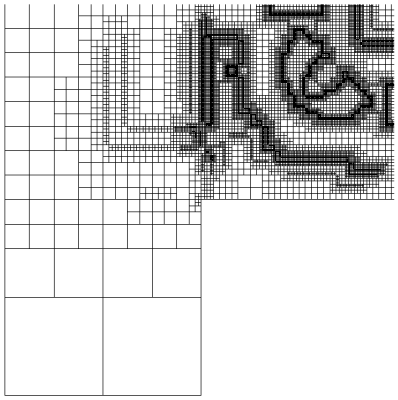

(b) Goal-oriented h-AFEM

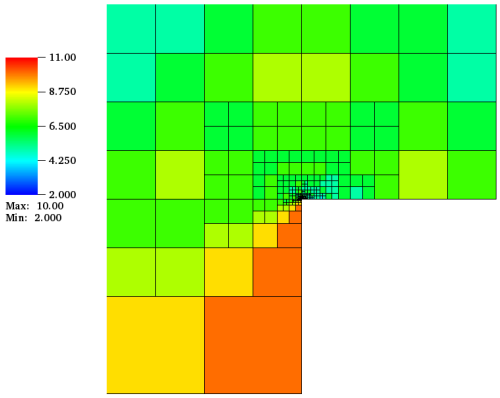

(c) hp-AFEM using Energy-estimate

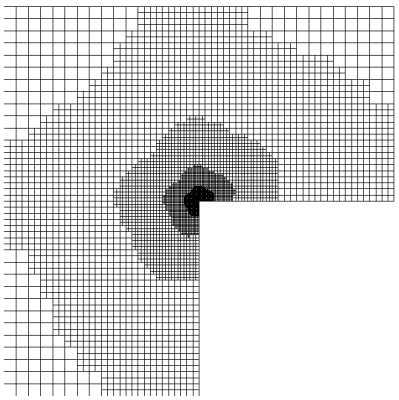

(d) h-AFEM using Energy-estimate

Figure 4.12: Example-2: (First row) triangulation produced by h- and hp-GO-AFEM; (Second row) h, hp-AFEM with almost the same number of degrees of freedom.

refinements show in that figure, the energy error estimator tries to refine the areas with large error contribution caused by singularities from the primal problem, whereas the triangulations generated by goal-oriented estimator captures the error in the area where the influence functional is large. The corresponding convergence plots between the functional error and the goal-oriented estimator for both h- and hp-adaptive cases can be seen in 4.13. As we can see in this figure, for both h and hp refinements, the goal-oriented estimator shows a reliable a posteriori estimator for the functional errors. Figure 4.14 shows the convergence rate comparison for the goal-oriented error

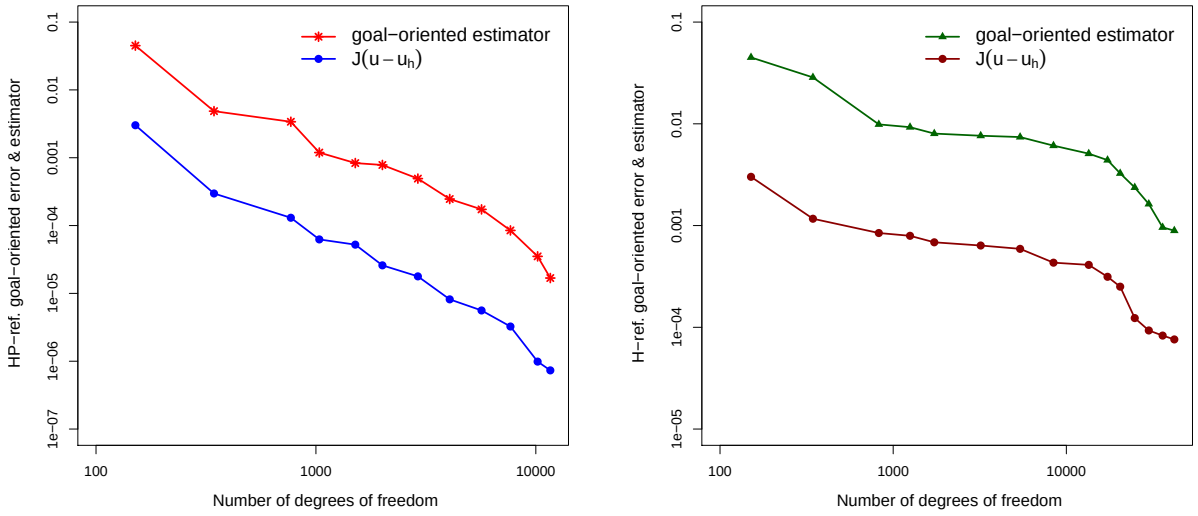

(a) hp-Goal-oriented

(b) h-Goal-oriented

Figure 4.13: Example-2: Convergence of goal estimator and the goal-functional error for both h- and hp-GO-AFEM.

estimator between h- and hp goal-oriented adaptive refinement. The last Figure in this example 4.15, demonstrates the convergence rate in the goal-estimator using GO-AFEM and AFEM by energy estimator. We give the results for both h- and hp-adaptive refinements. Considering the discussion on a priori error estimation for primal problem using $p_2 - p_1$ Taylor-Hood elements we expect the energy error converges with rate $\mathcal{O}(h^2) = \mathcal{O}(N^{-1})$, where N denotes the number of degrees of freedom. Therefore the expected optimal convergence rate for the goal oriented error would be $\mathcal{O}(N^{-2})$. We refer to [89] and [90] for deeper discussion in this regard. In this example, we solve the Stokes problem on an L-shape domain, the situation is different and we want to briefly discuss the expected error rate for problems on the L-shape domain. The L-Shape domain is a polyhedral domain with maximum edge opening angle $\omega = \frac{3\pi}{2}$. The re-entrant corner gives a corners singularity of the form $\rho_{\mathbf{edge}}^{\frac{\pi}{\omega}} = \rho^{\frac{2}{3}}$, such that $\rho_{\mathbf{edge}}$ is the distance to the given edge. In general, an adaptive method is called optimal, if it achieves the best possible convergence rate with respect to the polynomial degree that is $\mathcal{O}(N^{-\frac{p}{d}})$, where $d = 2$ in our case. So that we expect in this example using $p_2 - p_1$ elements for the primal or dual problem we achieve the rate $\mathcal{O}(\mathbf{DOF}^{-1})$.

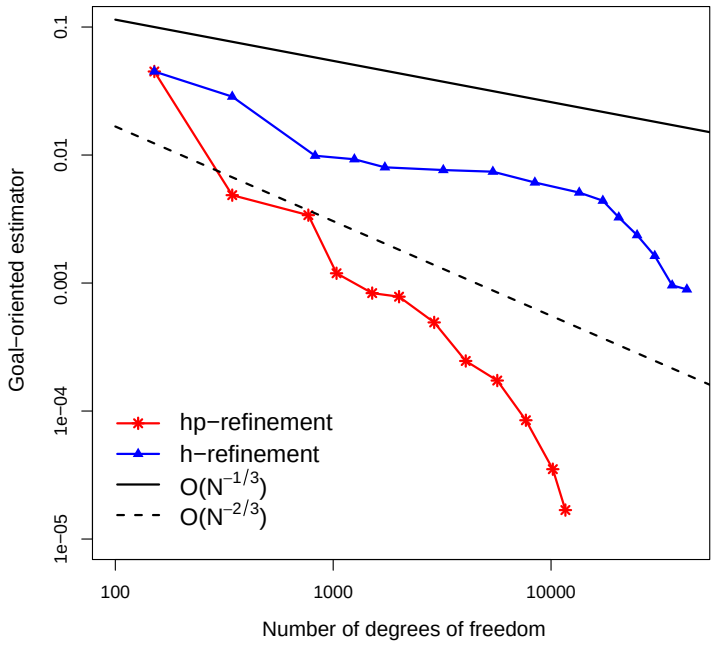

Figure 4.14: Example-2: Convergence rate comparison between h- and hp-GO-AFEM.

However, in our numerical experiments we observed using any $p_k - p_{k-1}$ finite elements the error rate did not go any better than $\mathcal{O}(h^{\frac{2}{3}}) = \mathcal{O}(N^{-\frac{1}{3}})$. In this case, using shape-regular finite elements of any higher degree won't improve the convergence rate, and it is just computational waste for no gain. To justify this result, it is important to remember that on a polyhedral domain with maximum edge opening angle ω, in this case the L-shape domain with $\omega = \frac{3\pi}{2}$, we will achieve a convergence rate of

$$\|\nabla(u - u_h)\|_{L^2(\Omega)} + \|\varrho - \varrho_h\|_{L^2(\Omega)} \lesssim \mathcal{O}(\mathbf{N}^{\frac{-s}{2}}), \quad s = \min(\frac{p}{2}, \frac{\pi}{\omega}). \tag{4.76}$$

Therefore based on the results in equation(4.76), the best possible convergence rate for the primal and dual problem is $\mathcal{O}(\mathbf{N}^{-\frac{1}{3}})$. For the goal-oriented h-AFEM error estimator, we expect to achieve the optimal convergence rate of $\mathcal{O}(\mathbf{N}^{-\frac{2}{3}})$. Our observation for both hp-AFEM and GO-hp-AFEM shows nice exponential convergence rate is achieved. Again as we expect in both figures 4.15a and 4.15b the values of functional error using the GO-AFEM is smaller than the AFEM. This is due

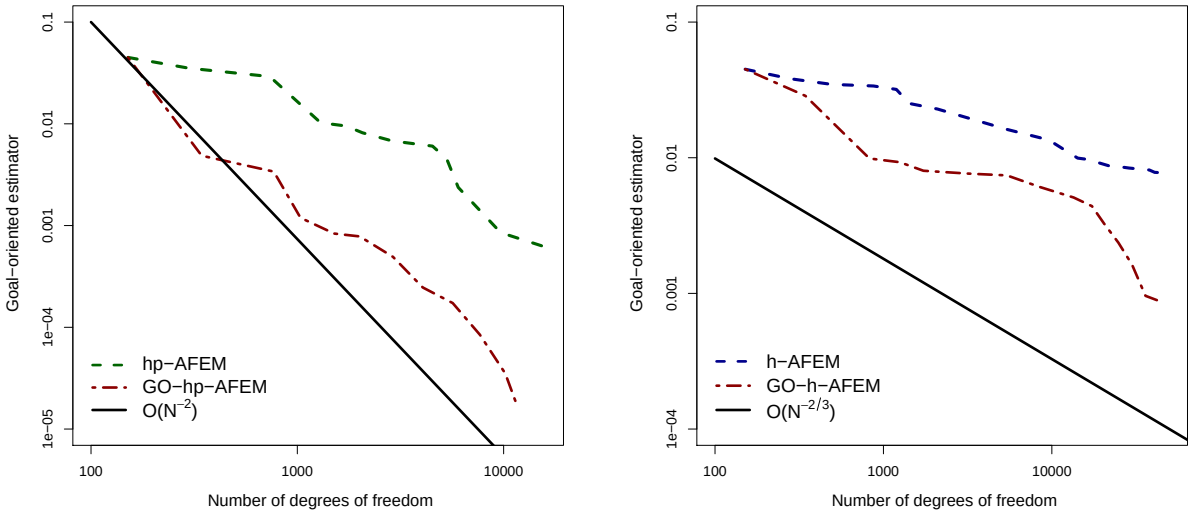

(a) GO-hp- vs. hp- error estimator

(b) GO-h- vs. h- error estimator

Figure 4.15: Example-2: Goal-oriented error estimator convergence rate using both GO-AFEM and AFEM.

to the fact that the goal-oriented refinement performs in such a way that it captures large errors in the vicinity of influence function domain, but standard AFEM refines just to minimize the error caused by the primal problem.

4.5.4 Example 3 - Fluid runs through a bent pipe

In this example, we consider the Stokes flows through a bent pipe. We prescribe the homogeneous Dirichlet boundary condition on the walls. For the inlet and outlet we set Parabolic profile. We are interested in computing the average values of velocity components over the sub-domain $\Omega_1 = [2, 2.5] \times [-1, -0.5]$. The exact solution of primal and dual problem are shown in Figure 4.16. Figures 4.17- 4.20 show both the h- and hp- adaptive refinement generated by using the locally defined dual-weighted goal-oriented error estimator, namely the GO-AFEM, and also using the energy estimator AFEM. Figure 4.21 presents the convergence rate comparison, for the goal-oriented error estimator between h- and hp goal-oriented adaptive refinements. The next Figure 4.22, demonstrates the convergence rate in the goal-estimator using GO-AFEM and AFEM by

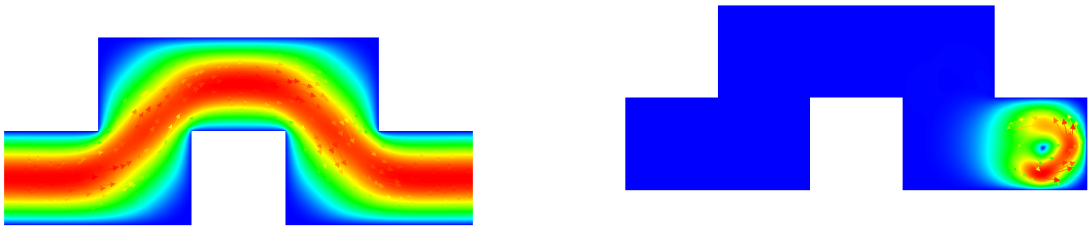

(a) Magnitude of the velocity component of the primal problem

(b) Magnitude of the velocity component of the influence function associated with the average of velocity on $\Omega_1 \subset \Omega$

Figure 4.16: Example-3: Exact solution of primal problem and the influence function of the dual problem.

energy estimator. In this example, we give the results for both h- and hp-adaptive refinements.

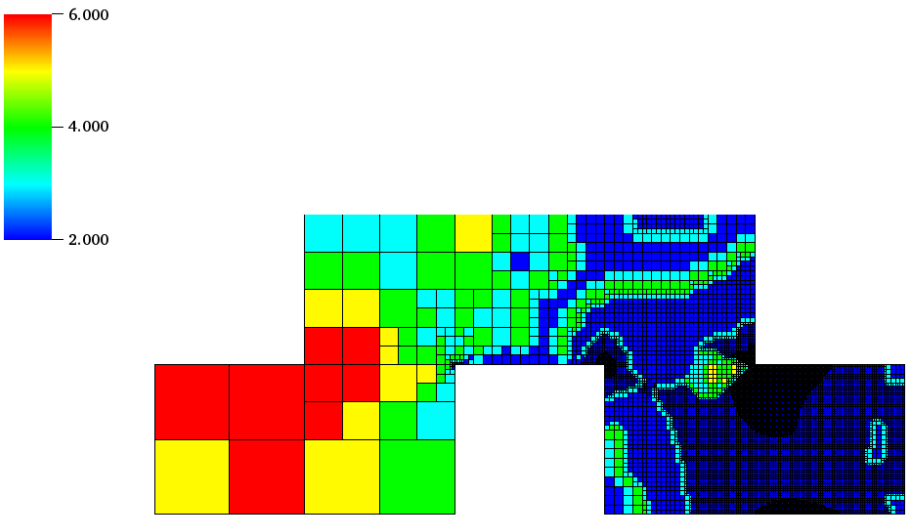

Figure 4.17: Goal-oriented hp-AFEM

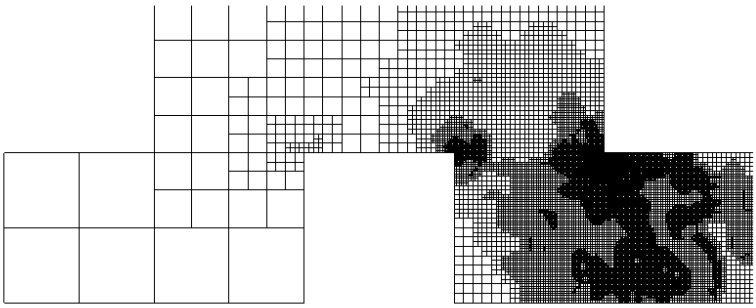

Figure 4.18: Goal-oriented h-AFEM

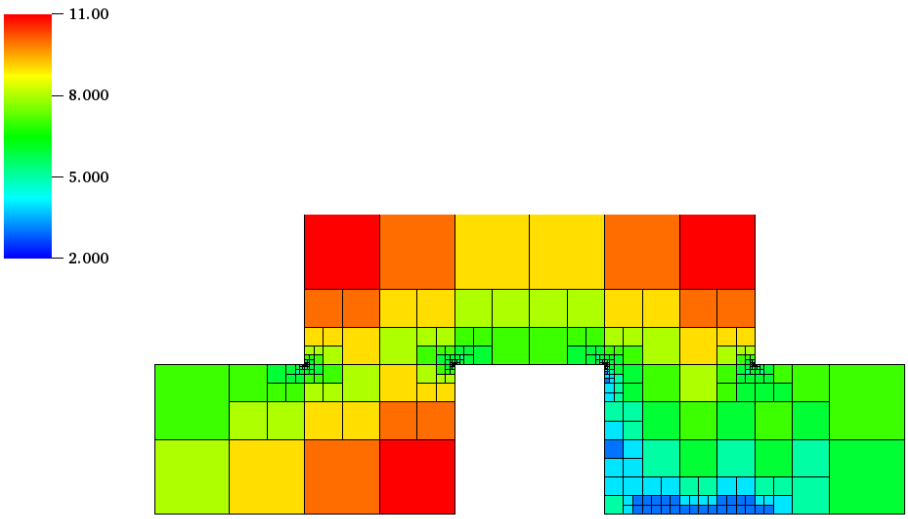

Figure 4.19: hp-AFEM using the energy error estimator

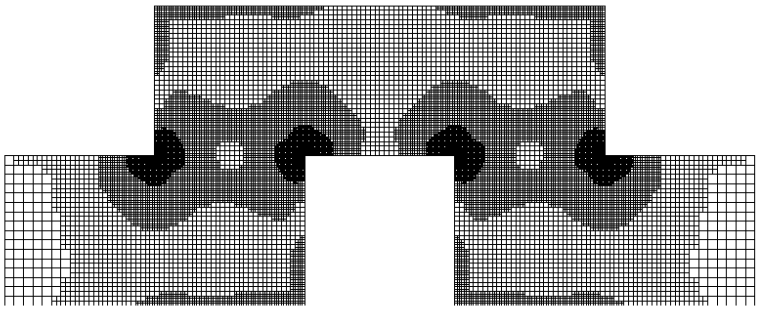

Figure 4.20: h-AFEM using the energy estimator

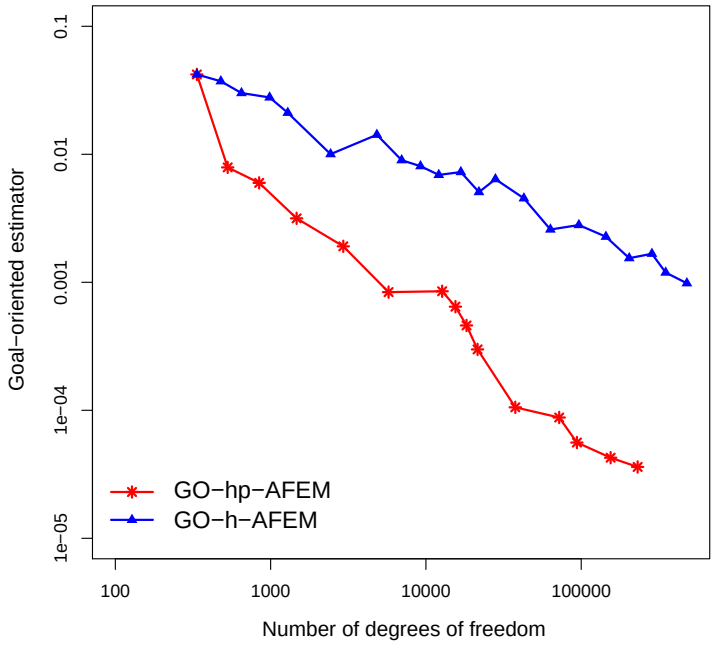

Figure 4.21: Example-3: Convergence rate comparison between h- and hp-GO-AFEM.

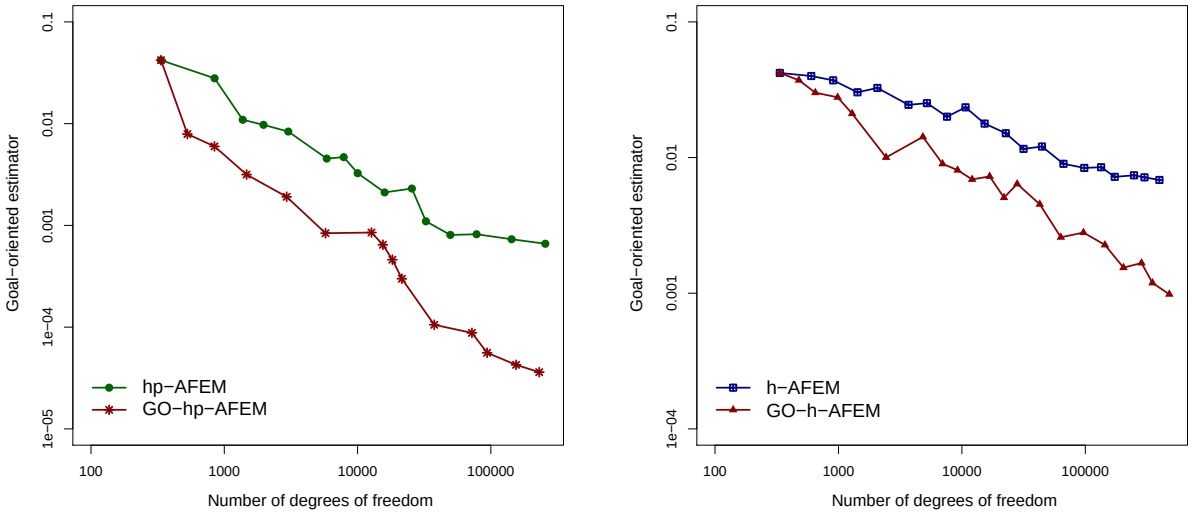

(a) GO-hp-AFEM vs. hp-AFEM

(b) GO-h-AFEM vs. h-AFEM

Figure 4.22: Example-3: Goal-oriented error estimator convergence rate using both GO-AFEM and AFEM.

5. ANALYSIS OF GOAL-ORIENTED H-AFEM WITH QUASI-OPTIMAL CONVERGENCE RATE FOR SYMMETRIC SECOND-ORDER LINEAR ELLIPTIC PDES

5.1 Introduction

In this chapter, we analyze a goal-oriented adaptive finite element method (GO-AFEM) for symmetric second-order linear elliptic PDEs as our model problem. For the marking in our proposed goal-oriented AFEM in Algorithm 5, we take the union of marking sets as a result of Dörfler marking on primal and dual problems. As we show in section 5.2.3 the primal and dual estimator product controls the error in the functional of interests in the goal-oriented adaptivity. Following the idea of Carstensen et al. [5], in section 5.3.3, we demonstrate these two estimators for primal and dual problems will satisfy the so-called *axioms of adaptivity* as the abstract properties needed to prove the optimal convergence rate. With the aforementioned tools in hand, and following the leads of Feischl et al. [3], we can establish a framework to show the linear convergence with optimal rate in primal and dual estimator products for our proposed goal-oriented adaptive finite element method.

5.1.1 Outline

In section 5.2, we present our model problem and its dual setting. Then in 5.2.1 and 5.2.2, we introduce the error estimators corresponding to the primal and dual problems. In section 5.2, we present both the goal-oriented algorithm proposed in [39], and our goal-oriented algorithm. Some preliminary definitions and required tools are presented in section 5.3. The important auxiliary results which provide us with an abstract framework for the optimality analysis are given in 5.3.3. In section 5.4, we apply the tools and results of the previous sections to prove the main result which is the optimality in our proposed goal-oriented marking strategy. Finally in section 5.5, we present some numerical examples showing that our goal-oriented algorithm is optimal, and we also compare our results with both dual-weighted goal-oriented algorithm introduced in [1], and

the standard AFEM using the energy error estimator.

5.2 Goal-oriented error estimator and GO-AFEM refinement algorithm

For the polygonal domain $\Omega \subset \mathbb{R}^2$ and the given data $f \in L^2(\Omega)$, let $u : \bar{\Omega} \longrightarrow \mathbb{R}$ be the solution of the following elliptic model problem, which we consider through this work,

$$\begin{aligned} -\Delta u &= f \qquad \text{in} \quad \Omega, \\ u &= 0 \qquad \text{on} \quad \partial\Omega. \end{aligned} \tag{5.1}$$

For simplicity we impose the zero boundary conditions, but the results hold for any type of boundary settings. Multiply by a test function $\phi \in H_0^1(\Omega) := V$ and applying integration by parts, the weak formulation for (5.1) reads as follows: find $u \in V$ such that

$$a(\phi, u) := \int_\Omega (\nabla\phi)^T \nabla u = \int_\Omega \phi f, \qquad \forall \phi \in V. \tag{5.2}$$

In the goal-oriented adaptive finite element method for the given linear bounded functional $\mathcal{J} \in H^{-1}(\Omega) := V^*$, the goal is to best approximate the function of interest $\mathcal{J}(u)$. Following the Riesz representation theorem, there exists some function $j \in L^2(\Omega)$ such that

$$\mathcal{J}(\phi) = \int_\Omega j\phi \qquad \forall \phi \in L^2(\Omega). \tag{5.3}$$

We find $z \in V$ as solution of the dual problem

$$a(z, \phi) := \int_\Omega (\nabla z)^T \nabla \phi = \mathcal{J}(\phi), \qquad \forall \phi \in V. \tag{5.4}$$

Now, assume $\mathcal{T} = \{K\}$ is family of triangulation associated with the problem domain $\Omega \in \mathbb{R}^2$. Further, we define the mesh size vector $h := (h_K)_{K\in\mathcal{T}}$, where $h_K := \operatorname{diam}(K)$. For the conforming finite element space $V_\mathcal{T} \subset V$, let $u_{\text{FE}} \in V_\mathcal{T}$ be the unique Galerkin solution to

$$a(\phi_{\text{FE}}, u_{\text{FE}}) = (\phi_{\text{FE}}, f) \qquad \forall \phi \in V_\mathcal{T}. \tag{5.5}$$

Then let z_{FE} be the Galerkin solution to

$$a(z_{\text{FE}}, \phi_{\text{FE}}) = (j, \phi_{\text{FE}}) \qquad \forall \phi \in V_{\mathcal{T}}. \tag{5.6}$$

The error in the functional of interest follows as

$$|\mathcal{J}(u) - \mathcal{J}(u_{\text{FE}})| = |a(z, u - u_{\text{FE}})| \leqslant |z - z_{\text{FE}}|_1 |u - u_{\text{FE}}|_1. \tag{5.7}$$

Here $|.|_1$ denotes the H^1-seminorm and z_{FE} is the Ritz projection of z. Before we move to the details of our algorithm and its related discussion, we present some preliminary results needed further on to demonstrate the results in the following sections.

5.2.1 A posteriori error estimator (Primal Problem)

Definition 5.2.1. *Consider $u_{FE} \in V_{\mathcal{T}}$ as the solution of (5.5), the primal residual-based a posteriori error estimator η is decomposed into a sum of local error indicators η_K,*

$$\eta^2 := \sum_{K \in \mathcal{T}} \eta_K^2. \tag{5.8}$$

for each η_K it is decomposed into a cell and an interface contribution:

$$\eta_K^2 := \eta_{K;R}^2 + \eta_{K;B}^2, \tag{5.9}$$

where the residual-based term $\eta_{K;R}$ and the jump-based term $\eta_{K;B}$ are defined as follows:

$$\begin{aligned} \eta_{K;R}^2 &:= h_K^2 \| I_K f + \Delta u_{FE} \|_{L^2(K)}^2 \\ \eta_{K;B}^2 &:= \frac{1}{2} \sum_{e \in \mathcal{E}(K)} h_e \left\| \left[\frac{du_{FE}}{dn_e} \right] \right\|_{L^2(e)}^2, \end{aligned} \tag{5.10}$$

where $I_K f$ denotes the local L^2-projection of f on cell K. h_e is the length of edge e and the $[\cdot]$ notation is the jump across the edge and n_e is the outward pointing unit normal vector of cell K

for each edge e. As it is proven in [68], the estimator is a reliable and also an efficient upper and lower bound for the energy error of the primal problem.

The following theorem states the aforementioned upper and lower bounds, typically referred to as the reliability and efficiency estimates.

Theorem 5.2.2. *Let $u \in H_0^1(\Omega)$ be solution of (5.2) and $u_{FE} \in V_{\mathcal{T}}$ be the solution of (5.5). Then there exists some constant $C_{rel} > 0$ independent of mesh size vector h, such that*

$$\|\nabla(u - u_{FE})\|^2_{L^2(\Omega)^2} \leqslant C_{rel}\left(\eta^2 + \sum_{K\in\mathcal{T}} h_K^2 \|f - I_K f\|^2_{L^2(K)}\right), \tag{5.11}$$

$$\eta^2 \leqslant C_{eff}\left(\|\nabla(u - u_{FE})\|^2_{L^2(\Omega)^2} + \sum_{K\in\mathcal{T}} h_K^2 \|f - I_K f\|^2_{L^2(\omega_{K,1})}\right) \tag{5.12}$$

Proof. See [68, Proposition 4.2]. □

5.2.2 A posteriori error estimator (Dual Problem)

Continuing, we state some auxiliary results from [1] which are used to define the error estimator for the energy error in the dual problem (5.4).

Lemma 5.2.3. *Let $z_{FE} \in V_{\mathcal{T}}$ be solution of (5.6) and consider λ_{FE} as solution of the following local variational equation*

$$\int_{\omega_{K,2}} (\nabla\lambda_{FE})^T \nabla\phi = \int_{\omega_{K,2}} j\phi - (\nabla z_{FE})^T \nabla\phi \qquad \forall\phi \in H_0^1(\omega_{K,2}), \tag{5.13}$$

then we have

$$\sup_{\phi\in H_0^1(\omega_{K,2})} \frac{\int_{\omega_{K,2}} j\phi - (\nabla z_{FE})^T \nabla\phi}{\|\nabla\phi\|_{L^2(\omega_{K,2})}} = \|\nabla\lambda^K\|_{L^2(\omega_{K,2})}$$

Proof. See [1, Lemma 1]. □

Following, we define the a posteriori error estimator for the patch problem associated with each cell K (5.13).

Definition 5.2.4. *Let λ_{FE}^K be the finite element solution associated of equation (5.13) and z_{FE} is the solution of (5.6), then the a posteriori error estimator $\tilde{\eta}(K)$ for each cell K is defined as follows:*

$$\tilde{\eta}(K)^2 := \sum_{T \in \omega_{K,2}} \tilde{\eta}_T^2(K), \tag{5.14}$$

where each local estimator is defined as:

$$\tilde{\eta}_T^2(K) := h_T^2 \| I_T j + \Delta z_{FE} + \Delta \lambda_{FE}^K \|_{L^2(T)}^2 + \frac{1}{2} \sum_{e \in \mathcal{E}(T)} h_e \left\| \left[\frac{dz_{FE}}{dn_e} + \frac{d\lambda_{FE}^K}{dn_e} \right] \right\|_{L^2(e)}^2, \tag{5.15}$$

and $I_K j$ denotes the local L^2-projection of j on cell T. h_e is the length of interior edge e, the $[\cdot]$ notation is the jump across the edge and n_e is the outward pointing unit normal vector of cell K for each edge e.

It has been proven in [1] that the above residual based error estimation is a reliable and efficient estimate for the energy error of equation (5.13).

Lemma 5.2.5. *Let $z \in H_0^1(\Omega)$ and $z_{FE} \in V_{\mathcal{T}}$ be the solution of (5.4) and (5.6), respectively. Furthermore, for each cell $K \in \mathcal{T}$ consider $\lambda^K \in H_0^1(\omega_{K,2})$ as the solution of (5.13) and $\lambda_{FE}^K \in V_{\mathcal{T}}$ be its finite element approximation, then there exists constants $C_{rel}^{patch} > 0$ and $C_{eff}^{patch} > 0$ independent of mesh size h_T, so that the following reliability and efficiency estimates hold:*

$$\| \nabla(\lambda - \lambda_{FE}) \|_{L^2(\omega_{K,2})}^2 \leqslant C_{rel}^{patch} \left(\tilde{\eta}(K)^2 + \sum_{T \in \omega_{K,2}} h_T^2 \| j - I_T j \|_{L^2(T)}^2 \right), \tag{5.16}$$

$$\tilde{\eta}(K)^2 \leqslant C_{eff}^{patch} \left(\| \nabla(\lambda^K - \lambda_{FE}^K) \|_{L^2(\omega_{T,1})}^2 + h_T^2 \| j - I_T j \|_{L^2(\omega_{K,1})}^2 \right). \tag{5.17}$$

Proof. See [1, Proposition 1]. □

Next, we define an a posteriori error estimator for the dual problem, which is used later on through our goal-oriented refinement algorithm 5, and also in the corresponding analysis therein.

Definition 5.2.6. *The associated error estimator for the dual problem (5.4) is defined as follows:*

$$\begin{aligned} \xi^2 &:= \sum_{K\in\mathcal{T}} \xi_K^2, \\ \xi_K^2 &:= \tilde{\eta}(K)^2 + \|\nabla \lambda_{FE}^K\|^2_{L^2(\omega_{K,2})}, \qquad \forall K \in \mathcal{T}. \end{aligned} \tag{5.18}$$

The next two theorems demonstrate the upper and the lower bounds for the energy error in the dual problem, which are the so-called reliability and efficiency estimates.

Theorem 5.2.7. *Let $z \in H_0^1(\Omega)$ be solution of (5.4) and $z_h \in V_h$ is solution of discrete problem (5.6), then the dual estimator introduced in (5.18) is a reliable error estimator for the energy error of the dual-problem, where there exists a constant $C_{rel}^{dual} > 0$ independent of mesh size h_k such that:*

$$\|\nabla(z - z_{FE})\|^2_\Omega \leqslant C_{rel}^{dual}\left(\xi^2 + \sum_{K\in\mathcal{T}} h_K^2 \|j - I_K j\|^2_{L^2(\omega_{K,2})}\right). \tag{5.19}$$

Proof. Proof follows exactly the lines of [1, Proposition 1, Theorem 3 and Lemma 5]. □

Theorem 5.2.8. *Let $z \in H_0^1(\Omega)$ be the solution of (5.4) and $z_{FE} \in V_\mathcal{T}$ the solution of discrete problem (5.6). Then the dual estimator introduced in (5.18) is an efficient error estimator for the energy error of the dual-problem where there exists a constant $C_{eff}^{dual} > 0$ independent of mesh size h_k such that:*

$$\xi^2 \leqslant C_{\text{eff}}^{\text{dual}}\left(\|\nabla(z - z_{\text{FE}})\|^2_{L^2(\Omega)} + \sum_{K\in\mathcal{T}} h_K \|j - I_K j\|^2_{L^2(\omega_{K,3})}\right) \tag{5.20}$$

Proof. See equation (5.17) in Lemma 5.2.5, and also [1, Lemma 6 and Theorem 3]. □

5.2.3 Goal-oriented adaptive algorithms

Additionally, from now on we assume some saturation assumption on data such that there exists some $\tau_p, \tau_d \in (0, 1]$

$$\begin{aligned} \sum_{K\in\mathcal{T}} h_K^2 \|f - I_K f\|^2_{L^2(K)} &\leqslant \tau_p^2 \eta^2, \\ \sum_{K\in\mathcal{T}} h_K^2 \|j - I_K j\|^2_{L^2(K)} &\leqslant \tau_d^2 \xi^2, \end{aligned} \tag{5.21}$$

where f and j are the data given for the primal and dual problems, respectively. η and ξ are the residual estimators for the primal and dual problems. From the upper bound for the error in the functional of interest given in (5.7), and the reliability estimates for both the primal and dual problem as given in Theorems 5.2.2, 5.19, and 5.20 the following holds:

$$|\mathcal{J}(u) - \mathcal{J}(u_{\text{FE}})| \leqslant \|\nabla(u - u_{\text{FE}})\|_{L^2(\Omega)} \|\nabla(z - z_{\text{FE}})\|_{L^2(\Omega)} \lesssim \eta\xi, \tag{5.22}$$

where $\lesssim$ denotes $\leqslant$ up to a constant $C > 0$ independent of the mesh size h. We want to propose a suitable marking strategy for our goal-oriented adaptive algorithm such that it gives us the tools to prove that the right hand side of (5.22) which is the product of primal and dual estimators $\eta\xi$, converges to zero with an optimal rate.

In order to set the preliminary and required tools for the analysis of optimal convergence rate, we consider two goal-oriented algorithms. The first one, Algorithm 4, is the goal-oriented refinement algorithm in [39] introduced by Mommer and Stevenson (MS). The second one is our proposed goal-oriented refinement strategy given in Algorithm 5, for which we aim to prove that the product of the primal and the dual estimators converges to zero with optimal rate.

It is important to mention that in [84], the article by Holst et al., the proposed goal-oriented algorithm follows exactly the adaptive Algorithm 4, except for the step **MARK**, where instead of taking the marking set with the smallest cardinality at each iteration step n, they consider the goal-oriented marked elements as being the union of primal and dual marking sets: $\mathcal{M}_n = \mathcal{M}_n^u \cup \mathcal{M}_n^z$.

Algorithm 4 Mommer-Stevenson (MS) goal-oriented algorithm, [39]

(Initialize): Set $n = 0$, a coarse mesh $\mathcal{T}_0$, $\theta \in (0, 1]$ and also tolerance TOL > 0. For all refinement cycles $n = 0, 1, 2, \cdots$

- **SOLVE**: Find the finite element solutions $(u^n_{\text{FE}}, z^n_{FE})$ of equations (5.5) and (5.6), respectively.
- **ESTIMATE**: For all elements $K \in \mathcal{T}_n$, compute the residual-based primal and dual refinement indicators $\eta_{u,n}(K)$ and $\eta_{z,n}(K)$.
  If $\eta_{u,n}(K)\eta_{z,n}(K) <$ TOL, then STOP the algorithm.
- **MARK**: Find a set of marked elements $\mathcal{M}_n \subseteq \mathcal{T}_n$ such that $\#\mathcal{M}_n = \min\{\#\mathcal{M}^u_n, \#\mathcal{M}^z_n\}$, where the following Dörfler markings hold:

$$\eta^2_{u,n}(\mathcal{M}^u_n) \geqslant \theta\eta^2_{u,n}, \qquad and \qquad \eta^2_{z,n}(\mathcal{M}^z_n) \geqslant \theta\eta^2_{z,n}. \tag{5.23}$$

- **REFINE**: Refine all the marked elements $K \in \mathcal{M}_n$, such that $\mathcal{T}_{n+1} :=$ refine$(\mathcal{T}_n, \mathcal{M}_n)$.

Algorithm 5 Goal-oriented adaptive algorithm

(Initialize): Set $n = 0$, a coarse mesh $\mathcal{T}_0$, $\theta \in (0, 1]$ and also tolerance TOL > 0. For all refinement cycles $n = 0, 1, 2, \cdots$

- **SOLVE**: Find the finite element solutions $(u^n_{\text{FE}}, z^n_{\text{FE}}, \lambda^n_{\text{FE}})$ of equations (5.5), (5.6) and (5.13), respectively.
- **ESTIMATE**: For all elements $K \in \mathcal{T}_n$, compute the primal and dual refinement indicators $\eta_{K,n}$ and $\xi_{K,n}$, as is defined in (5.10) and (5.18).
  If $\eta_{K,n}\xi_{K,n} <$ TOL, then STOP the algorithm.
- **MARK**: Find a set of marked elements $\mathcal{M}_n \subseteq \mathcal{M}^u_n \bigcup \mathcal{M}^z_n$ such that

$$\eta^2_n(\mathcal{M}_n)\xi^2_n(\mathcal{M}_n) \geqslant \theta^2\eta^2_n\xi^2_n, \tag{5.24}$$

  where that the Dörfler marking holds for both our primal and dual estimator

$$\eta^2_n(\mathcal{M}^u_n) \geqslant \theta\eta^2_n, \qquad and \qquad \xi^2_n(\mathcal{M}^z_n) \geqslant \theta\xi^2_n. \tag{5.25}$$

- **REFINE**: Refine all the marked elements $K \in \mathcal{M}_n$, such that $\mathcal{T}_{n+1} :=$ refine$(\mathcal{T}_n, \mathcal{M}_n)$.

In that article, Holst et al. showed that while the estimator product is linearly convergent, but in [84, Sec. 4] they could only prove a suboptimal convergence rate $\min\{s,t\}$, where s and t are used to show the approximation rate in primal and dual solutions. In this work, for my proposed primal and dual estimators, and the marking strategy in Algorithm 5, I prove that the decay rate in the estimators product happens with an optimal convergence rate $s+t$.

5.3 Preliminary definitions and tools for optimality analysis

In this section, we try to assemble all the required definitions and lemmas to set the ground in order to use them effectively for representing our main results in the next section.

5.3.1 Introduction to approximation class

As we will show further on in Theorem 5.4.3, even though the linear convergence shows the reduction in quasi-error and therefore in the error estimator, but despite of a priori error estimators discussed in section 3.2.1, here nothing is noted about the regularity of solution nor about the polynomial degree used for approximation. The optimality analysis tries to make a relation between the smoothness of the solution and the optimal decay rate in the adaptive finite element refinement. The idea of optimality in the standard AFEM is showing that the proposed adaptive refinement algorithm constructs a set of triangulations such that error reduction happens in optimal rate. Consider $\mathbb{T} := \text{refine}(\mathcal{T}_0)$ as the set of all triangulations that can be obtained from $\mathcal{T}_0$, where $\mathcal{T}_0$ is the initial triangulation for both aforementioned Algorithms 4 and 5. Let $\mathbb{T}_{\mathrm{N}} := \{\mathcal{T} \in \mathbb{T} | \#\mathcal{T} - \#\mathcal{T}_0 \leqslant \mathrm{N}\}$, be the set of all conforming triangulations generated from $\mathcal{T}_0$ which have at most N elements more than $\mathcal{T}_0$. In order to be able to demonstrate the quality of the adaptive refinement algorithm, we need to introduce the approximation class $\mathbb{A}_s$ for some $s > 0$.

Definition 5.3.1. *The nonlinear approximation class $\mathbb{A}_s$, for some $s > 0$ is defined as*

$$\mathbb{A}_s := \left\{ u \in H_0^1(\Omega) : \|u\|_{\mathbb{A}_s} := \sup_{N>0} \left((N+1)^s \min_{\mathcal{T}^* \in \mathbb{T}_n} \eta_u^* \right) < \infty \right\},$$

here η_u^* denotes the primal or dual error estimator associated with the conforming triangulation

$\mathcal{T}^* \in \mathbb{T}_n$. *The finite norm* $\|u\|_{\mathbb{A}_s} < \infty$ *means that, if we find the optimal conforming triangulation* $\mathcal{T}^*$*, the algebraic convergence rate for the error estimators would be* $\mathcal{O}(N^{-s})$.

5.3.2 Assumption on mesh refinement

In the analysis of optimal convergence rates, the refinement procedure has an important impact on discussion therein. For any triangulation $\mathcal{T}$ of Ω and any set of marked elements $\mathcal{M} \subset \mathcal{T}$ in both Algorithms 4 and 5, the notation $\mathcal{T}_* = \text{REFINE}(\mathcal{T}, \mathcal{M})$ implies at least all the marked elements $\mathcal{M}$ are refined.

Lemma 5.3.2 (Complexity of REFINE)**.** *Consider the initial conforming triangulation* $\mathcal{T}_0$*. For* $n > 0$ *let* $\{\mathcal{T}_n\}$ *be a sequence of refinements of* $\mathcal{T}_0$ *such that* $\mathcal{T}_{n+1} := \textit{REFINE}(\mathcal{T}_n, \mathcal{M}_n)$*, where* $\mathcal{M}_n \subset \mathcal{T}_n$*. Then there exists a constant* $C_{\textit{complex}} > 0$ *that only depends on* $\mathcal{T}_0$ *such that*

$$\#\mathcal{T}_n - \#\mathcal{T}_0 \leq C_{\textit{complex}} \sum_{j=0}^{n-1} \#\mathcal{M}_j \qquad \forall n \geqslant 1.$$

Proof. The above complexity condition, for conforming triangulations using bisection methods is well known due to work done by Binev et al. [26, 89] for $d = 2$, and Stevenson [91] for $d > 2$. More specifically for our refinement on quadrilaterals, Bonito and Nochetto in [88, Lemma 6.5] provide the proof of complexity of REFINE. □

Lemma 5.3.3 (Mesh overlay)**.** *For any conforming triangulations* $\mathcal{T}_1, \mathcal{T}_2 \in \mathbb{T}$ *of initial triangulation* $\mathcal{T}_0$*, the overlay is the smallest conforming triangulation* $\mathcal{T} : \mathcal{T}_1 \bigoplus \mathcal{T}_2$ *that satisfies*

$$\#\mathcal{T} \leqslant \#\mathcal{T}_1 + \#\mathcal{T}_2 - \mathcal{T}_0$$

Proof. See [4, Lemma 3.7]. □

5.3.3 Auxiliary results

Lemma 5.3.4 (Stability of energy estimators on non-refined elements)**.** *Let* $w_{\textit{FE}} \in \{u_{\textit{FE}}, z_{\textit{FE}}\}$ *be the solution of primal equation (5.2) or dual problem (5.4). Consider* $\widehat{w}_h \in \widehat{V}_{\mathcal{T}}$ *and* $w_{\textit{FE}} \in V_{\mathcal{T}}$

be the finite element solutions such that $\widehat{\mathcal{T}} := \textit{REFINE}(\mathcal{T})$. *Then for all sets of non-refined cells* $\Upsilon \subset \mathcal{T} \cap \widehat{\mathcal{T}}$ *there exists a constant* $C_{stab} > 0$ *such that*

$$\left| \left(\sum_{K \in \Upsilon} \eta_K^2(\widehat{w}_{FE}, \widehat{\mathcal{T}}) \right)^{\frac{1}{2}} - \left(\sum_{K \in \Upsilon} \eta_K^2(w_{FE}, \mathcal{T}) \right)^{\frac{1}{2}} \right| \leqslant C_{stab} \|\nabla(\widehat{w}_{FE} - w_{FE})\|_{L^2(\Omega)} \tag{5.26}$$

Proof. The result follows by using the triangle inequality $|\|\cdot\| - \|\cdot\|| \leqslant \|\cdot - \cdot\|$, and also the efficiency estimate which holds for both estimators for primal and dual equations in (5.12) and (5.20), respectively. □

Lemma 5.3.5 (Error estimator reduction for primal problem)**.** *For* $\mathcal{T} \in \mathbb{T}$ *and* $\mathcal{M} \subset \mathcal{T}$, *let* $\widehat{\mathcal{T}} \in \mathbb{T}$ *be the conforming refinement of* $\mathcal{T}$ *such that* $\widehat{\mathcal{T}} := \textit{REFINE}(\mathcal{T}, \mathcal{M})$ *and also* $u_{FE} \in V_{\mathcal{T}}$, $\widehat{u}_{FE} \in \widehat{V}_{\mathcal{T}}$ *be the finite element solutions of (5.5). Assume that there exists some constant* $0 < \rho < 1$ *independent of the mesh size vector* h *so that for all refined cells* $\tilde{K} \in \mathcal{T}$ *and all* $K \in \widehat{\mathcal{T}}$ *with* $K \subseteq \tilde{K}$, *we have* $h_K \leqslant \rho h_{\tilde{K}}$. *Moreover, assume there exists some* $\tau \in (0, 1]$ *such that*

$$\sum_{K \in \mathcal{T}} h_K^2 \|f - I_K f\|_{L^2(K)}^2 \leqslant \tau^2 \eta(u, \mathcal{T}). \tag{5.27}$$

Then for all $\delta > 0$ *it holds*

$$\begin{aligned} \eta^2(\widehat{u}_{FE}, \widehat{\mathcal{T}}) \leqslant & (1+\delta) \left\{ \left(1 + \frac{\rho^2 \tau^2}{2\delta} \right) \eta^2(u_{FE}, \mathcal{T}) - (1-\rho^2) \eta^2(u_{FE}, \mathcal{M}) \right\} \\ & + (1 + \delta^{-1}) \|\nabla(\widehat{u}_{FE} - u_{FE})\|_{L^2(\Omega)^2}^2. \end{aligned} \tag{5.28}$$

Proof. The proof is inspired by the proof of [92, Lemma 3.18]. By Definition 5.2.1 we have

$$\eta^2(\widehat{u}_{\mathrm{FE}}, \widehat{\mathcal{T}}) = \sum_{K \in \widehat{\mathcal{T}}} \left(\eta_{K;R}^2(\widehat{u}_{\mathrm{FE}}, \widehat{\mathcal{T}}) + \eta_{K;B}^2(\widehat{u}_{\mathrm{FE}}, \widehat{\mathcal{T}}) \right). \tag{5.29}$$

From (5.10) the cell contribution is defined as:

$$\eta_{K;R}(\widehat{u}_{\mathrm{FE}}, \widehat{\mathcal{T}}) = h_K \|I_{\widehat{K}} f + \Delta \widehat{u}_{\mathrm{FE}}\|_{L^2(K)}^2. \tag{5.30}$$

Then the Minkowski inequality yields

$$\eta_{K;R}(\widehat{u}_{\text{FE}}, \widehat{\mathcal{T}}) \leqslant h_k \Big(\|I_K f + \Delta u_{\text{FE}}\|_{L^2(K)} + \|I_{\widehat{K}} f - I_K f\|_{L^2(K)} + \|\Delta(\widehat{u}_{\text{FE}} - u_{\text{FE}})\|_{L^2(K)} \Big). \quad (5.31)$$

Consider $\mathcal{R} := \{K \in \mathcal{T} : \text{K is refined}\}$, it is clear that $\mathcal{M} \subseteq \mathcal{R}$. First suppose there is some $\tilde{K} \in \mathcal{R}$ such that $K \subseteq \tilde{K}$, then it yields the followings

$$h_K \|I_K f + \Delta u_{\text{FE}}\|_{L^2(K)} \leq \rho h_{\tilde{K}} \|I_K f + \Delta u_{\text{FE}}\|_{L^2(K)}, \quad (5.32)$$

$$h_K \|I_{\widehat{K}} f - I_K f\|_{L^2(K)} \leqslant \rho h_K \|f - I_K f\| \leqslant \rho h_{\widehat{K}} \|f - I_K f\|. \quad (5.33)$$

Now, let us consider there exists no $K \in \mathcal{R}$, then for $\widehat{K} \in \mathcal{T}$ it holds

$$h_{\widehat{K}} \|I_K f + \Delta u_{\text{FE}}\|_{L^2(K)} = \eta_{K;R}(u_{\text{FE}}, \mathcal{T}), \quad (5.34)$$

and of course

$$\|I_{\widehat{K}} f - I_K f\|_{L^2(K)} = 0. \quad (5.35)$$

The inverse estimate implies

$$\|\Delta(\widehat{u}_{\text{FE}} - u_{\text{FE}})\|_{L^2(K)} \leqslant C_{\text{inv}} \|\nabla(\widehat{u}_{\text{FE}} - u_{\text{FE}})\|_{L^2(K)^2}. \quad (5.36)$$

By using equations (5.32)-(5.36) in (5.31), for the case that there exists such a cell $\tilde{K} \in \mathcal{R}$ where $K \subseteq \tilde{K}$, we get

$$\begin{aligned} \eta_{K;R}(\widehat{u}_{\text{FE}}, \widehat{\mathcal{T}}) \leqslant & \rho h_{\tilde{K}} \Big(\|I_K f + \Delta u_{\text{FE}}\|_{L^2(K)} + \|f - I_K f\|_{L^2(K)} \Big) \\ & + C_{\text{inv}} \|\nabla(\widehat{u}_{\text{FE}} - u_{\text{FE}})\|_{L^2(K)^2}. \end{aligned} \quad (5.37)$$

And if there exists no such cell in the set of refined elements $\mathcal{R}$, the following holds

$$\eta_{K;R}(\widehat{u}_{\text{FE}}, \widehat{\mathcal{T}}) \leqslant \eta_{K;R}(u_{\text{FE}}, \mathcal{T}) + C_{\text{inv}} \|\nabla(\widehat{u}_{\text{FE}} - u_{\text{FE}})\|_{L^2(K)^2}. \tag{5.38}$$

For the edge contribution of error estimator defined in (5.10) we get

$$\begin{aligned} \eta^2_{K;B}(\widehat{u}_{\text{FE}}, \widehat{\mathcal{T}}) =& \frac{1}{2} \sum_{e \in \mathcal{E}(K)} h_e \left\| \left[\frac{d\widehat{u}_{\text{FE}}}{dn_e} \right] \right\|^2_{L^2(e)} \\ \leqslant& \frac{1}{2} \sum_{e \in \mathcal{E}(K)} h_e \left\| \left[\frac{d\widehat{u}_{\text{FE}}}{dn_e} \right] \right\|_{L^2(e)} \left(\left\| \left[\frac{du_{\text{FE}}}{dn_e} \right] \right\|_{L^2(e)} + \left\| \left[\frac{d(\widehat{u}_{\text{FE}} - u_{\text{FE}})}{dn_e} \right] \right\|_{L^2(e)} \right). \end{aligned} \tag{5.39}$$

The Cauchy-Schwarz inequality gives

$$\eta^2_{K;B}(\widehat{u}_h, \widehat{\mathcal{T}}) \leqslant \eta_{K;B}(\widehat{u}_{\text{FE}}, \widehat{\mathcal{T}})(T_1 + T_2), \tag{5.40}$$

where T_1 and T_2 are given as

$$\begin{aligned} T_1^2 &:= \frac{1}{2} \sum_{e \in \mathcal{E}(K)} h_e \left\| \left[\frac{du_{\text{FE}}}{dn_e} \right] \right\|^2_{L^2(e)}, \\ T_2^2 &:= \frac{1}{2} \sum_{e \in \mathcal{E}(K)} h_e \left\| \left[\frac{d(\widehat{u}_{\text{FE}} - u_{\text{FE}})}{dn_e} \right] . \right\|_{L^2(e)}. \end{aligned} \tag{5.41}$$

If there exists some $\tilde{K} \in \mathcal{R}$ such that $K \subseteq \tilde{K}$, then

$$T_1^2 \leqslant \frac{\rho}{2} \sum_{e \in \mathcal{E}(K)} h_e \left\| \left[\frac{du_{\text{FE}}}{dn_e} \right] \right\|^2_{L^2(e)}, \tag{5.42}$$

and else

$$T_1^2 \leqslant \eta^2_{K;B}(u_{\text{FE}}, \mathcal{T}), \tag{5.43}$$

Using the trace inequality, for T_2 we get the following upper bound for either or not there exists a $\tilde{K} \in \mathcal{R}$ so that $K \subseteq \tilde{K}$,

$$T_2^2 \leqslant C_{\text{trace}} \|\nabla(\widehat{u}_{\text{FE}} - u_{\text{FE}})\|^2_{L^2(K)^2}. \tag{5.44}$$

Insert equations (5.42)-(5.43) into (5.40) for the case that there exists some $\tilde{K} \in \mathcal{R}$ such that $K \subseteq \tilde{K}$, and we will get

$$\eta_{K;B}(\widehat{u}_{\text{FE}}, \widehat{\mathcal{T}}) \leqslant \left(\frac{\rho}{2} \sum_{e \in \mathcal{E}(K)} h_e \left\| \left[\frac{du_{\text{FE}}}{dn_e} \right] \right\|^2_{L^2(e)} \right)^{\frac{1}{2}} + C^{1/2}_{\text{trace}} \|\nabla(\widehat{u}_{\text{FE}} - u)\|_{L^2(K)^2} \tag{5.45}$$

and if there is no such a cell $\tilde{K} \in \mathcal{R}$

$$\eta_{K;B}(\widehat{u}_{\text{FE}}, \widehat{\mathcal{T}}) \leqslant \eta_{K;B}(u_{\text{FE}}, \mathcal{T}) + C^{1/2}_{\text{trace}} \|\nabla(\widehat{u}_{\text{FE}} - u_{\text{FE}})\|_{L^2(K)^2} \tag{5.46}$$

Now, applying equations (5.37), (5.38), (5.45) and (5.46) to (5.29) and using Young's inequality completes the proof:

$$\begin{aligned} \eta(\widehat{u}_{\text{FE}}, \widehat{\mathcal{T}}) \leqslant & (1+\delta) \left(\left(1 + \frac{\rho^2 \tau^2}{2\delta} \right) \eta^2(u_{\text{FE}}, \mathcal{T}) - (1-\rho^2) \eta(u_{\text{FE}}, \mathcal{M}) \right) \\ & + \left(1 + \frac{1}{\delta} \right) \|\nabla(\widehat{u}_{\text{FE}} - u_{\text{FE}})\|^2_{L^2(\Omega)^2}. \end{aligned} \tag{5.47}$$

□

Lemma 5.3.6 (Error estimator reduction for dual problem)**.** *For $\mathcal{T} \in \mathbb{T}$ and $\mathcal{M} \subset \mathcal{T}$, let $\widehat{\mathcal{T}} \in \mathbb{T}$ be the conforming refinement of $\mathcal{T}$ such that $\widehat{\mathcal{T}} := \textit{REFINE}(\mathcal{T}, \mathcal{M})$ and also $z_{FE} \in V_{\mathcal{T}}$, $\widehat{z}_{FE} \in \widehat{V}_{\mathcal{T}}$ be the finite element solution of (5.5). Consider there exists some constant $\rho > 0$ independent of mesh size vector h so that for all refined cells $\tilde{K} \in \mathcal{T}$ and all $K \in \widehat{\mathcal{T}}$ with $K \subseteq \tilde{K}$, we have $h_K \leqslant \rho h_{\tilde{K}}$. Moreover, assume there exists some $\tau \in (0, 1]$ such that*

$$\sum_{K \in \mathcal{T}} h_K^2 \|j - I_K j\|^2_{L^2(K)} \leqslant \tau^2 \xi(u, \mathcal{T}). \tag{5.48}$$

Then for all $\delta > 0$ it holds

$$\begin{aligned} \xi^2_{\widehat{\mathcal{T}} \setminus \mathcal{T}}(\widehat{z}_{FE}, \widehat{\mathcal{T}}) \leqslant & (1+\delta) \left\{ \left(1 + \frac{\rho^2 \tau^2}{2\delta} \right) \xi^2(z_{FE}, \mathcal{T}) - (1-\rho^2) \xi^2(z_{FE}, \mathcal{M}) \right\} \\ & + (1 + \delta^{-1}) \|\nabla(\widehat{z}_{FE} - z_{FE})\|^2_{L^2(\Omega)}. \end{aligned} \tag{5.49}$$

Proof. The proof starts with Definition 5.2.6 for the dual-error estimator, and follows exactly the same discussion as described in the proof of the error reduction in primal estimator given in Lemma 5.3.5. □

To provide the main result regarding the optimality of our goal-oriented estimator, for both primal and the dual problems, we need to demonstrate that the energy error between the solution of two iterative refinements can be estimated by using the error indicators of the set of refined elements, namely $\mathcal{R} \subseteq \mathcal{T}$.

Lemma 5.3.7 (Discrete reliability for primal problem)**.** *Let $\mathcal{T}, \widehat{\mathcal{T}} \in \mathbb{T}$ such that $\widehat{\mathcal{T}}$ be the conforming refinement of $\mathcal{T}$, $\widehat{\mathcal{T}} := REFINE(\mathcal{T}, \mathcal{M})$. Consider the set of refined elements $\mathcal{R} = \mathcal{R}_{\mathcal{T} \longrightarrow \widehat{\mathcal{T}}}$. For discrete solutions $u_{FE} \in V_{\mathcal{T}}$ and $\widehat{u}_{FE} \in \widehat{V}_{\mathcal{T}}$ of (5.5), there exists constant C_{rel}^{local} for which following discrete reliability holds,*

$$\|\nabla(\widehat{u}_{FE} - u_{FE})\|^2_{L^2(\Omega)^2} \leqslant C_{rel}^{local}\, \eta^2(u_{FE}, \mathcal{R}). \tag{5.50}$$

Proof. See [4, Lemma 3.6] for a complete proof for elliptic problems. □

Lemma 5.3.8 (Discrete reliability for the dual problem)**.** *Let $\mathcal{T}, \widehat{\mathcal{T}} \in \mathbb{T}$ such that $\widehat{\mathcal{T}}$ be the conforming refinement of $\mathcal{T}$, $\widehat{\mathcal{T}} := REFINE(\mathcal{T}, \mathcal{M})$. Consider the set of refined elements $\mathcal{R} = \mathcal{R}_{\mathcal{T} \longrightarrow \widehat{\mathcal{T}}}$. For discrete solutions $z_{FE} \in V_{\mathcal{T}}$ and $\widehat{z}_{FE} \in \widehat{V}_{\mathcal{T}}$ of (5.6), there exists constant C_{rel}^{local} for which following discrete reliability holds,*

$$\|\nabla(\widehat{z}_{FE} - z_{FE})\|^2_{L^2(\Omega)^2} \leqslant C_{rel}^{local}\, \xi^2(Z, \mathcal{R}). \tag{5.51}$$

Proof. The dual problem is again a symmetric elliptic PDE. Therefore, again following the lines of discussion on localized upper bound or discrete reliability in [4, Lemma 3.6], the proof completes. □

The next lemma is an important statement which we use in the next section for the proofs of the main theorems on optimality.

Lemma 5.3.9 (Orthogonality)**.** *Let $w_h \in \{u_h, z_h\}$ be the finite element solution of primal (5.5) or dual (5.6) problems, and $\mathcal{T}, \widehat{\mathcal{T}} \in \mathbb{T}$ such that $\widehat{\mathcal{T}} :=$ REFINE$(\mathcal{T})$. Then the following orthogonality condition holds:*

$$\|w - w_{FE}\|^2_{H^1_0(\Omega)} = \|w - \widehat{w}_{FE}\|^2_{H^1_0(\Omega)} + \|\widehat{w}_{FE} - w_{FE}\|^2_{H^1_0(\Omega)}. \tag{5.52}$$

Proof. The nestedness of finite element spaces $V_{\mathcal{T}} \subset \widehat{V}_{\mathcal{T}}$ and the Galerkin orthogonality $a(w - \widehat{w}_{\text{FE}}, \widehat{w}_{\text{FE}}) = 0,\ \forall \widehat{w}_{\text{FE}} \in \widehat{V}_{\mathcal{T}}$, implies

$$\begin{aligned}
\|w - w_{\text{FE}}\|^2_{H^1_0(\Omega)} &= a(w - w_{\text{FE}}, w - w_{\text{FE}}) \\
&= a(w - \widehat{w}_{\text{FE}}, w - w_{\text{FE}}) + a(\widehat{w}_{\text{FE}} - w_{\text{FE}}, w - w_{\text{FE}}) \\
&= a(w - \widehat{w}_{\text{FE}}, w) + a(\widehat{w}_{\text{FE}}, w - w_h) - a(w_{\text{FE}}, \widehat{w}_{\text{FE}} - w_{\text{FE}}) \\
&= a(w - \widehat{w}_{\text{FE}}, w - \widehat{w}_{\text{FE}}) + a(\widehat{w}_{\text{FE}}, \widehat{w}_{\text{FE}} - w_{\text{FE}}) - a(w_h, \widehat{w}_{\text{FE}} - w_{\text{FE}}) \\
&= a(w - \widehat{w}_{\text{FE}}, w - \widehat{w}_{\text{FE}}) + a(\widehat{w}_{\text{FE}} - w_{\text{FE}}, \widehat{w}_{\text{FE}} - w_{\text{FE}}) \\
&= \|w - \widehat{w}_{\text{FE}}\|^2_{H^1_0(\Omega)} + \|\widehat{w}_{\text{FE}} - w_{\text{FE}}\|^2_{H^1_0(\Omega)}.
\end{aligned} \tag{5.53}$$

□

5.4 Main results

In this section, we strongly rely on the auxiliary tools presented as Lemmas 5.3.4-5.3.9 in section 5.3.

Proposition 5.4.1 (Quasi-Monotonicity of Primal and Dual Error Estimator)**.** *Let $w_{FE} \in \{u_{FE}, z_{FE}\}$ be the finite element solution of primal (5.5) or dual (5.6) problems, and $\mathcal{T}, \widehat{\mathcal{T}} \in \mathbb{T}$ such that $\widehat{\mathcal{T}} :=$ REFINE$(\mathcal{T})$. Assuming that the following properties hold: the stability of energy estimators on non-refined elements (Lemma 5.3.4), error estimator reduction for primal and dual problems (Lemmas 5.3.5 and 5.3.6), and finally the discrete reliability for primal and dual problems (Lemmas 5.3.7 and 5.3.8). Then the quasi-monotonicity of the estimator holds, which implies there exists a*

constant C_{mono} such that

$$\widehat{\eta}(\widehat{w}_{FE}, \widehat{\mathcal{T}}) \leqslant C_{mono}\, \eta(w_{FE}, \mathcal{T}). \tag{5.54}$$

Proof. The proof follows [5, Lemma 3.5]. The stability of energy estimator Lemma 5.3.4, and the error estimator reduction Lemmas 5.3.5 and 5.3.6 imply

$$\begin{aligned} \widehat{\eta}(\widehat{w}_{\mathrm{FE}}, \widehat{\mathcal{T}}) \leqslant & C_{\mathrm{red}_1} \sum_{K \in \mathcal{T} \setminus \widehat{\mathcal{T}}} \eta_K^2(w_{\mathrm{FE}}, \mathcal{T}) + C_{\mathrm{red}_2} \|\nabla(\widehat{w}_{\mathrm{FE}} - w_{\mathrm{FE}})\|_{L^2(\Omega)}^2 \\ & + \sum_{K \in \mathcal{T} \cap \widehat{\mathcal{T}}} \eta_K^2(w_{\mathrm{FE}}, \mathcal{T}) + C_{\mathrm{stab}} \|\nabla(\widehat{w}_{\mathrm{FE}} - w_{\mathrm{FE}})\|_{L^2(\Omega)}^2 := \mathrm{RHS}, \end{aligned} \tag{5.55}$$

where $0 < C_{\mathrm{red}_1} < 1$. Now after using the results on local upper bound in Lemmas 5.3.7 and 5.3.8 we get

$$\begin{aligned} \mathrm{RHS} \leqslant & C\eta^2(w_{\mathrm{FE}}, \mathcal{T}) + (C_{\mathrm{red}_2} + C_{\mathrm{stab}}) C_{\mathrm{rel}}^{\mathrm{local}} \eta^2(w_{\mathrm{FE}}, \mathcal{T}) \\ = & C_{\mathrm{mono}} \eta^2(w_{\mathrm{FE}}, \mathcal{T}), \end{aligned} \tag{5.56}$$

where $C_{\mathrm{mono}} := C + (C_{\mathrm{red}_2} + C_{\mathrm{stab}}) C_{\mathrm{rel}}^{\mathrm{local}}$ for some constant $C > 0$. □

The following Proposition demonstrates a relation between error estimator reduction from $\mathcal{T}$ to its refinement $\widehat{\mathcal{T}}$ and AFEM through the Dörfler marking. The statement simply says if the estimator reduces after refinement, then the error indicators on the set of refined elements $\mathcal{R}_{\mathcal{T} \longrightarrow \widehat{\mathcal{T}}}$ should satisfy the Dörfler property.

Proposition 5.4.2 (Optimal Marking)**.** *Let $w_{FE} \in \{u_{FE}, z_{FE}\}$ be the finite element solution of primal (5.5) or dual (5.6) problems, and $\mathcal{T}, \widehat{\mathcal{T}} \in \mathbb{T}$ such that $\widehat{\mathcal{T}} := REFINE(\mathcal{T})$. Moreover, assume the stability condition in Lemma 5.3.4 and the discrete reliability noted in Lemmas 5.3.7 and 5.3.8 hold. Then for any $0 < \mu < 1$, there exists $0 < \theta_0 < 1$ such that for all $0 < \theta < \theta_0$ the following holds*

$$\widehat{\eta}(\widehat{w}_{FE}, \widehat{\mathcal{T}})^2 \leqslant \mu\, \eta(w_{FE}, \mathcal{T})^2 \Longrightarrow \sum_{K \in \mathcal{R}} \eta_K(w_{FE}, \mathcal{T})^2 \geqslant \theta\, \eta(w_{FE}, \mathcal{T})^2 \tag{5.57}$$

where θ_0 depends only on constants μ, C_{stab} and C_{rel}^{local}.

Proof. The proof follows the line of [5, Proposition 4.12]. From the stability in Lemma 5.3.4 and applying the Young inequality for any $\delta > 0$ we have

$$\begin{aligned}\eta(w_{\mathrm{FE}},\mathcal{T})^2 &= \sum_{K\in\mathcal{T}\setminus\widehat{\mathcal{T}}}\eta_K(w_{\mathrm{FE}},\mathcal{T})^2 + \sum_{K\in\mathcal{T}\cap\widehat{\mathcal{T}}}\eta_K(w_{\mathrm{FE}},\mathcal{T})^2 \\ &\leqslant \sum_{K\in\mathcal{T}\setminus\widehat{\mathcal{T}}}\eta_K(w_{\mathrm{FE}},\mathcal{T})^2 + (1+\delta)\sum_{K\in\mathcal{T}\cap\widehat{\mathcal{T}}}\eta_K(\widehat{w}_{\mathrm{FE}},\widehat{\mathcal{T}})^2 \\ &\quad + (1+\delta^{-1})C_{\mathrm{stab}}^2\|\nabla(w_{\mathrm{FE}}-\widehat{w_{\mathrm{FE}}})\|_{L^2(\Omega)} := \mathrm{RHS}\end{aligned} \tag{5.58}$$

where $\mathcal{T}\cap\widehat{\mathcal{T}}$ is the set of unrefined elements and $\mathcal{T}\setminus\widehat{\mathcal{T}}\subseteq\mathcal{R}$. Now from the assumption $\widehat{\eta}(\widehat{w}_{\mathrm{FE}},\widehat{\mathcal{T}})^2 \leqslant \mu\,\eta(w_{\mathrm{FE}},\mathcal{T})^2$ and Lemmas 5.3.7 and 5.3.8 on discrete reliability we get

$$\mathrm{RHS} \leqslant \mu(1+\delta)\eta(w_{\mathrm{FE}},\mathcal{T})^2 + (1+C_{\mathrm{stab}}C_{\mathrm{rel}}^{\mathrm{local}}(1+\delta^{-1}))\sum_{K\in\mathcal{R}}\eta_K(w_{\mathrm{FE}},\mathcal{T})^2, \tag{5.59}$$

which implies

$$\left(1+C_{\mathrm{stab}}C_{\mathrm{rel}}^{\mathrm{local}}(1+\delta^{-1})\right)\sum_{K\in\mathcal{R}}\eta_K(w_{\mathrm{FE}},\mathcal{T})^2 \geqslant (1-(1+\delta))\mu\eta(w_{\mathrm{FE}},\mathcal{T})^2 \tag{5.60}$$

where for $0<\mu<1$ and $\delta>0$ small enough, we get $0<\theta=\frac{(1-(1+\delta))\mu}{1+C_{\mathrm{stab}}C_{\mathrm{rel}}^{\mathrm{local}}(1+\delta^{-1})}<1$ which completes the proof. □

In the analysis of optimality, it is essential to find an appropriate error quantity and define its associated approximation class $\mathbb{A}_s$. It is beneficial to demonstrate the relation between the frequently used error quantities. The reliability and efficiency properties of the error estimator imply the following equivalent results for the total error that is a measure of approximability for both data and solution, which is described as $\|u-u_h\|^2_{H^1_0(\Omega)}+\mathrm{osc}^2$:

$$\left(\text{Error Estimator}\right)^2 := \eta^2 \approx \|u-u_{\mathrm{FE}}\|^2_{H^1_0(\Omega)} + \mathrm{osc}^2 =: \left(\text{Total Error}\right)^2. \tag{5.61}$$

It is important to recall that all the decisions made in module **MARK** in any adaptive refinement

strategies, depend on the error estimator η. Moreover, based on the above equivalence relation the convergence rate for the total error is also closely related to the error estimator. On the other hand, the error estimator is equivalent to the sum of the energy error and the scaled error estimator which is called the quasi-error. In [4, Theorem 4.1] the contraction property is proved that guarantees the reduction of quasi-error at each refinement cycle in the adaptive refinement strategy:

$$\left(\text{Error Estimator}\right)^2 := \eta^2 \approx \|u - u_{\text{FE}}\|^2_{H^1_0(\Omega)} + \gamma\eta^2 =: \left(\text{Quasi Error}\right)^2, \quad \text{for some } \gamma > 0. \tag{5.62}$$

The following theorem is an important consequence of using the aforementioned lemmas about the reliability of estimators, the error estimator reduction for both primal and dual settings, and finally the orthogonality condition, to prove the following contraction property.

Theorem 5.4.3 (Contraction for Quasi-Error)**.** *Assuming the reliability assumption in Lemmas 5.11 and 5.19, error estimation reduction described in Lemmas 5.3.5 and 5.3.6, and finally the orthogonality property in Lemma 5.3.9 hold. Then we can prove the quasi-error decreases at each refinement step of AFEM, which implies there exists a contraction constant* $0 < C_{contraction} < 1$ *and* $\gamma > 0$ *such that*

$$\|w - w^{n+1}_{FE}\|^2_{H^1_0(\Omega)} + \gamma\,\eta^2(w^{n+1}_{FE}) \leqslant C_{contraction}\left(\|w - w^{n+1}_{FE}\|^2_{H^1_0(\Omega)} + \gamma\,\eta^2(w^{n}_{FE})\right) \tag{5.63}$$

where $w_{FE} \in \{u_{FE}, z_{FE}\}$ *is the finite element solution of the primal (5.5) or dual (5.6) problems, and* $\mathcal{T}_{n+1}$ *be a refined triangulation such that* $\mathcal{T}_{n+1} \in REFINE(\mathcal{T}_n)$.

Proof. See [4, Theorem 4.1]. □

As we showed in (5.22), the product of primal and dual estimators $\eta\,\xi$ is a quantity to control the error in the goal-oriented adaptive refinement. Therefore, it is important to prove the contraction property for both primal and dual error estimators. In this regard, the next proposition implies if the Dörfler marking is used, then we can prove the contraction property for the error estimator and therefore we can get $\lim_{n\longrightarrow\infty}\eta(w_{\text{FE}}, \mathcal{T}) = 0$, where n denotes the refinement cycle and $w_{\text{FE}} \in$

$\{u_{\text{FE}}, z_{\text{FE}}\}$ is the solution of the primal or dual problem.

Proposition 5.4.4 (Linear Convergence for Error Estimator)**.** *Let $w_{FE} \in \{u_{FE}, z_{FE}\}$ be the finite element solution of the primal (5.5) or dual (5.6) problem, and $\mathcal{T}_n$ is a sequence of refined triangulation such that $\mathcal{T}_n \in$ REFINE$(\mathcal{T}_{n-1})$. Assume that all the auxiliary results introduced in Lemmas 5.3.4 to 5.3.8 and the orthogonality condition in Lemma 5.3.9 hold. Let $0 < \theta \leqslant 1$ be the parameter in Dörfler marking. Then there exists $C > 0$ and a convergence factor $0 < \mu_{conv} < 1$ such that if for $n, k \in \mathbb{N}_0$ there exists at least $k' \leqslant k$ indices $n \leqslant n_1 < n_2 < n_3 < \cdots < n_{k'} < n + k$ satisfying the following Dörfler property*

$$\eta_{n_j}(w_{FE}, \mathcal{T}_{n_j} \backslash \mathcal{T}_{n_j+1})^2 \geqslant \theta \eta^2(w_{FE}, \mathcal{T}_{n_j}), \qquad j = 1, 2, \cdots, k', \tag{5.64}$$

then the following linear convergence holds for the error estimator

$$\eta^2(w_{\text{FE}}, \mathcal{T}_{n+k}) \leqslant C \mu_{\text{conv}}^{k'} \eta^2(w_{\text{FE}}, \mathcal{T}_k). \tag{5.65}$$

Proof. See [5, Proposition 10]. □

This theorem guarantees the linear convergence for the product of primal and dual error estimators.

Theorem 5.4.5 (Linear Convergence for the Estimator Product)**.** *Assume all the auxiliary results stated in Lemmas 5.3.4 to 5.3.8, and the orthogonality condition 5.3.9 hold, then there exist constants $0 < \mu_{lin} < 1$ and $C_{lin} > 0$ such that the product of primal and dual error estimators are linearly convergent so that*

$$\eta(u_{FE}, \mathcal{T}_{n+k})\, \eta(z_{FE}, \mathcal{T}_{n+k}) \leqslant C_{lin}\, \mu_{lin}^k\, \eta(u_{FE}, \mathcal{T}_n)\, \eta(z_{FE}, \mathcal{T}_n), \tag{5.66}$$

where u_{FE} and z_{FE} are the finite element solutions of primal and dual equations (5.5) and (5.6).

Proof. First consider the Mommer-Stevenson (MS) algorithm 4, which implies at each iterative step the marked elements in $\mathcal{M}_j$ either satisfy the Dörfler marking for the primal estimator $\eta(u_{\text{FE}}, \mathcal{T}_j)$, or for the dual estimator $\eta(z_{\text{FE}}, \mathcal{T}_j)$. Moreover, we have $\mathcal{M}_j \subseteq \mathcal{T}_j \backslash \mathcal{T}_{j+1}$ as relation between the set of marked elements and the set of refined elements. The set of marked elements in the MS-algorithm implies, for any k successive triangulations $\mathcal{T}_j$, that $\mathcal{T}_j \backslash \mathcal{T}_{j+1} \subseteq \mathcal{R}$ satisfies k' times Dörfler marking for the primal estimator $\eta(u_{\text{FE}}, \mathcal{T}_j)$ and $k - k'$ times Dörfler marking for the dual estimator $\eta(z_{\text{FE}}, \mathcal{T}_j)$. Therefore Proposition 5.4.4 shows after k refinement steps the following linear convergence for primal and dual error estimators:

$$\eta^2(u_{\text{FE}}, \mathcal{T}_{n+k}) \leqslant C\mu_{\text{conv}}^{k'}\, \eta^2(u_{\text{FE}}, \mathcal{T}_n), \qquad \eta^2(z_{\text{FE}}, \mathcal{T}_{n+k}) \leqslant C\mu_{\text{conv}}^{k-k'}\, \eta^2(z_{\text{FE}}, \mathcal{T}_n) \tag{5.67}$$

which implies

$$\eta^2(u_{\text{FE}}, \mathcal{T}_{n+k})\, \eta^2(z_{\text{FE}}, \mathcal{T}_{n+k}) \leqslant C^2\mu_{\text{conv}}^{k}\, \eta^2(u_{\text{FE}}, \mathcal{T}_n)\eta^2(z_{\text{FE}}, \mathcal{T}_n). \tag{5.68}$$

That completes the proof for MS-algorithm 4.

Now it is time to prove the linear convergence in the estimators product for our proposed goal-oriented algorithm 5. As we presented in equation (5.24) in module MARK, we have $\mathcal{M}_n \subseteq \mathcal{M}_n^u \bigcup \mathcal{M}_n^z$:

$$\eta_n^2(\mathcal{M}_n)\, \xi_n^2(\mathcal{M}_n) \geqslant \theta^2\, \eta_n^2\, \xi_n^2, \tag{5.69}$$

where

$$\eta_n^2(\mathcal{M}_n) \geqslant \theta\eta_n^2, \qquad and \qquad \xi_n^2(\mathcal{M}_n) \geqslant \theta\xi_n^2. \tag{5.70}$$

In other words, the algorithm enforces that in each iteration step n, the Dörfler marking holds for both primal and the dual estimators. Hence, by assumption of Proposition 5.4.4 we conclude that at each iterative step n we have the linear convergence for both our primal and the dual estimators. This concludes the linear convergence for the product of estimators. □

The following lemma gives an important tool to prove the next two theorems associated with the

optimal convergence rate for both MS algorithm 4 and also our goal-oriented algorithm presented in Algorithm 5.

Lemma 5.4.6. *Suppose there exists* $0 < \theta < \theta_0 := \frac{1}{1+C_{stab}C_{rel}^{local}}$ *, and* $\mathcal{T}_n, \widehat{\mathcal{T}} \in \mathbb{T}$ *such that* $\widehat{\mathcal{T}}$ *is a conforming refinement of* $\mathcal{T}_n$*,* $\widehat{\mathcal{T}} := REFINE(\mathcal{T}_n, \mathcal{M})$*. Moreover, consider the refined sets* $\mathcal{R}^u_{\mathcal{T}_n \longrightarrow \widehat{\mathcal{T}}}$ *and* $\mathcal{R}^z_{\mathcal{T}_n \longrightarrow \widehat{\mathcal{T}}}$ *that satisfy the discrete reliability property noted in Lemmas 5.3.7 and 5.3.8. For all* $t, s > 0$ *such that* $(u, z) \in \mathbb{A}_s \times \mathbb{A}_t$*, the following holds*

$$\max\left\{\#\mathcal{R}^u_{\mathcal{T}_n \longrightarrow \widehat{\mathcal{T}}}, \#\mathcal{R}^z_{\mathcal{T}_n \longrightarrow \widehat{\mathcal{T}}}\right\} \leqslant C_1(C_2\|u\|_{\mathbb{A}_s}\|z\|_{\mathbb{A}_t})^{\frac{1}{s+t}}(\eta(u_{FE}, \mathcal{T}_n)\eta(z_{FE}, \mathcal{T}_n))^{\frac{-1}{(s+t)}}, \tag{5.71}$$

where C_1, C_2 *depend on* θ *and also on the stability constant* C_{stab} *in Lemma 5.3.4, estimator reduction constants in Lemmas 5.3.5 and 5.3.6, and finally depend on the discrete reliability constant* C_{rel}^{local} *introduced in Lemmas 5.3.7 and 5.3.8. Further we can prove that the sets* $\mathcal{R}^u_{\mathcal{T}_n \longrightarrow \widehat{\mathcal{T}}}$ *and* $\mathcal{R}^z_{\mathcal{T}_n \longrightarrow \widehat{\mathcal{T}}}$ *satisfy the Dörfler marking*

$$\begin{aligned}\eta^2(u_{FE}, \mathcal{R}^u_{\mathcal{T}_n \longrightarrow \widehat{\mathcal{T}}}) &\geqslant \theta\eta^2(u_{FE}, \mathcal{T}_n),\\ \eta^2(z_{FE}, \mathcal{R}^z_{\mathcal{T}_n \longrightarrow \widehat{\mathcal{T}}}) &\geqslant \theta\eta^2(z_{FE}, \mathcal{T}_n).\end{aligned} \tag{5.72}$$

Proof. See [5, Lemma 15]. □

The next is the main theorem which shows optimal decay rate for the estimator product in the Mommer-Stevenson (MS) algorithm 4. The reason that first we bring Theorem 5.4.7, is because we will use the result of this theorem in the last theorem of this section to prove the optimal convergence rate for our goal-oriented Algorithm 5.

Theorem 5.4.7 (Optimal convergence rate, for Algorithms 4 and 5)**.** *Assume our conforming mesh refinement satisfies both complexity of refinement 5.3.2 and the mesh overlay 5.3.3, and* $0 < \theta < \theta_0 := \frac{1}{1+C_{stab}C_{rel}^{local}}$*. Moreover let all the auxiliary results discussed in section 5.3, namely Lemmas 5.3.4 to 5.3.8 and Lemma 5.3.9 on orthogonality, hold. Then for all* $s, t > 0$ *where* $(u, z) \in \mathbb{A}_s \times \mathbb{A}_t$*, applying the MS-algorithm guarantees there exists an optimality constant* C_{opt} *which depends only*

on θ and $C_{complex}$ such that for all iterative cycles $n \in \mathbb{N}_0$,

$$\eta(u_{FE}, \mathcal{T}_n)\eta(z_{FE}, \mathcal{T}_n) \leqslant \frac{C_{opt}^{1+s+t}}{\left(1 - q_{lin}^{\frac{1}{s+t}}\right)^{s+t}} \|u\|_{\mathbb{A}_s} \|z\|_{\mathbb{A}_t} \left(\#\mathcal{T}_n - \#\mathcal{T}_0\right)^{-(s+t)}. \tag{5.73}$$

Proof. See [3, Theorem 13]. □

Theorem 5.4.8 (Optimal convergence rate, our goal-oriented Algorithm 5)**.** *Let $0 < \theta < \theta_0 := \frac{1}{1+C_{stab}C_{rel}^{local}}$ and assume all the auxiliary results discussed in section 5.3, namely Lemmas 5.3.4 to 5.3.8 and the orthogonality condition 5.3.9 hold. Then for our goal-oriented Algorithm 5, we can show the optimal convergence rate for the primal and dual estimator product in our goal-oriented algorithm 5,*

$$\eta(u_{FE}, \mathcal{T}_n)\xi(z_{FE}, \mathcal{T}_n) \leqslant \frac{C_{opt}^{1+s+t}}{\left(1 - q_{lin}^{\frac{1}{s+t}}\right)^{s+t}} \|u\|_{\mathbb{A}_s} \|z\|_{\mathbb{A}_t} \left(\#\mathcal{T}_n - \#\mathcal{T}_0\right)^{-(s+t)}. \tag{5.74}$$

where η and ξ denote the primal and dual estimators, and all other notations are exactly the same as been defined in Theorem 5.4.7.

Proof. As the proof of [3, Theorem 13] shows, the only missing part that we need to prove is showing that at each iterative cycle, the set of our marking cells $\mathcal{M}_n$ will satisfy

$$\#\mathcal{M}_n \leqslant C \max\left\{\#\mathcal{R}^u_{\mathcal{T}_n \longrightarrow \widehat{\mathcal{T}}}, \#\mathcal{R}^z_{\mathcal{T}_n \longrightarrow \widehat{\mathcal{T}}}\right\}. \tag{5.75}$$

for some $C > 0$, and the rest is the direct use of the Lemma 5.4.6. To show equation (5.75), we start with the result of Lemma 5.4.6 as it implies

$$\begin{aligned} \eta^2(u_{\text{FE}}, \mathcal{R}^u_{\mathcal{T}_n \longrightarrow \widehat{\mathcal{T}}}) &\geqslant \theta\eta^2(u_{\text{FE}}, \mathcal{T}_n) \\ \eta^2(z_{\text{FE}}, \mathcal{R}^z_{\mathcal{T}_n \longrightarrow \widehat{\mathcal{T}}}) &\geqslant \theta\eta^2(z_{\text{FE}}, \mathcal{T}_n). \end{aligned} \tag{5.76}$$

Let $\mathcal{R}_{\mathcal{T}_n \longrightarrow \widehat{\mathcal{T}}} = \left(\mathcal{R}^u_{\mathcal{T}_n \longrightarrow \widehat{\mathcal{T}}} \bigcup \mathcal{R}^z_{\mathcal{T}_n \longrightarrow \widehat{\mathcal{T}}} \right)$, which gives

$$\eta^2(u_{\text{FE}}, \mathcal{R}_{\mathcal{T}_n \longrightarrow \widehat{\mathcal{T}}})\, \eta^2(z_{\text{FE}}, \mathcal{R}_{\mathcal{T}_n \longrightarrow \widehat{\mathcal{T}}}) \geqslant \theta^2\, \eta^2(u_{\text{FE}}, \mathcal{T}_n)\, \eta^2(z_{\text{FE}}, \mathcal{T}_n), \tag{5.77}$$

according to the module MARK in our goal-oriented Algorithm 5,

$$\#\mathcal{M}_n \leqslant C \#\mathcal{R}_n \leqslant 2C \max\{\#\mathcal{R}^u_{\mathcal{T}_n \longrightarrow \widehat{\mathcal{T}}}, \#\mathcal{R}^z_{\mathcal{T}_n \longrightarrow \widehat{\mathcal{T}}}\}. \tag{5.78}$$

Now that equation (5.78) holds for our goal-oriented algorithm, the rest follows exactly the lines of proof [3, Theorem 13] which guarantees the existence of an optimality constant C_{opt}, and consequently the optimal decay rate for the estimator products. □

5.5 Numerical experiments

We consider the Poisson model problem with finite element space of continuous piecewise polynomials of degree $p = 1$. All the goal-oriented adaptive algorithms described in this section are implemented within the deal.II library [76]. In test cases we consider three adaptive refinement strategies and compare their h-refinement patterns, and more importantly we show their corresponding convergence plots. In summary, the first refinement is done based on the energy error estimator, for the second one we consider the locally defined dual-weighted goal-oriented estimator as introduced in [1] for the Poisson problem. Finally, we compare the results of these two methods with our goal oriented strategy presented in Algorithm 5. In the analysis of optimal convergence rate demonstrated in section 5.4, we proved in our goal-oriented strategy using linear polynomials to approximate finite element solutions $Q = 1$, the product of primal and dual estimators $\eta\, \xi$ attains the optimal convergence rate of order $\mathcal{O}(N^{-(\frac{1}{d}+\frac{1}{d})})$, where d denotes the space dimension, and N is the number of degrees of freedom. It is also notable that we use the same order of finite element space for the solution of primal and dual problems.

Example 1 - Square annulus

Consider the Poisson problem described in equation (5.1) on square annulus domain $\Omega = [-1,1] \times [-1,1] \backslash [-0.5,0.5] \times [-0.5,0.5]$. We set the data function $f(x,y)$ and the Dirichlet boundary values such that the exact solution is

$$u(x,y) = \frac{\sin(\pi x) sin(\pi y)}{(x-0.2)^2 + (y-0.2)^2 + 10^{-10}}. \tag{5.79}$$

In our numerical experiments we are interested in the average functional in two sub-domains $\Omega_1, \Omega_2 \subset \Omega$ as we describe in the following two examples.

5.5.1 Example 1-a : Average value over sub-domain Ω_1

For the first case, we are interested in the average of solution values on sub-domain $\Omega_1 = [0.5,1] \times [0.5,1]$. The exact solution of primal and dual problem is shown in Figure 5.1. Figure 5.2 visualizes the meshes generated by the three aforementioned adaptive refinement strategies. As we can see the standard adaptive algorithm using the energy error estimator can not successfully capture the singularities for the primal and dual problems at the same time. The convergence plot for the goal error against the number of degrees of freedom is presented in Figure 5.3. Here we can see the linear reduction of goal error with respect to the number of degrees of freedom. In this example, the influence function applies to the top right area of the domain in the close vicinity of the region where the primal solution itself is non-smooth. Therefore, one can see that the standard AFEM strategy that uses the energy error estimator performs good and is able to resolve the singularities close to the sub-domain $\Omega_1 \subset \Omega$ where the influence function is imposed. However, still we observe AFEM got larger error values and does not exactly decrease linearly. The other two plots in this figure are associated with the goal-oriented refinements. One is the locally defined dual-weighted goal-oriented error estimator introduced by Bürg-Nazarov (BN) in [1], and the third plot in this figure is our proposed goal-oriented strategy in Algorithm 5. As the convergence plots in this figure show, the goal-oriented algorithms perform better than standard AFEM in terms of value and also the rate such that they both decrease linearly. The last Figure 5.4,

(a) Primal solution

(b) Dual solution on Ω_1

(c) Dual solution on Ω_2

Figure 5.1: Analytic solutions for primal and dual problems.

illustrates how nicely the product of our primal and dual estimators $\eta\ \xi$ gives a reliable upper bound for the error in the goal functional. The dashed line in these two figures represents the optimal convergence rate expected for the goal-oriented AFEM using Q_1 shape-regular finite elements, namely $\mathcal{O}(\mathbf{DOF})^{-(\frac{1}{2}+\frac{1}{2})} = \mathcal{O}(\mathbf{DOF})^{-1}$.

5.5.2 Example 1-b : Average value over sub-domain Ω_2

For the second test case, we are interested in the average of solution values on the sub-domain $\Omega_2 = [-1, -0.5] \times [-1, -0.5]$. The exact solution of primal and dual problem is shown in Figure 5.1. Figure 5.5 visualizes the meshes generated by the three aforementioned adaptive refinement strategies. As we can see the standard adaptive algorithm 5.5a using the energy error estimator

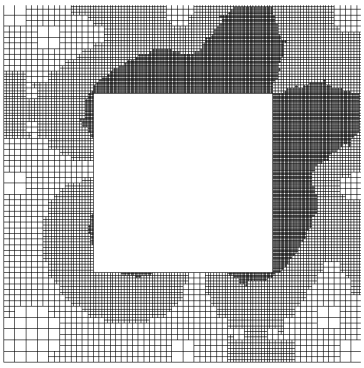

(a) Standard AFEM, using energy estimator.

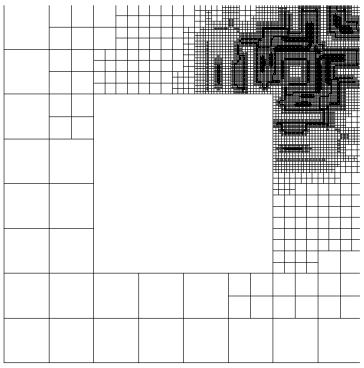

(b) GO-AFEM, using BN estimator [1].

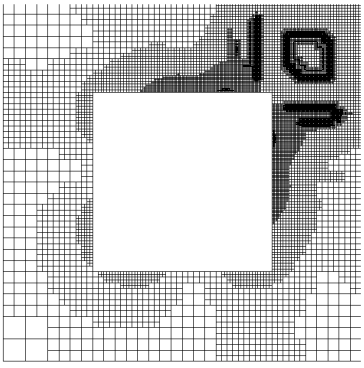

(c) GO-AFEM, using the union of primal and dual marking sets (Algorithm 5).

Figure 5.2: Triangulations generated using different error estimators and marking strategies.

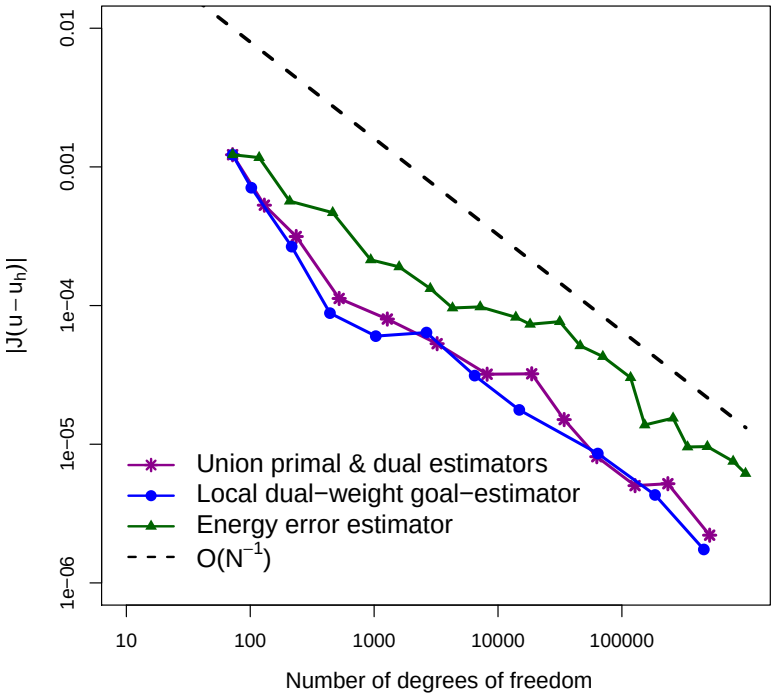

Figure 5.3: Error in the functional vs. number of DOFs. The plots represent the convergence rate for the following: 1) AFEM refinement using energy estimators, 2) the GO-AFEM using local dual-weighted estimator introduced in [1], and 3) our proposed goal-oriented strategy given in Algorithm 5.

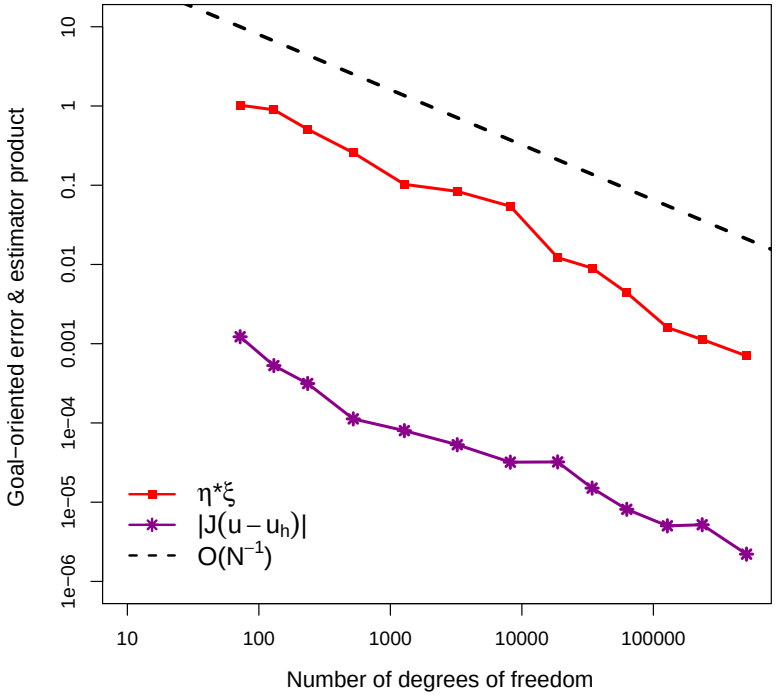

Figure 5.4: Product of primal and dual estimators $\eta\xi$, as well as goal error $J(u - u_h)$ as output of Algorithm 5.

can only resolve the singularities in the areas with high primal residual and is not able to do more local refinements on the bottom left sub-domain $\Omega_2 \subset \Omega$ where the influence function is imposed. In the locally defined dual-weighted goal-oriented estimator Figure 5.5b refinement happens in the areas with larger residual associated with dual problem. In our goal-oriented refinement 5.5c the refinement is done for both cells with the largest primal and dual residuals. The convergence plots corresponding to these methods for the goal-oriented error against the number of degrees of freedom is presented in Figure 5.6. As we expect the AFEM does not perform well both in terms of error values and the rate which is due to the fact that it just focuses on the large residuals for the primal problem. As the figure shows, both goal-oriented strategies decrease linearly. The last Figure 5.7 illustrates how nicely the estimator product gives a reliable upper bound for the error in the goal functional. The dashed line in these two figures represents the optimal convergence rate expected for the goal-oriented AFEM using Q_1 shape-regular finite elements, which is $\mathcal{O}(\mathbf{DOF})^{-(\frac{1}{2}+\frac{1}{2})} = \mathcal{O}(\mathbf{DOF})^{-1}$.

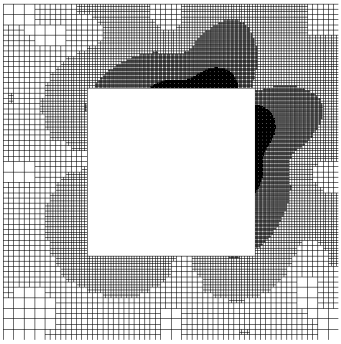

(a) Standard AFEM, using energy estimator.

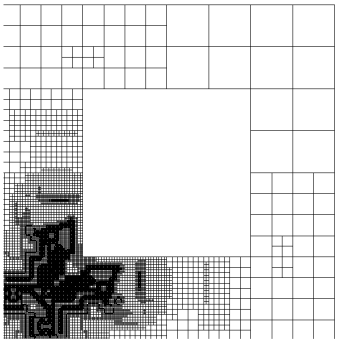

(b) GO-AFEM, using BN estimator [1].

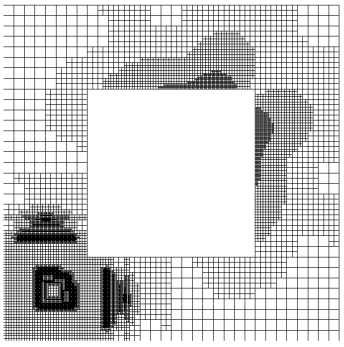

(c) GO-AFEM, using the union of primal and dual marking sets (Algorithm 5).

Figure 5.5: Triangulations generated using different error estimators and marking strategies.

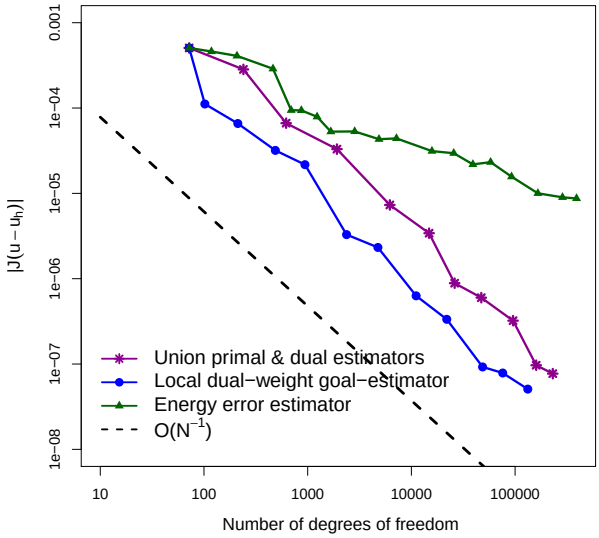

Figure 5.6: Error in the functional vs. number of DOFs. The plots represent the convergence rate for the following: 1) AFEM refinement using energy estimators, 2) the GO-AFEM using local dual-weighted estimator introduced in [1] , and 3) our proposed goal-oriented strategy in Algorithm 5.

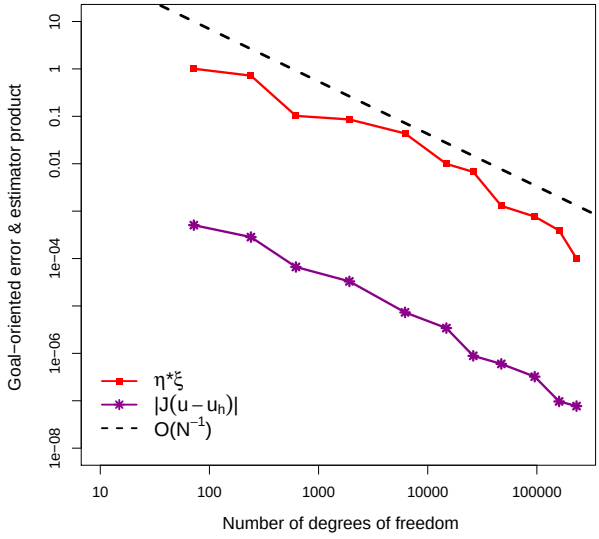

Figure 5.7: Product of primal and dual estimators $\eta\xi$, as well as goal error $J(u - u_h)$ as output of Algorithm 5.

6. CONCLUSIONS

In this dissertation, we focused on the development and application of h- and hp-adaptive refinement strategies for the Stokes and Poisson problems. We devoted separate chapters for each study, and extensively discussed their corresponding analysis, and results of numerical examples. In the following, all the main achievements for each chapter are shortly summarized.

First, in the spirit of Melenk [54, 2], we introduced a residual based a posteriori error estimator for the Stokes problem for hp-adaptive finite elements. In this work, we presented a family $\eta_\alpha,\ \alpha \in [0, 1]$ of residual based error estimators for the hp-AFEM. We proved upper and lower bounds for the estimators applied to the Stokes problems. We were inspired by Dörfler and Heuveline's work [62] for one-dimensional problems and the later works on higher space dimensions by Bürg [**?**]. Following the aforementioned works, we established the hp-adaptive refinement algorithm for our application. In order to decide which refinement gives the best possible hp-refinement, in terms of the largest error reduction, we solve local patch problems in parallel for each individual cell. The numerical examples demonstrate the exponential convergence rate for hp-AFEM in comparison with h-AFEM.

The next chapter was devoted to presenting our analytical and numerical results on investigating a new approach for the goal-oriented AFEMs. This idea in 2015 was introduced for the Poisson equation in [1]. Here, we considered the Stokes problems. The idea of Clément and Scott-Zhang interpolation operators is used. The novelty in this work is the definition of locally formulated error estimators for the goal-oriented refinement. Moreover, we proved the reliability and efficiency of the goal estimator for the Stokes model problem. In the numerical experiments, we compared the h- and hp-AFEM using the energy estimators with the goal-oriented h- and hp-refinement. The comparison of convergence rates confirms our goal-oriented strategy is a promising method to capture the singularities in the areas of influence function. The numerical examples illustrate the expected optimal convergence rate using Taylor-Hood $P_2 - P_1$ elements in the h-GO-AFEM, and the results on the hp-GO-AFEM show the exponential convergence rate.

The last chapter of this dissertation is about applying an abstract framework introduced in [5] to prove the optimality of goal-oriented adaptive refinement. We set the groundwork and demonstrate that all the requirements being noted as the "axioms of adaptivity" hold for our proposed goal-oriented refinement strategy. Next, inspired by the approach of Feischl et al. [3], we prove that the decay rate in the product of the primal and dual estimators is optimal for our goal-oriented refinement algorithm. Numerical experiments show the optimal convergence behavior of the algorithm.

REFERENCES

[1] M. Bürg and M. Nazarov, "Goal-oriented adaptive finite element methods for elliptic problems revisited," *J. of Comput. and Appl. Math.*, vol. 287, pp. 125–147, 2015.

[2] J. M. Melenk and B. I. Wohlmuth, "On residual-based a posteriori error estimation in hp-FEM," *Adv. in Comput. Math.*, vol. 15, pp. 311–331, 2001.

[3] M. Feischl, D. Praetorius, and K. G. V. der Zee, "An abstract analysis of optimal goal-oriented adaptivity," *SIAM J. on Numer. Anal.*, vol. 54, no. 3, pp. 1423–1448, 2016.

[4] J. M. Cascon, C. Kreuzer, R. H. Nochetto, and K. G. Siebert, "Quasi-optimal convergence rate for an adaptive finite element method," *SIAM J. on Numer. Anal.*, vol. 46, no. 5, pp. 2524–2550, 2008.

[5] C. Carstensen, M. Feischl, M. Page, and D. Praetorius, "Axioms of adaptivity," *Comput. & Math. with Appl.*, vol. 67, no. 6, pp. 1195–1253, 2014.

[6] I. Babuška, "Finite element method for domains with corners," *Computing*, vol. 6, no. 3-4, pp. 264–273, 1970.

[7] I. Babuška, "Error estimates for adaptive finite element computations," *SIAM J. Math. Anal.J. Numer. Anal.*, vol. 15(4), pp. 736–754, 1978.

[8] I. Babuška and W. Rheinboldt, "Adaptive approaches and reliability estimations in finite element analysis," *Comput. Meth. Appl. Mech. Engrg.*, vol. 17, pp. 519–540, 1979.

[9] I. Babuška, B. Szabó, and I. Katz, "The p-version of the finite element method," *SIAM J. Numer. Anal.,*, vol. 18, pp. 515–545, 1981.

[10] I. Babuška and M. Dorr, "Error estimates for the combined h- and p-versions of the finite element method," *Numer. Math.*, vol. 37(2), pp. 257–277, 1981.

[11] C. Schwab, *p- and hp-Finite element methods*. Clarendon Press, Oxford, 1998.

[12] J. M. Melenk and C. Schwab, "hp-fem for reaction-diffusion equations, robust exponential convergence," *SIAM J. Numer. Anal.*, vol. 35, pp. 1520–1557, 1998.

[13] D. Schötzau and C. Schwab, "Exponential convergence in a galerkin least squares hp-fem for stokes flow," *IMA J. Numer. Anal.*, vol. 21, pp. 53–80, 2001.

[14] M. Costabel, M. Dauge, and C. Schwab, "Exponential convergence of hp-fem for maxwell's equations with weighted regularization in polygonal domains," *M3AS*, vol. 15(4), pp. 575–622, 2005.

[15] R. Verfürth, *A review of a posteriori error estimation and adaptive mesh-refinement techniques*. C. Wiley, 1996.

[16] T. Eibner and J. Melenk, "An adaptive strategy for hp-fem based on testing for analyticity," *Comput. Mech.*, vol. 39, pp. 575–595, 2007.

[17] T. P. Wihler, "An hp-adaptive strategy based on continuous sobolev embeddings," *J. Comput. Appl. Math*, vol. 235, pp. 2731–2739, 2011.

[18] L. Demkowicz, W. Rachowicz, and P. Devloo, "A fully automatic hp-adaptivity," *J. Sci. Comput.,*, vol. 17, pp. 127–155, 2002.

[19] W. Rachowicz, J. T. Oden, and L. Demkowicz, "Toward a universal h-p adaptive finite element strategy part 3. design of h-p meshes," *Comput. Methods Appl. Mech. Eng.*, vol. 77(1-2), pp. 181–212, 1989.

[20] M. Ainsworth and B. Senior, "An adaptive refinement strategy for hp-finite-element computations," *Appl. Numer. Math.*, vol. 26, pp. 165–178, 1998.

[21] M. Bürg and W. Dörfler, "Convergence of an adaptive hp finite element strategy in higher space-dimensions," *Appl. Numer. Math*, vol. 61, pp. 1132–1146, 2011.

[22] V. Heuveline and R. Rannacher, "Duality-based adaptivity in the hp-finite element method," *J. Numer. Math.*, vol. 11(2), pp. 95–113, 2003.

[23] W. Dörfler, "A convergent adaptive algorithm for poissons equation," *SIAM J. on Numer. Anal.*, vol. 33, no. 3, pp. 1106–1124, 1996.

[24] P. Morin, R. H. Nochetto, and K. G. Siebert, "Data oscillation and convergence of adaptive fem," *SIAM J. on Numer. Anal.*, vol. 38, no. 2, pp. 466–488, 2000.

[25] P. Morin, R. H. Nochetto, and K. G. Siebert, "Convergence of adaptive finite element methods," *SIAM Review*, vol. 44, no. 4, pp. 631–658, 2002.

[26] P. Binev, W. Dahmen, and R. DeVore, "Adaptive finite element methods with convergence rates," *Numerische Mathematik*, vol. 97, no. 2, pp. 219–268, 2004.

[27] K. Mekchay and R. H. Nochetto, "Convergence of adaptive finite element methods for general second order linear elliptic pdes," *SIAM J. on Numer. Anal.*, vol. 43, no. 5, pp. 1803–1827, 2005.

[28] R. Stevenson, "Optimality of a standard adaptive finite element method," *Found. of Comput. Math.*, vol. 7, no. 2, pp. 245–269, 2007.

[29] P. Morin, K. G. Siebert, and A. Veeser, "A basic convergence result for conforming adaptive finite elements," *Math. Models and Methods in Appl. Sci.*, vol. 18, no. 05, pp. 707–737, 2008.

[30] W. Bangerth and R. Rannacher, *Adaptive finite element methods for differential equations*. Birkhäuser Verlag, 2003.

[31] R. Becker and R. Rannacher, "An optimal control approach to a posteriori error estimation in finite element methods," *Acta Numerica 2001*, vol. 10, pp. 1–102, 2001.

[32] C. Johnson and A. Szepessy, "Adaptive finite element methods for conservation laws based on a posteriori error estimates," *Comm. Pure Appl. Math.*, vol. 48, pp. 199–234, 1995.

[33] S. Prudhomme and J. T. Oden, "On goal-oriented error estimation for elliptic problems: application to the control of pointwise errors," *Comput. Methods in Appl. Mech. and Eng.*, vol. 176, no. 1-4, pp. 313–331, 1999.

[34] M. Giles and E. Süli, "Adjoint methods for pdes: a posteriori error analysis and postprocessing by duality," *Acta Numerica*, vol. 11, pp. 145–236, 2002.

[35] K. Eriksson, D. Estep, P. Hansbo, and C. Johnson, "Introduction to adaptive methods for differential equations," *Acta numerica*, vol. 4, pp. 105–158, 1995.

[36] R. Becker and R. Rannacher, *A feed-back approach to error control in finite element methods: basic analysis and examples*. IWR, 1996.

[37] W. Dahmen, A. Kunoth, and J. Vorloeper, "Convergence of adaptive wavelet methods for goal-oriented error estimation," *Numer. Math. and Adv. Appl.*, pp. 39–61, 2006.

[38] K. S. Moon, E. von Schwerin, A. Szepessy, and R. Tempone, "Convergence rates for an adaptive dual weighted residual finite element algorithm," *BIT*, vol. 46 (2), pp. 367 – 407, 2006.

[39] M. S. Mommer and R. Stevenson, "A goal-oriented adaptive finite element method with convergence rates," *SIAM J. Numer. Anal.*, vol. 47(2), pp. 861–886, 2009.

[40] R. Becker, E. Estecahandy, and D. Trujillo, "Weighted marking for goal-oriented adaptive finite element methods," *SIAM J. on Numer.l Anal.*, vol. 49, no. 6, pp. 2451–2469, 2011.

[41] W. Rudin, *Functional analysis. International series in pure and applied mathematics*. McGraw-Hill, Inc., New York, 1991.

[42] S. Brenner and R. Scott, *The mathematical theory of finite element methods*. Springer Science & Business Media, 2007.

[43] I. Babuška and T. Strouboulis, *The finite element method and its reliability*. Oxford university press, 2001.

[44] F. Brezzi and M. Fortin, *Mixed and hybrid finite element methods*, vol. 15. Springer Science & Business Media, 2012.

[45] P. G. Ciarlet, *The finite element method for elliptic problems*. SIAM, 2002.

[46] A. Ern and J. L. Guermond, *Theory and practice of finite elements*. 2013.

[47] F. Brezzi, "On the existence, uniqueness, and approximation of saddle-point problems arising from lagrangian multipliers," *RAIRO Anal. Num.*, vol. 8, pp. 129–151, 1974.

[48] V. Girault and P. A. Raviart, *Finite element approximation of the Navier-Stokes equations. series in computational mathematics.* Berlin Heidelberg New York: Springer, 1986.

[49] A. N. Douglas, F. Brezzi, and M. Fortin, "A stable finite element for the stokes equations," *Calcolo*, vol. 21, no. 4, pp. 337–344, 1984.

[50] P. Clément, "Approximation by finite element functions using local regularization," *RAIRO Anal. Num*, vol. 9, pp. 77–84, 1975.

[51] L. R. Scott and S. Zhang, "Finite element interpolation of nonsmooth functions satisfying boundary conditions," *Math. Comput.*, vol. 54 (190), pp. 483–493, 1990.

[52] L. Demkowicz and I. Babuška, "p-interpolation error estimates for edge finite elements of variable order in two dimensions," *SIAM J. on Numer. Anal.*, vol. 41, no. 4, pp. 1195–1208, 2003.

[53] L. Demkowicz and A. Buffa, "H^1, h(curl) and h-(div)-conforming projection-based interpolation in three dimensions: Quasi-optimal p-interpolation estimates," *Comput. Meth. in Appl. Mech. and Eng.*, vol. 194, no. 2, pp. 267–296, 2005.

[54] J. M. Melenk, "hp-interpolation of nonsmooth functions and an application to hp-a posteriori error estimation," *SIAM J. Numer. Anal.*, vol. 43, pp. 127–155, 2005.

[55] M. Bürg, "A residual-based a posteriori error estimator for the hp-finite element method for Maxwell's equations," *Appl. Numer. Math.*, vol. 62, pp. 922–940, 2012.

[56] C. Bernardi, R. G. Owens, and J. Valenciano, "An error indicator for mortar element solution to the Stokes problem," *SIAM J. Numer. Anal.*, vol. 21, pp. 857–886, 2001.

[57] M. Ainsworth and J. T. Oden, "A posteriori error estimation in finite element analysis," *Comput. Methods. Appl. Mech. Eng.*, vol. 142, pp. 1–88, 1997.

[58] I. Babuška and A. K. Aziz, *The mathematical foundations of the finite element method with applications to partial differential equations*. Proc. Sympos., Univ. Maryland, Baltimore, 1972.

[59] I. Babuška and M. Suril, "The hp version of the finite element method with quasiuniform meshes," *RAIRO-Modélisation mathématique et analyse numérique*, vol. 21, no. 2, pp. 199–238, 1987.

[60] I. Babuška and M. Suri, "The p and hp versions of the finite element method, basic principles and properties," *SIAM review*, vol. 36, no. 4, pp. 578–632, 1994.

[61] W. Bangerth and O. Kayser-Herold, "Data structures and requirements for hp finite element software," *ACM Trans. Math. Softw.*, vol. 36, no. 1, pp. 4/1–4/31, 2009.

[62] W. Dörfler and V. Heuveline, "Convergence of an adaptive hp-finite element strategy in one space dimension," *Appl. Numer. Math.*, vol. 57, pp. 1108–1124, 2007.

[63] I. Babüska and W. Rheinboldt, "A posteriori error estimates for the finite element method," *Int. J. Numer. Methods Eng.*, vol. 12, pp. 1597–1615, 1978.

[64] R. Verfürth, "A posteriori error estimator for the stokes equations," *Numer. Math.*, vol. 55, pp. 309–325, 1989.

[65] I. Bubuška and M. Vogelius, "Feedback and adaptive finite element solution of one-dimensional boundary value problems," *Numerische Mathematik*, vol. 44, no. 1, pp. 75–102, 1984.

[66] I. Babuška and W. C. Rheinboldt, "Analysis of optimal finite-element meshes in r," *Math. of Comput.*, vol. 33, no. 146, pp. 435–463, 1979.

[67] R. H. Nochetto, "Pointwise a posteriori error estimates for elliptic problems on highly graded meshes," *Math. of Comput.*, vol. 64, no. 209, pp. 1–22, 1995.

[68] R. Verfürth, "A posteriori error estimation and adaptive mesh-refinement techniques," *Jour. of Comput. and Appl. and Math.*, vol. 50, no. 1-3, pp. 67–83, 1994.

[69] I. Babuška and A. Miller, "A feedback finite element method with a posteriori error estimation: Part i. the finite element method and some basic properties of the a posteriori error estimator," *Comput. Meth. in Appl. Mech. and Eng.*, vol. 61, no. 1, pp. 1–40, 1987.

[70] I. Babuška and W. C. Rheinboldt, "A-posteriori error estimates for the finite element method," *Int. J. for Numer. Methods in Eng.*, vol. 12, no. 10, pp. 1597–1615, 1978.

[71] R. E. Bank and A. Weiser, "Some a posteriori error estimators for elliptic partial differential equations," *Math. of comput.*, vol. 44, no. 170, pp. 283–301, 1985.

[72] D. W. Kelly, "The self-equilibration of residuals and complementary a posteriori error estimates in the finite element method," *Int. J. for Numer. Methods in Eng.*, vol. 20, no. 8, pp. 1491–1506, 1984.

[73] T. Cao, D. W. Kelly, and I. H. Sloan, "Local error bounds for post-processed finite element calculations," *Int. J. for Numer. Methods in Eng.*, vol. 45, no. 8, pp. 1085–1098, 1999.

[74] M. Paraschivoiu, J. Peraire, and A. T. Patera, "A posteriori finite element bounds for linear-functional outputs of elliptic partial differential equations," *Comput. Methods in Appl. Mech. and Eng.*, vol. 150, no. 1-4, pp. 289–312, 1997.

[75] B. Turcksin, M. Kronbichler, and W. Bangerth, "Workstream–a design pattern for multicore-enabled finite element computations," *ACM Transactions on Math.l Software (TOMS)*, vol. 43, no. 1, p. 2, 2016.

[76] W. Bangerth, R. Hartmann, and G. Kanschat, "deal.II a general purpose object oriented finite element library," *ACM Trans. Math. Software*, vol. 33(4), pp. 24/1–24/27, 2007.

[77] P. Houston, D. Schötzau, and T. P. Wihler, "Energy norm shape a posteriori error estimation for mixed discontinuous galerkin approximations of the stokes problem," *J. of Sci. Comput.*, vol. 22, no. 1, pp. 347–370, 2005.

[78] M. Dauge, "Stationary stokes and navier–stokes systems on two-or three-dimensional domains with corners. part i. linearized equations," *SIAM J. on Math. Anal.*, vol. 20, no. 1, pp. 74–97, 1989.

[79] E. Bänsch, P. Morin, and R. H. Nochetto, "An adaptive uzawa fem for the stokes problem: Convergence without the inf-sup condition," *SIAM J. on Numer. Anal.*, vol. 40, no. 4, pp. 1207–1229, 2002.

[80] R. Becker and R. Rannacher, "Feed-back approach to error control in finite element methods: basic analysis and examples," *East-West Journal of Numer. Math.*, vol. 4, pp. 237–264, 1996.

[81] J. T. Oden and S. Prudhomme, "New apapproach to error estimation and adaptivity for the stokes and oseen equations," *Int. J. for Num. Methods in Fluids*, vol. 31, pp. 3–15, 1999.

[82] M. Nazarov and J. Hoffman, "An adaptive finite element method for inviscid compressible flow," *Int. J. Numer. Methods Fluids*, vol. 10, pp. 1102 – 1128, 2010.

[83] M. Nazarov and J. Hoffman, "Residual-based artificial viscosity for simulation of turbulent compressible flow using adaptive finite element methods," *Int. J. Numer. Methods Fluids*, vol. 71(3), pp. 339–357, 2013.

[84] M. Holst and S. Pollock, "Convergence of goal-oriented adaptive finite element methods for nonsymmetric problems," *Numer. Methods for Partial. Diff. Equ.*, vol. 32(2), pp. 479 – 509, 2015.

[85] H. Melbø and T. Kvamsdal, "Goal oriented error estimators for stokes equations based on variationally consistent postprocessing," *Comput. Meth. in Appl. Mech. and Eng.*, vol. 192, no. 5, pp. 613–633, 2003.

[86] K. G. van der Zee, E. H. van Brummelen, and R. D. Borst, "Goal-oriented error estimation for stokes flow interacting with a flexible channel," *Int. J. for Numer. Meth. in Fluids*, vol. 56, no. 8, p. 1551, 2008.

[87] R. Becker and R.Rannacher, "Weighted a posteriori error control in FE methods," *Proc. ENUMATH-97, World Scientific Publ., Singapore*, vol. 5, pp. 621 – 637, 1997.

[88] A. Bonito and R. H. Nochetto, "Quasi-optimal convergence rate of an adaptive discontinuous galerkin method," *SIAM J. on Numer.l Anal.*, vol. 48, no. 2, pp. 734–771, 2010.

[89] P. Binev, W. Dahmen, R. DeVore, and P. Petrushev, "Approximation classes for adaptive methods," *Serdica Mathematical J.*, vol. 28, no. 4, pp. 391–416, 2002.

[90] A. Bonito, R. A. DeVore, and R. H. Nochetto, "Adaptive finite element methods for elliptic problems with discontinuous coefficients," *SIAM J. on Numer. Anal.*, vol. 51, no. 6, pp. 3106–3134, 2013.

[91] R. Stevenson, "The completion of locally refined simplicial partitions created by bisection," *Math. of Comput.*, vol. 77, no. 261, pp. 227–241, 2008.

[92] M. Bürg, *A Fully Automatic hp-Adaptive Refinement Strategy*. Ph. D. dissertation, des Karlsruher Instituts für Technologie (KIT), 2012.